January 2011

Well-defined molecular brushes: Synthesis by a "grafting through" strategy and self assembly into complicated hierarchical nanostructures

Zhou Li
Washington University in St. Louis

WASHINGTON UNIVERSITY IN ST. LOUIS

Department of Chemistry

Dissertation Examination Committee

Professor Karen Wooley, Chair
Professor John-Stephen Taylor, Co-Chair
Professor Donald Elbert
Professor Kevin Moeller
Professor Jacob Schaefer
Professor Jay Turner

Well-defined molecular brushes: Synthesis by a "grafting through" strategy and self assembly into complicated hierarchical nanostructures

By

Zhou Li

A dissertation presented to the
Graduate School of Arts and Sciences
of Washington University in
partial fulfillment of the
requirements for the degree
of Doctor of Philosophy

August 2011

Saint Louis, Missouri

ABSTRACT OF THE DISSERTATION

Well-defined molecular brushes:

Synthesis by a "grafting through" strategy and

self assembly into complicated hierarchical nanostructures

By

Zhou Li

Doctor of Philosophy in Chemistry

Washington University in St. Louis, 2011

Professor Karen L. Wooley, Chairperson

This dissertation focuses on the development of a "grafting through" methodology to synthesize molecular brushes with well-defined structures, as an attempt to construct nanostructures by covalent bonds totally. Detailed synthetic procedures for and characterization of molecular brushes, as well as complicated hierarchical nanostructures resulted from their self-assembly are reported. The synthesis of molecular brushes is achieved by combining orthogonal living polymerization techniques rationally, such as living/controlled radical polymerization, ring opening polymerization and ring opening metathesis polymerization. Generally, the strategy can be divided into two steps: the first step involves the preparation of linear macromonomers whose chain ends are functionalized with polymerizable groups and the second step is the polymerization of chain end functional groups. In this dissertation, living/controlled radical polymerization, ring opening polymerization and chain end modification have been applied in the first step to afford chain end functional macromonomers and ring opening metathesis

polymerization is used in the second step to achieve the molecular brush architectures. Due to the high tolerance of Grubbs' catalysts towards functional groups, various functionalities can be incorporated into the molecular brush frameworks by changing the side chain structures, including poly(4-acetoxystyrene), poly(pentafluorostyrene), poly(methyl acrylate), poly(t-butyl acrylate), poly(methyl methacrylate), poly(t-butyl methacrylate), polylactide, poly(ethylene glycol) and polyhedral oligomeric silsesquioxane (POSS). The high versatility of our strategy is also used to increase the complexity of the resulting molecular brushes, by introducing block structures to either backbone or side chains, using the "livingness" characters of the employed polymerization techniques. Those block molecular brushes can be used as building blocks to construct more complicated hierarchical nanostructures, which are self assembled from simpler precursory nanostructures. The confinement of triblock copolymers within molecular brush architecture changes their self assembly behaviors. Dynamic cylindrical nanostructures are constructed from the PS-PMA-PAA triblock amphiphilic molecular brushes, while the same triblock copolymers, when not pre-connected into the molecular brush architectures, organize only into globular assemblies. The vast scope of macromonomers that are compatible with this strategy can also be applied to prepare molecular brushes with fine tunable properties, by introducing several functionalities to the molecular brush frameworks and adjusting their ratios accordingly.

For my parents,

who have provided me with unconditional love and support;

and Ting,

who has made many special changes in my life.

Acknowledgement

With deep sincerity, I would like to express my appreciation to my Ph. D. advisor, Prof. Karen L. Wooley. She has been there to help me throughout my graduate school career not only as an excellent research advisor but also as an amazing teacher and mentor. A brilliant scientist, an intelligent woman, and a respectable human being, her contribution to the progress of this work and the valuable lessons learned under her guidance cannot be overestimated. Karen embodies a wonderful "spicy" mixture of intelligence, enthusiasm and compassion. Her concern for me and my career is forever remembered and she will always be a great friend.

Through this research effort there have been several people with whom I have worked extensively. Dr. Chong Cheng is now a professor at University of Buffalo. Dr. Cheng helped me initiate my research project during his last month as a post-doctoral research associate in Wooley group and we have maintained our friendship since then. He taught me much about polymer chemistry and spread an enthusiasm for research. Members of Wooley group who have assisted me over the years with some aspects of my research include Dr. Jun Ma, Dr. Ke Zhang, Dr. Nam Lee, Mr. Ang Li, Dr. Eric Du, Dr. Guorong Sun, Mr. Shiyi Zhang, Dr. Jeremy Bartles, Ms. Yun Lin, Dr. Zicheng Li, and Dr. Yali Li. All of these individuals have contributed to this work in one fashion or another either through direct collaboration or simply sharing of ideas and woes. I feel blessed to have worked with each of them. I would also like to express my gratitude to all Wooley group members, who have created an enjoyable laboratory environment and make the research life joyful.

Special recognition must also be given to professors who have served as my instructors and members of committee. Prof. John-Stephen Taylor and Prof. Kevin Moeller have been my research committee members for years and I have been fortunate to receive inspiration and feedbacks from them. I also appreciate Prof. Jacob Schaefer, Prof. Jay Turner and Prof. Donald Elbert for providing help and critical suggestions while serving in my defense committee.

The support from McDonnell International Scholars Academy is crucial to my career as my scientific abilities. What the academy provided to me is far beyond the financial support for my graduate career at Washington University. Prof. James V. Wertsch is the director of our academy. He is an enjoyable and inspiring person; communicating with him is a true pleasure. He and his wife, Mrs. Mary Wertsch, provided me many beneficial suggestions regarding to my life and my career. Ms. Kristin Williams, Ms. Angie Rahaman, and Ms. Carla Koberna are appreciated for their boundless help to the scholars. The wonderful events and activities they organized helped build my global vision of current and future crisis in the world, develop my leadership and prepare me for the coming global challenges.

There can be no adequate acknowledgement of the loving encouragement I have received from my parents, my sister and my fiancée throughout these years. Their boundless love and tremendous support continue to be an inspiration.

Financial support from National Science Foundation (grant numbers DMR-0906815 and DMR-1032267) is acknowledged. I also thank the electron microscopy facilities at Washington University in St. Louis, Department of Otolaryngology, Research Center for Auditory and Visual Studies funded by NIH P30 DC004665.

TABLE OF CONTENTS

LIST OF FIGURES

Chapter 5

LIST OF SCHEMES

Chapter 1

Introduction

1.1 Introduction of nanoscience

Nanoscience is the study of nanometer (10^{-9} meter) scale functional systems on the atomic and molecular level. Generally, it deals with structures sized between 1 to 100 nanometers in at least one dimension, and involves developing materials or devices within that size.(1-3) The concept of nanoscience was first developed in a famous talk - *There's Plenty of Room at the Bottom* - given by Nobel Laureate physicist Richard Feynman on December 29, 1959.(4) Dr. Feynman described a process by which the ability to manipulate several atoms and molecules might be developed, using "one set of precise tools to build and operate another proportionally smaller set", and so on down to the needed scale. However, long before that, Nature had "adopted" nanoscience and technology for millions of years. For example, the superhydrophobicity exhibited by the leaves of the lotus flowers, which makes them self-cleaning, is due to nanoscopic architectures of the leaf surface.(5) There are many unique features and properties accompanied with nanostructures, which cannot be observed in macroscopic objects (*i.e.* inert matter becomes an active catalyst such as Au; stable matter becomes flammable such as Al (6)). The surface to bulk ratio is reciprocal to the dimension and increases significantly in nanomaterial, making nanomaterials promising in efficient catalysis and controlled drug delivery.(7) All of these distinctive properties and promises of nanoscience and technology have drawn attention of scientists and engineers across multiple disciplines. Significant advances have been achieved from their research efforts

to understand the properties of nanostructures, to manipulate and construct nanoscale devices, and to apply them in practice to benefit human beings. Worldwide, nanoscience has been profoundly influencing scientific research and manufacture, such as fabrication of small high-performance electromagnetic or mechanic devices,(8-12) design of efficient and robust catalysts(13-15) and development of "smart" and versatile drug carriers.(16-20) These achievements, combined with significant promises for the future have given nanoscience and technology tremendous momentum toward continued growth.

Many approaches have been established to construct nanostructures or nanopatterns, and they can be divided into two categories based on the strategies involved. The first "top-down"(21-27) approach follows the principles that were described in Dr. Feynman's talk, by which nanostructures are constructed using larger devices to direct the assembly of atoms and molecules. The most successful example of this approach is the fabrication of microprocessors by lithography,(24, 28) which is now capable of creating features smaller than 100 nm and makes the blooming information technology possible. The manufacturing of these nanopatterns is only possible with the invention of precision instruments such as the atomic force microscope (AFM) and the scanning tunneling microscope (STM). In the second "bottom-up" approach,(29-36) complex assemblies are constructed from simpler and smaller precursory components by some interactions. The forces are usually inherent within their structures and include covalent bonds, hydrogen bonds, van der Waals forces, electrostatic forces and coordination bonds, *etc*.(37-42) Nature has been a master at constructing sophisticated systems starting from single atoms by the "bottom-up" approach.(43) The genetic process, in which complicated proteins with diverse functionalities are built from simple primitive amino acids, is one of the

most elegant example of Nature in constructing complex structures. One research effort to mimic Nature's "bottom-up" approach is the DNA nanotechnology that combines Watson-Crick basepairing and computer-programing to construct well-defined structures from nucleic acids. The complicated synthesis of structures like smiley-face nanostructures illustrates the ability of this approach.(44, 45) Both "top-down" and "bottom-up" approaches provide specific capacities that can complement by each other.

"Bottom-up" approaches should be capable of producing devices in parallel and be cheaper than "top-down" methods which involve expensive precision equipment. However, "bottom-up" approaches can potentially be overwhelmed as the size and complexity of the desired assembly increases. From the perspective of synthetic chemistry, assembling small molecules to complicated structures requires the expertise to design their structures and manipulate their behaviors precisely. The vast advance in modern synthetic chemistry in the past few decades has achieved the point where it is possible to prepare small molecules to almost any structure. These methods have enabled the production of various useful chemicals such as pharmaceuticals and commercial polymers. However, total prediction of the properties, behaviors and thus interactions of those molecules is still not possible. Perhaps the system that has been best studied is the interactions among nucleic acids and their polymers, by which DNA nanotechnology has achieved precise control over the morphologies, structures, compositions and dimensions of nanostructures. The hindrance to reach such a control in other systems lies in the difficulty to predict what is going to happen in a complicated system, especially when multiple interactions account for driving the assembly process, including chemical bonds, hydrogen bonding, coordination boding, electrostatic forces and van der Waals forces, *etc.*

Among all the forces that may be present in the system, covalent bonds have been studied most extensively by synthetic chemists in the rational synthesis of small molecules with specific structures. This ability raises the question of extending this kind of control to the next-larger level, seeking methods to assemble single molecules into complex assemblies consisting of many molecules arranged in a well-defined manner.(46, 47) In this dissertation, a common "bottom up" approach to building robust nanostructures by covalent bonds will be discussed. Moreover, the organization of those covalent nanostructures in the formation of complex hierarchically-assembled materials will be evaluated.

Self-assembly, the autonomous organization of separated disordered components into assembled ordered structures by non-covalent interaction,(43, 48) is a common phenomenon throughout Nature and technology and has been exploited as a basis for "bottom up" approaches to build nanostructures. Molecules with varying chemical structures are synthesized or separated to drive the assembly, and this has been achieved in surfactants,(49, 50) proteins,(51, 52) DNAs,(44, 53, 54) peptides(55-57) and block copolymers, (58-62) *etc.* Among them, block copolymers, in which two or more homopolymer subunits are connected by covalent bonds, provide a great opportunity to develop self-assembly strategies to build nanostructures with complex functionalities.(58-62) Amphiphilic block copolymers can be assembled into micellar structures due to the incompatibility of the subunit homopolymers in selective solvents.(63-65) By varying the compositions and self-assembly conditions, the dimensions, morphologies, functionalities, and sizes of the resulting structures can be tuned accordingly.(58-62, 66, 67) In most of these studies, the building blocks are primitive linear copolymers and

there is no architectural arrangement of them before the assembly. In this dissertation, we attempt to use covalent bonds to confine polymers/copolymers within a nanoscopic framework first and then study their self assembly behaviors. Complicated nanostructures can be built from block copolymers after increasing the complexity of the building blocks from block copolymers to molecular brushes.

1.2 Molecular brushes

Molecular brushes are bottlebrush-like macromolecular architectures in which many side chains are densely distributed along a backbone (**Figure 1-1**).(68, 69) Due to the steric interactions among the densely grafted side chains, the backbone usually adopts entropically unfavored extended chain extension, which leads to cylindrical morphologies of molecular brushes if the backbone is longer than the side chains. The multibranched nature of molecular brushes leads to compact molecular dimensions compared with linear polymers with the same molecular weight.

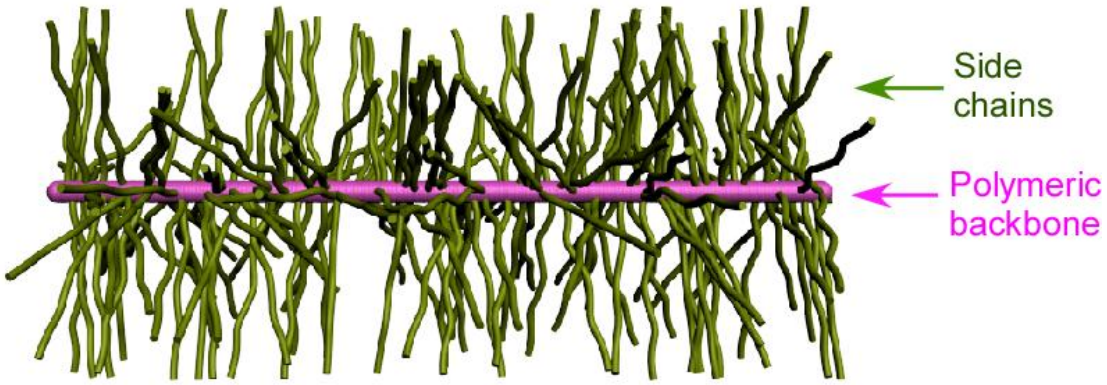

Figure 1-1. Schematic illustration of a molecular brush, composed of a polymeric backbone (pink) from which many side chains (yellow-green) emanate.

Although there are molecular brushes which are created by non-covalent forces, most of them are constructed from covalent bonds exclusively. This provides us the opportunity to utilize our expertise in synthetic chemistry to build well-controlled soft nanostructures unit-by-unit using "bottom-up" approach. Within the development of living/controlled polymerizations,(70-75) the lengths, dimensions and compositions of both the backbone and side chains can be controlled precisely. Generally, there are three strategies to synthesize molecular brushes (**Figure 1-2**): "grafting from",(76-82) "grafting onto"(83-85) and "grafting through".(86, 87) Each of the methods has its own utility and it is often advantageous to employ a combination of methods to prepare brushes with structures which cannot be obtained by a single technique.

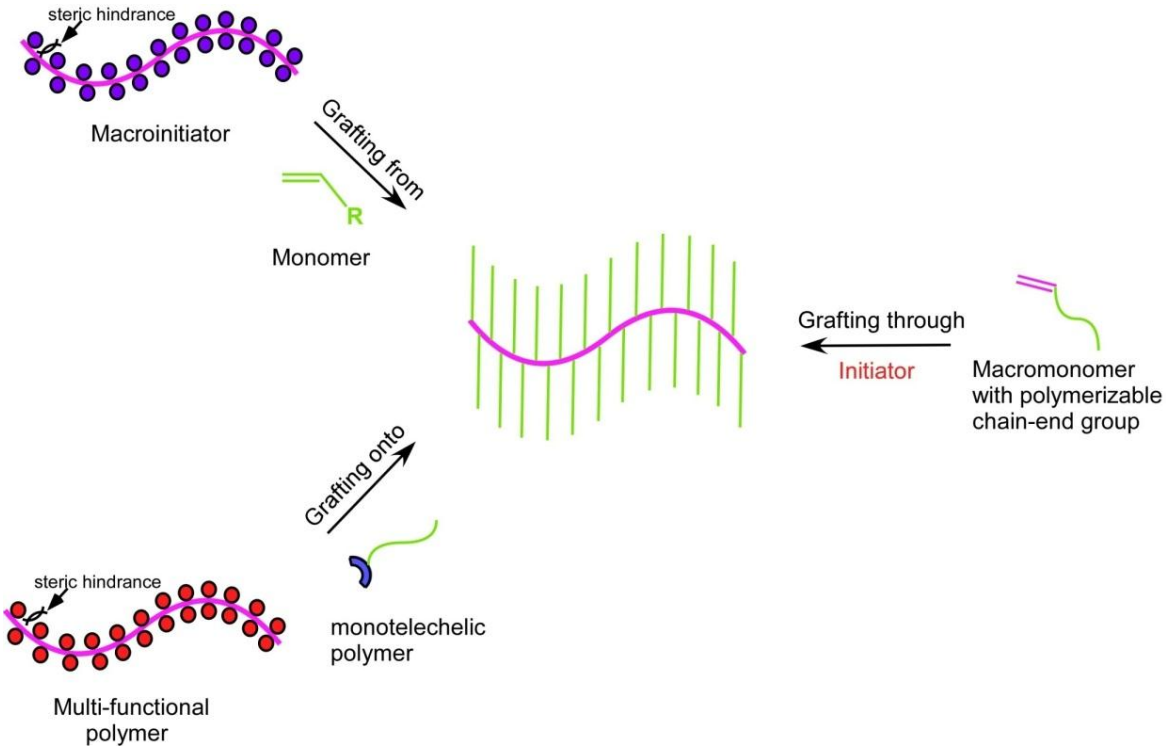

Figure 1-2. Three strategies to construct molecular brushes – "grafting from", "grafting onto" and "grafting through".

1.2.1 "Grafting from" (Grafting the side chains from a multi-initiator)

"Grafting from" synthesis of molecular brushes starts with the preparation of a backbone polymer (multi-initiator) with pre-determined number of initiation sites which are subsequentially used to initiate polymerizations. Depending on polymerization techniques are used in both steps, the initiating groups can be incorporated directly or protected and introduced later after the first-step polymerization.(88, 89) Since the backbone is synthesized first, its composition and length can be controlled. However, there are significant steric effects from initiating groups in proximity with each other along the backbone, which usually lead to incomplete initiation of the polymerization.(90, 91) Because the degree of polymerization is usually controlled by a feeding ratio of

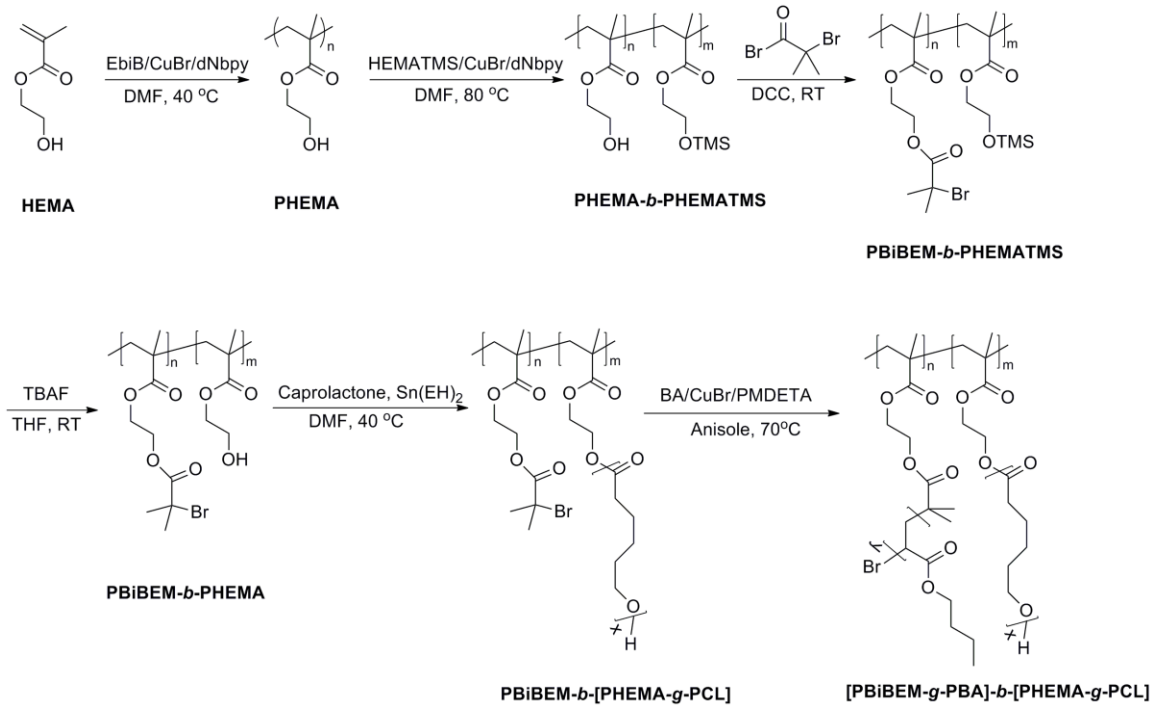

Scheme 1-1. An example of the "grafting from" strategy – synthesis of PCL-*b*-PBA hetero-grafted diblock molecular brushes by a total "grafting from" method. (89)

monomer to initiator, loss control over the initiation efficiency results in loss control over the length of side chains as well. An example of the "grafting from" strategy is shown in **Scheme 1-1**.(89) Besides of all the drawbacks mentioned before, there were multiple steps of protection and deprotection involved in the synthesis of the hetero-grafted diblock molecular brushes, which increases step numbers in the synthesis and the number of deficient sites (sites along the backbone which are not functionalized with initiating groups or initiating groups which do not initiate polymerization) may increase.

1.2.2 "Grafting onto" (Attachment of the side chains to a backbone)

In the "grafting onto" strategy, the backbone and the side chains are synthesized separately. This method involves the reaction of end functional polymers with a precursory polymer backbone bearing multiple complimentary functional groups. Because both backbone and side chains are synthesized independently, the control over their compositions and lengths is good if proper polymerization techniques can be applied to prepare them from respective monomers. However, the limitations in "grafting onto" strategy are obvious. The reaction of the chain ends of large macromolecules and functional groups along the backbone, which are close with each other, is unfavored both thermodynamically and kinetically. The steric effect is more predominant than that in "grafting from" strategy (reactions between two giant macromolecules *vs.* reaction of a small monomer and a macromolecule) and leads to low grafting density.

1.2.3 "Grafting through" (Polymerization of the chain end groups of pre-synthesized polymers)

The "grafting through" strategy contains two steps: first, the synthesis of polymers whose chain ends are polymerizable; second, polymerization of these chain end groups to afford the brush structures. Because the side chains are synthesized by appropriate polymerization techniques first, their structures can be controlled as well as those in "grafting onto" strategy and well-defined polymers can be synthesized. The grafting density is controlled as well as that every monomer moiety (chain end group of macromonomer) incorporated into the backbone bears a defined number of side chains. If a living polymerization is used to polymerize the chain end groups in the second step, the length of the backbone is controlled as well. Therefore, it can provide molecular brushes with best controlled structures in all the three strategies. Some early attempts to apply "grafting through" strategy to synthesize molecular brushes did not show sufficient results because the polymerization of the chain end groups of the side chains is too challenging.(86, 87, 92)

1.3 Tutorial of the developed "grafting through" strategy

1.3.1 Living polymerizations and controlled polymerizations

Living polymerizations or controlled polymerizations are addition polymerizations where the possibility of a growing chain to terminate is significantly lowered down. Chain termination and chain transfer reactions are suppressed and the rate of chain initiation is also much larger than the rate of propagation. As a result, in such polymerization

systems, the polymer chains grow at a more constant rate and their lengths remain similar. Living/controlled polymerization techniques are required in the development of the "grafting through" strategy because the control over the dimensions of molecular brushes is expected. Main living/controlled polymerization techniques include living anionic polymerizations, living/ controlled radical polymerizations, ring opening metathesis polymerizations, and ring opening polymerizations.

1.3.1.1 Living anionic polymerization

Scheme 1-2 showed the general mechanism of living anionic polymerizations.(93, 94) In the absence of impurities, the repetitive conjugate addition reaction of unsaturated monomers to the terminus of growing chains will continue until the monomers are consumed. Since all the chains are initiated at the same time and terminated deliberately, the resulting polymers can be controlled precisely in terms of molecular weight, molecular weight distribution and chain end functional groups. Various polymers/copolymers have been synthesized by this method. The anionic polymerization system may be ceased or interfered by any impurities that are sensitive to anions. The main drawbacks of anionic polymerizations are the limited choice of monomer and the extremely demanding reaction conditions.

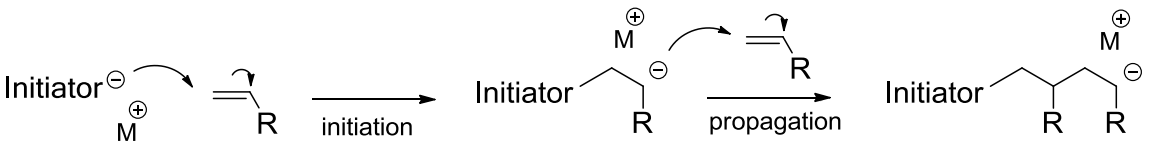

Scheme 1-2. General mechanism of living anionic polymerizations.

1.3.1.2 Living/controlled radical polymerizations

There have been great advances in the development of living/controlled radical polymerizations in the past two decades. A living radical polymerization is a free radical polymerization that aims at display living characters. For example, the growing polymer chains do not terminate or transfer and are able to continue polymerization by addition of more monomers. However, termination processes are inherent to radical reactions (bi-radical coupling), and this side reaction can be suppressed by various mechanisms in different LRP techniques. There are several distinct LRP techniques, including nitroxide-mediated polymerizations (NMP),(95-97) atom transfer radical polymerization (ATRP)(98-101) and reversible addition-fragmentation chain transfer (RAFT) polymerizations.(102-105) The principles of those polymerizations are similar – decrease the concentration of propagating radicals by capping them with protecting groups using reversible reactions.

Scheme 1-3 is the general mechanism of RAFT polymerization. This control is achieved by a molecular transfer agent that reacts with initiating and propagating radicals and then fragments to form both a new radical center capable of initiation and a dormant species that can transfer to another growing chain, which in turn liberates new propagating radicals. The great advantages of radical polymerizations are their wide range of monomers, tolerance of various functional groups and their facile reaction conditions.

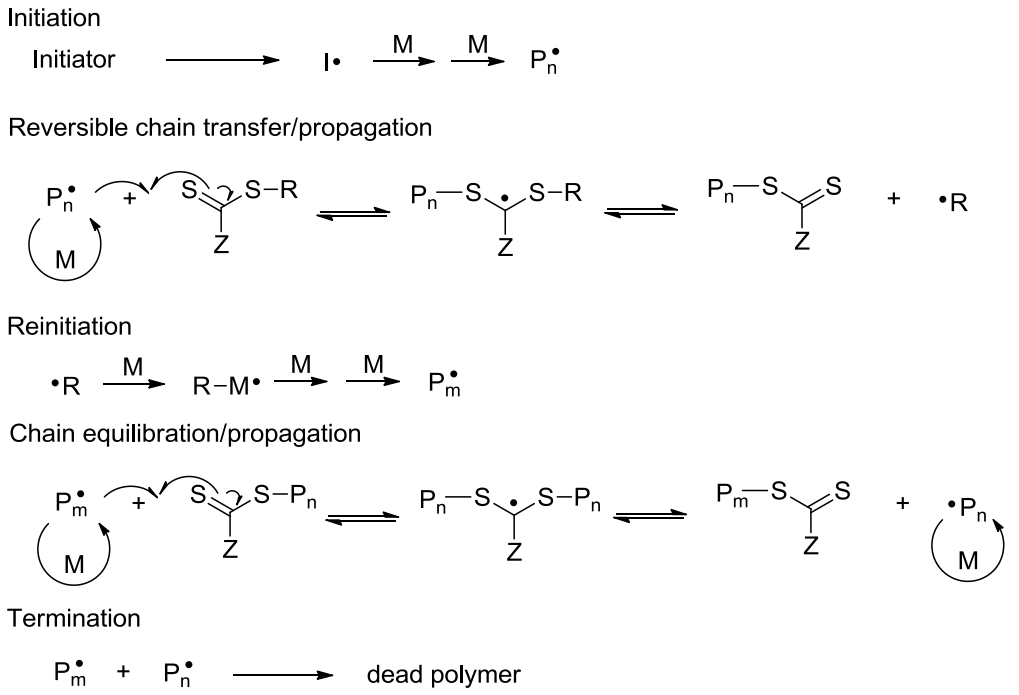

Scheme 1-3. General mechanism of RAFT polymerizations.

1.3.1.3 Ring opening metathesis polymerizations (ROMP)

Ring opening metathesis polymerization (ROMP) is a variant of the olefin metathesis reaction, which can polymerize strained cyclic olefins to produce monodispersed polymers and copolymers. The general mechanism of ROMP is shown in **Scheme 1-4**. Metal-alkylidene complexes, which are derived from metathesis catalysts, are capable of reacting with strained cyclic olefins to open the ring structures. The "new" olefins generated by metathesis reaction remain attached to the metal species, forming new metal-alkylidiene complexes. Although the size of the resulting complexes has increased due to the incorporation of monomers, their reactivity toward strained cyclic olefins is similar. Analogous catalytic cycles occurs continuously until all the monomers are

consumed. The driving force of ROMP reaction is the enthalpy released from the ring strains and thus the polymerization is essentially irreversible.

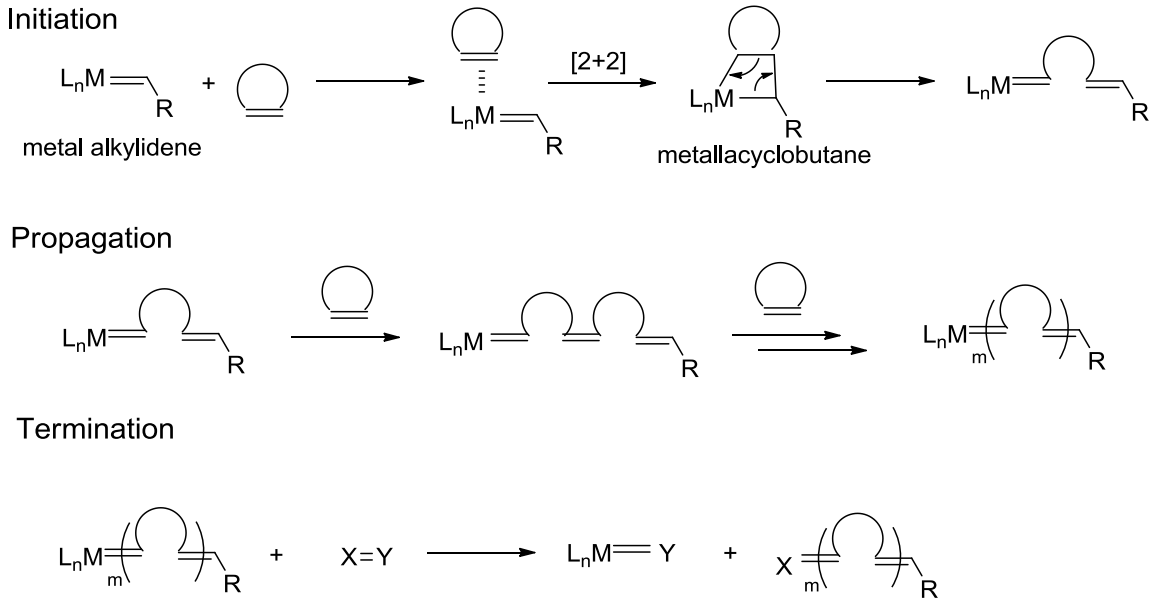

Scheme 1-4. General mechanism of ring opening metathesis polymerization (ROMP).

1.3.1.4 Ring opening polymerizations (ROP)

In polymer chemistry, ring opening polymerization falls into the category of chain-growth polymerization, in which the chain end of a polymer acts as a reactive center, where further cyclic monomers be incorporated to form a longer polymer. By definition, ROMP is a specific form of ROP, but it is discussed separately in this dissertation due to its irreplaceable role in our "grafting through" strategy. **Scheme 1-5** showed an example of ROP and its mechanism. Initiation occurs when a nucleophile such as an alcohol reacts with a lactide-DMAP complex (activated monomer) to form the mono adduct, and the terminal ω-hydroxyl group acts as a nucleophile to facilitate further chain growth.

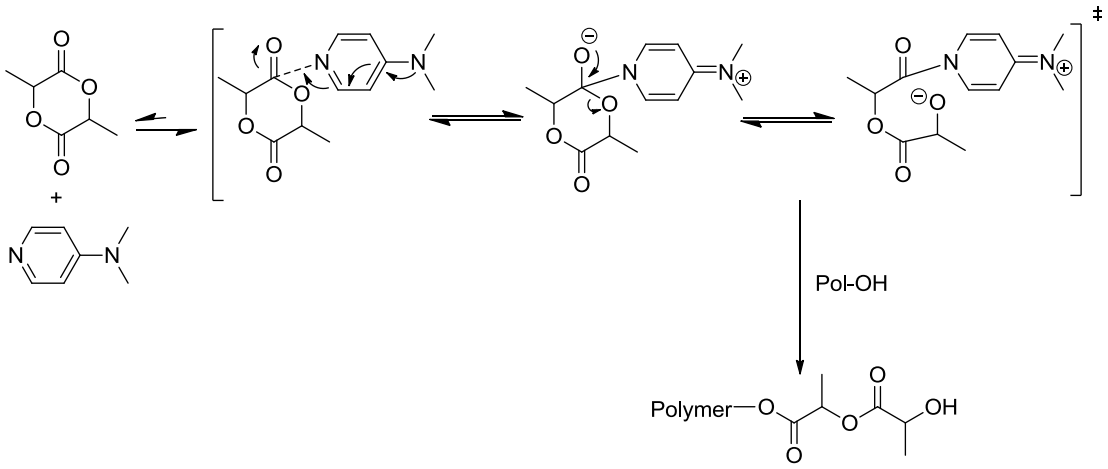

Scheme 1-5. Mechanism of ring opening polymerization of lactide using DMAP as a catalyst.

1.3.2 Choice of the right polymerization techniques

The "grafting through" strategy involves two steps - synthesis of macromonomers whose chain end is a polymerizable functional group and polymerization of these chain end groups. The second step is more challenging due to the low effective concentration of polymerizable end groups and high steric hindrance of the propagating chain end. Hence, polymerizations can be slow and not proceed to high conversion. There have been several reports on anionic polymerizations or controlled radical polymerizations of various macromonomers to construct molecular brushes. Hadjichristidis N. *et al.* studied the anionic polymerization of polyisoprene, polybutadiene and polystyrene with terminal styrenic functionalities.(106) They have found that impurities that are introduced during the isolation of macromonomers by pouring the macromonomer solution to nonsolvent usually terminate the anionic polymerization of macromonomers at early stage. Instead, they have to develop complicated special glass apparatus to synthesize and polymerize macromonomers in the same reactor without isolating them. Although successful, this

method has proved inefficient and expensive. The limited scope of monomers that are compatible with anionic polymerization restricts the expansion of such a strategy to incorporate other monomers into molecular brushes.

Conventional free radical polymerization has been used to construct molecular brushes from a wide range of monomers and reaction conditions by "grafting through" strategy; however, their poor control over molecular weight precludes its application to prepare well-defined structures. To maintain the tolerance of functional groups of radical polymerizations, controlled radical polymerization becomes a candidate which can overcome this issue by increasing control over molecular weight. However, the polymerization rate of CRP processes is determined by activation/deactivation equilibria, the polymerization becomes very slow and often limited to low polymerization degrees when monomer size is increased. When the steric hindrance of the macromonomer is decreased to a certain extent, this method can be successful. Matyjaszewski K. *et al*. polymerized poly(ethylene glycol) methyl ether methacrylate, where the length of poly(ethylene glycol) (PEG) is tuned.(107) When the DP of PEG is 5, molecular brushes with long backbone ($DP_{backbone}$ > 400) and low polydispersity index (PDI = 1.18 – 1.47) can be synthesized; while the DP of PEG is increased to 23, the PDI of the resulting molecular brushes increased and $DP_{backbone}$ is significantly lowered, indicating the loss of the controlled manner of polymerizations when the bulkiness of the macromonomers increases. Moreover, to eliminate the bi-radical coupling side reactions which can terminate radical polymerizations, CRP is usually ceased deliberately at early stage when the conversion of monomers is still low. This feature of CRP presents a challenge to

separate molecular brushes from their representative macromonomers, since they usually have similar solubility.

Ring opening metathesis polymerization (ROMP) was chosen to polymerize macromonomers in our "grafting through" strategy because it can address those challenges presented by anionic polymerizations and CRP. First, the grafting density of side chains in molecular brushes is lower, providing a kinetically favorable environment for propagation reactions. Second, ring strain released from the polymerization provides dramatic thermodynamic forces to drive the reaction to high completion, which is critical to polymerize the polymerizable end groups, whose concentration is low. Third, unlike CRP, the degree of polymerization of ROMP is controlled totally by the feeding ratio of monomer to initiator when the reaction condition is optimized. Last, ROMP is tolerated with many functional groups if proper catalysts are selected as initiators, which promises the versatility of the developed strategy to incorporate various functionalities into the framework.

1.3.3 Macromonomer synthesis

1.3.3.1 RAFT

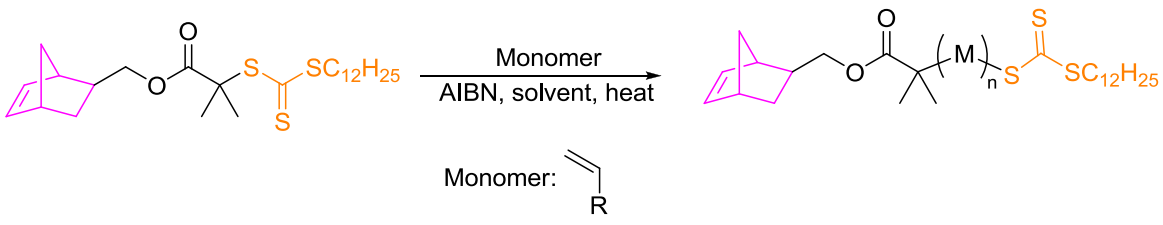

Scheme 1-6. Scheme of the synthesis of macromonomers bearing norbornenyl chain end groups by RAFT polymerization.

RAFT polymerization can be used to synthesize polymers whose chain ends are norbornenyl groups, starting from a norbornenyl functionalized RAFT chain transfer agent, as shown in **Scheme 1-6**.(108, 109) The detailed synthesis of this norbornenyl functionalized RAFT chain transfer agent can be found in **Chapter 2**. The general mechanism of RAFT polymerization has been described previously in **Scheme 1-3**. In this polymerization, azobisisobutyronitrile (AIBN) is used as initiator to provide the initial radicals upon heating. The molecular weight of the resulting polymers is controlled by the addition/fragmentation processes that is tuned by the chain transfer agent. The main side reaction is the participation of norbornenyl groups to radical polymerization, leading to bi-modal molecular weight distribution of the resulting polymers. Moreover, this side reaction also leads to inaccurate calculation of the amount of norbornenyl groups in the second step in "grafting through" strategy. The success of the synthesis of macromonomers by RAFT was accomplished by carefully tuning the polymerization conditions, including adjusting polymerization temperature, selecting proper solvent, changing the feeding ratio of monomer / chain transfer agent / initiator, and controlling the monomer conversions.

Temperature is known to influence the RAFT polymerization.(105) The initiation of the polymerization system requires the production of initiating radicals from certain starting reagents by thermo or photo-induced splitting. In our polymerization system, we try to avoid high temperature to preserve the norbornenyl functionalities. AIBN has a half-life of 10 h in toluene at 65 ^{o}C decomposition temperature,(110) which falls into an acceptable range that norbornenyl groups can tolerate. In practice, the temperature is

usually lowered further to 50 ^{o}C to decrease the concentration of radicals in the system as well as the polymerization rate and, thereby, achieve better control.

Adding solvent to the polymerization system can reduce the viscosity of the reaction and thus decrease the autoacceleration at high monomer concentrations. Another benefit of adding solvent is that the concentration of living radicals is decreased as well. If the polymerization proceeds at a relatively low rate, adding solvent may not be helpful (such as polymerization of styrene by RAFT whose polymerization rate is around 1.5% - 2% conversion of monomers per hour at 60 ^{o}C). However, when the polymerization rate is high, control over the polymerization can be improved significantly by adding proper solvents. In the polymerizations of acrylates, whose reaction rate is around 15% - 25% conversion of monomers per hour, the polymerization can easily become uncontrolled easily if no solvent is added.

The feeding ratio of monomer / chain transfer agent / initiator determines the target length of the resulting polymers, partially. It also affects the concentration of living radicals in the polymerization system. Larger amount of initiators will produce more radicals at a definite time and thus lead to undesired side reactions. Also, too much initiator will result in some macromonomers whose chain ends are capped by AIBN half radicals instead of the norbornenyl groups. In the synthesis of homo-macromonomers (macromonomers synthesized from one monomer), the initiator / chain transfer agent ratio is usually controlled around 5%. In the synthesis of block-macromonomers (macromonomers synthesized from two or more monomers by sequential polymerization), the initiator / chain transfer agent ratio becomes more important and subtle, which will be discussed further in the following chapters.

Controlling the monomer conversion represents a unique feature of controlled radical polymerization (CRP). As shown in **Scheme 1-3**, RAFT polymerization can be terminated by bi-radical coupling, which becomes dominant when monomer concentration is low. Quenching the polymerization at an early stage can diminish this side reaction. In the RAFT polymerization using norbornenyl functionalized chain transfer agent, similar principles can be utilized to increase the reaction selectivity toward monomer olefins and suppress the side reaction of norbornenyl olefins and radicals. The presence of large amounts of unreacted olefin monomers helps with the protection of the norbornenyl groups. In all cases, the conversion of monomers is less than 55%.

Given any monomer, all of these conditions should be tuned carefully to achieve good control over the polymerization reaction. Only after that can well-defined macromonomers be synthesized by RAFT polymerizations.

1.3.3.2 ATRP

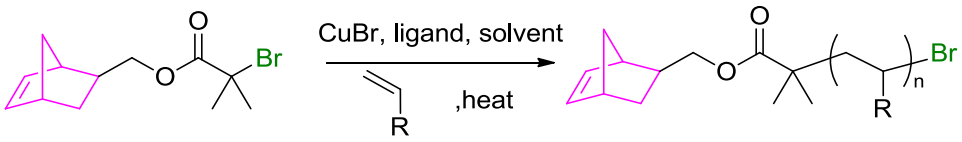

Scheme 1-7. Scheme of the synthesis of macromonomers bearing norbornenyl chain end groups by ATRP.

Atom transfer radical polymerization (ATRP) is another example of a controlled radical polymerization, which was discovered independently by Sawamoto(111) and

Matyjaszewski.(99) Its mechanism involves reversible equilibria between active propagating radicals and inactive dormant forms of the polymers, by reversibly capping them with halogens. Although different in mechanism, ATRP shared many features in common with RAFT. Thus, the principles to adjust polymerization conditions to achieve good control over polymer structures are similar to those of RAFT (**Scheme 1-7**).

1.3.3.3 ROP

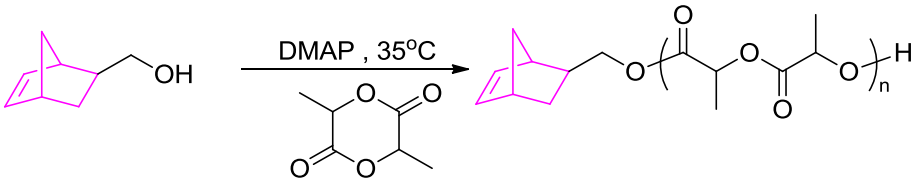

Scheme 1-8. Scheme of the synthesis of *a*-norbornenyl polylactide by ROP.

Exo-5-norbornene-2-methanol acts as a nucleophile to initiate the ring opening polymerization of L-lactide (**Scheme 1-8**). Activated by DMAP, the reaction condition is mild and can afford polylactide whose chain end is functionalized by norbornenyl group at 35 ^{o}C.(112, 113) Due to the ionic pathways in its mechanism, this polymerization does not require the control of the monomer conversion like that in radical polymerizations. However, it was observed that significant chain transfer reactions occur in the presence of DMAP if the polymerization solution is kept untreated under room temperature for a long time.

1.3.3.4 Post modification of chain end

The chain ends of well-defined polymers synthesized from living / controlled polymerizations can be usually capped with functional groups deliberately. Grubbs R. *et al.* synthesized linear homopolymers by ATRP and replaced halogens in the chain ends by azide groups, which were used to incorporate norbornenyl functionalities by "click chemistry".(114, 115) This similar strategy can be applied to functionalize dendrimers(116) and polyhedral oligomeric silsesquioxane (POSS). The reaction that is used to modify the end groups of macromolecules should be highly efficient and it is usually practiced with excess feeding of other reagents to drive the modification to high completion. By post-polymerization modification, incorporation of ROMP active moieties is required for every newly synthesized polymer, which may decrease the research efficiency if many polymers are involved in.

1.3.4 Polymerization of the chain end groups

1.3.4.1 Cleanness of macromonomers

Macromonomers that are synthesized by living /controlled radical polymerization are purified by pouring the polymerization solution into a nonsolvent when the monomer conversion is below 100%. By this method, the resulting macromonomers usually bear trace amounts of unpolymerized vinyl monomers and those residual olefins may present potential problems in the second step of polymerization of norbornenyl groups. A controlled experiment has been done to demonstrate the influence of unreacted monomers to ROMP. Norbornenyl polystyrene macromonomers (NB-PS_{32}) were mixed

with styrene at 2: 1 mole ratio before ROMP. The mole ratio may seem extraordinarily high at first glance, however, the mass ratio of NB-PS_{32} to styrene is about 70: 1, which approaches the possible compositions of an "unclean sample". Compared to ROMP of pure NB-PS_{32} at macromonomer/initiator (M/I) = 100, the molecular brushes from "uncleaned" macromonomers under the same reaction conditions showed smaller molecular weight (78k Da for "uncleaned" *vs.* 380k Da for pure). Also, the polymerizations of "uncleaned" macromonomers at different M/I ratios produced molecular brushes with similar molecular weight (78k Da at M/I = 100 *vs.* 98k Da at M/I = 200). All these results suggest that the presence of styrene can trigger chain transfer reactions of ROMP and that this side reaction can be avoid by carefully purifying the macromonomers.

1.3.4.2 Selection of catalysts

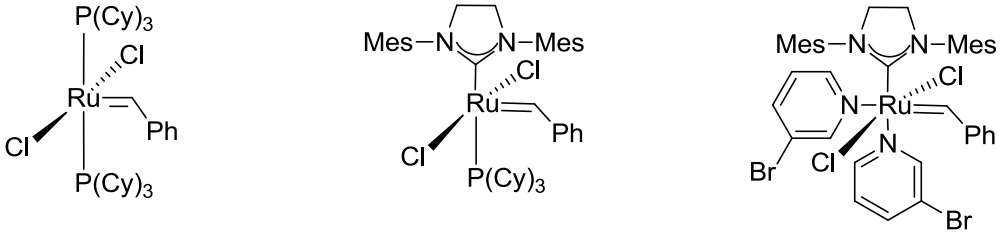

(1) **(2)** **(3)**

Figure 1-3. Chemical structures of several Grubbs' catalysts.

Well-defined olefin-metathesis catalysts are essential for ROMP in our research. Without them, controlled living polymerization cannot be possible. Most of the well-defined catalysts are molybdenum based (Schrock's catalysts)(117) or ruthenium based (Grubbs' catalysts). Grubbs' catalysts (**Figure 1-3**) are chosen in our research because Ru shows

low oxophilicity, which makes it inherently stable toward many polar functional groups, promising the versatile functionalities that can be achieved by the "grafting through" strategy. In general, there are two generations of Grubbs' catalysts. The first generation catalyst is a bisphosphine Ru alkyldiene (**1**)(118) while in the second generation catalyst a phosphine ligand is replaced a N-heterocyclic carbene (NHC) ligand (**2** and **3**).(119) We have found that the propagation in ROMP of macromonomers is often terminated unexpectedly when **1** is used as the initiator. This may be attributed to the labile nature of the phosphine ligands and thus catalyst decomposition occurs during the reaction. NHC ligands are strong σ-donors and less likely to dissociate from the catalyst.(120) However, ROMP using catalyst **2** as initiator usually went uncontrolled because the catalyst exhibits slow initiation rates and fast propagation rates ($k_i < k_p$). Catalyst **3** was found to initiate more rapidly than **2**(121) and can initiate living polymerization of macromonomers.

1.3.4.3 Concentration of macromonomer solutions

The effective concentration of the polymerizable end groups (norbornenyl groups) is very low because it is only a small portion of the whole macromonomer structure. The mass ratio of norbornenyl end group to the whole polymer chain is usually around 1:15 to 1: 40, depending on the molecular weight of the macromonomers. Driven by the ring strain released from ROMP, polymerization does occur even the concentration of the chain end moieties is low. However, in ROMP to build polynorbornene backbones, it is beneficial to run the reaction with high concentration of macromonomers. It should also be pointed

out that the viscosity of polymerization solution may increase significantly when the concentration of macromonomers is too high, resulting in early termination of the polymerization because residual macromonomers cannot access to propagating sites easily.

1.4 Scope of the dissertation

This dissertation demonstrates our research efforts to develop a "bottom-up" approach to construct robust well-defined nanostructures, by using the expertise in synthetic polymer chemistry to assemble small molecules strategically. More specifically, a highly efficient, versatile "grafting through" synthetic methodology has been established by combining "controlled radical polymerizations" (CRP), "ring opening polymerization" (ROP), "chain end modification" and "ring opening metathesis polymerization" (ROMP). The exploitation of living polymerizations techniques and quantitative functional group modification enables us to control the composition, molecular weight, chain length, and structures of both backbone and side chains. We have achieved the preparation of molecular brushes with well-defined structures and diverse types of architectures. Various molecular brushes with different structures were designed based on the structure-property relationships, synthesized by the "grafting-through" strategy and their unique properties were investigated.

Chapter 2 is focused on the synthesis of homo-grafted molecular brushes, which are synthesized by polymerization of macronomers which are homopolymers. As an example, the ROMP of α-norbornenyl-functionalized poly(*t*-butyl acrylate), catalyzed by the modified

2nd generation Grubbs' catalyst, achieved completion in minutes under air. Following hydrolysis, functionalizable water-soluble poly(acrylic acid) molecular brushes were afforded. The versatility of this strategy is also demonstrated by expanding macromonomer structures to other polymers, including polystyrene, poly(4-acetyl styrene), poly(methyl acrylate), poly(*t*-butyl acrylate), poly(methyl methacrylate), poly(*t*-butyl methacrylate), polylactide and polyhedral oligomeric silsesquioxane. A wide range of macronomers that are compatible with this strategy enables us to prepare a variety of molecular brushes with tunable structures and compositions.

In **Chapter 3**, "livingness" of ROMP is utilized to develop a facile and efficient "grafting through" strategy to synthesize hetero-grafted diblock molecular brushes with precisely controlled structure, which exhibit block structures along the backbone. These diblock molecular brushes were prepared by polymerizing different homopolymer macromonomers sequentially in one-pot. Some of them are chemically transformed to amphiphilic nanostructures, whose aqueous solution self-assembly behaviors are studied.

In **Chapter 4,** livingness of controlled radical polymerization is applied to increase the complexity of molecular brush structures. We optimized polymerization conditions to prepare macromonomers which are block copolymers and polymerized them into molecular brushes. The "grafting through" strategy guarantees the compositional consistency of molecular brushes and corresponding macromonomers and enables us to study the difference of their self assembly behaviors, which may be caused by macromolecular architecture only. In this study, we have demonstrated a hierarchical process that combines linear triblock copolymers into concentric globular sub-units through strong chemical bonds and is followed by their supramolecular assembly *via*

weak non-covalent interactions to afford one-dimensionally-assembled, dynamic cylindrical nanostructures.

In **Chapter 5**, the efficiency of the "grafting through" strategy is further utilized to synthesize PPFS-POSS molecular brush copolymers (9 polymers at one time), whose PPFS/POSS ratio is adjusted simply by changing the feeding amounts of the macromonomers. Characterization of nanostructures assembled from them suggests that their sizes and morphologies are independent with PPFS/POSS ratios. However, PPFS content in molecular brush architecture affects the mechanical properties of the resulting nanostructures significantly. Lower PPFS/PPFS ratio leads to flexible and looser nanostructures. It is also revealed that the geometric regularity of the nanostructures may also be influenced by the arrangement of PPFS blocks and POSS blocks in molecular brushes.

References

(1) C. M. Lieber "Nanoscale science and technology: Building a big future from small things." *MRS Bull.* **2003**, *28*, 486-491.

(2) C. N. R. Rao and A. K. Cheetham "Science and technology of nanomaterials: current status and future prospects." *J. Mater. Chem.* **2001**, *11*, 2887-2894.

(3) G. M. Whitesides "Nanoscience, nanotechnology, and chemistry." *Small* **2005**, *1*, 172-179.

(4) R. P. Feynman "There's plenty of room at the bottom. ." **1960**, *23*, 22-36.

(5) T. L. Sun, L. Feng, X. F. Gao and L. Jiang "Bioinspired surfaces with special wettability." *Accounts Chem. Res.* **2005**, *38*, 644-652.

(6) G. C. Bond and D. T. Thompson "Catalysis by gold." *Catal. Rev.-Sci. Eng.* **1999**, *41*, 319-388.

(7) C. Allen, D. Maysinger and A. Eisenberg "Nano-engineering block copolymer aggregates for drug delivery." *Colloid Surf. B-Biointerfaces* **1999**, *16*, 3-27.

(8) J. Xiang, W. Lu, Y. J. Hu, Y. Wu, H. Yan and C. M. Lieber "Ge/Si nanowire heterostructures as high-performance field-effect transistors." *Nature* **2006**, *441*, 489-493.

(9) G. D. Scholes and G. Rumbles "Excitons in nanoscale systems." *Nat. Mater.* **2006**, *5*, 683-696.

(10) V. Balzani, M. Clemente-Leon, A. Credi, B. Ferrer, M. Venturi, A. H. Flood and J. F. Stoddart "Autonomous artificial nanomotor powered by sunlight." *Proc. Natl. Acad. Sci. U. S. A.* **2006**, *103*, 1178-1183.

(11) S. Tiwari, F. Rana, H. Hanafi, A. Hartstein, E. F. Crabbe and K. Chan "A silicon nanocrystals based memory." *Appl. Phys. Lett.* **1996**, *68*, 1377-1379.

(12) E. R. Kay, D. A. Leigh and F. Zerbetto "Synthetic molecular motors and mechanical machines." *Angew. Chem.-Int. Edit.* **2007**, *46*, 72-191.

(13) A. T. Bell "The impact of nanoscience on heterogeneous catalysis." *Science* **2003**, *299*, 1688-1691.

(14) M. C. Daniel and D. Astruc "Gold nanoparticles: Assembly, supramolecular chemistry, quantum-size-related properties, and applications toward biology, catalysis, and nanotechnology." *Chem. Rev.* **2004**, *104*, 293-346.

(15) A. Zaluska, L. Zaluski and J. O. Strom-Olsen "Structure, catalysis and atomic reactions on the nano-scale: a systematic approach to metal hydrides for hydrogen storage." *Appl. Phys. A-Mater. Sci. Process.* **2001**, *72*, 157-165.

(16) S. M. Moghimi, A. C. Hunter and J. C. Murray "Nanomedicine: current status and future prospects." *Faseb J.* **2005**, *19*, 311-330.

(17) E. Boisselier and D. Astruc "Gold nanoparticles in nanomedicine: preparations, imaging, diagnostics, therapies and toxicity." *Chem. Soc. Rev.* **2009**, *38*, 1759-1782.

(18) X. Michalet, F. F. Pinaud, L. A. Bentolila, J. M. Tsay, S. Doose, J. J. Li, G. Sundaresan, A. M. Wu, S. S. Gambhir and S. Weiss "Quantum dots for live cells, in vivo imaging, and diagnostics." *Science* **2005**, *307*, 538-544.

(19) Y. Kakizawa and K. Kataoka "Block copolymer micelles for delivery of gene and related compounds." *Adv. Drug Deliv. Rev.* **2002**, *54*, 203-222.

(20) R. Duncan "The dawning era of polymer therapeutics." *Nat. Rev. Drug Discov.* **2003**, *2*, 347-360.

(21) Y. N. Xia and G. M. Whitesides "Soft lithography." *Annu. Rev. Mater. Sci.* **1998**, *28*, 153-184.

(22) S. Y. Chou, P. R. Krauss and P. J. Renstrom "Imprint lithography with 25-nanometer resolution." *Science* **1996**, *272*, 85-87.

(23) O. Lehtinen, J. Kotakoski, A. V. Krasheninnikov and J. Keinonen "Cutting and controlled modification of graphene with ion beams." *Nanotechnology* **2011**, *22*,

(24) L. T. Canham "Silicon quantum wire array fabrication by electrochemical and chemical dissolution of wafers." *Appl. Phys. Lett.* **1990**, *57*, 1046-1048.

(25) R. S. Kane, S. Takayama, E. Ostuni, D. E. Ingber and G. M. Whitesides "Patterning proteins and cells using soft lithography." *Biomaterials* **1999**, *20*, 2363-2376.

(26) C. Journet, W. K. Maser, P. Bernier, A. Loiseau, M. L. delaChapelle, S. Lefrant, P. Deniard, R. Lee and J. E. Fischer "Large-scale production of single-walled carbon nanotubes by the electric-arc technique." *Nature* **1997**, *388*, 756-758.

(27) R. D. Piner, J. Zhu, F. Xu, S. H. Hong and C. A. Mirkin ""Dip-pen" nanolithography." *Science* **1999**, *283*, 661-663.

(28) S. Y. Chou, P. R. Krauss, W. Zhang, L. J. Guo and L. Zhuang "Sub-10 nm imprint lithography and applications." *J. Vac. Sci. Technol. B* **1997**, *15*, 2897-2904.

(29) M. H. Huang, S. Mao, H. Feick, H. Q. Yan, Y. Y. Wu, H. Kind, E. Weber, R. Russo and P. D. Yang "Room-temperature ultraviolet nanowire nanolasers." *Science* **2001**, *292*, 1897-1899.

(30) T. J. Trentler, K. M. Hickman, S. C. Goel, A. M. Viano, P. C. Gibbons and W. E. Buhro "Solution-liquid-solid growth of crystalline III-V semiconductors - an analogy to vapor-liquid-solid growth." *Science* **1995**, *270*, 1791-1794.

(31) J. M. J. Frechét "Dendrimers and other dendritic macromolecules: From building blocks to functional assemblies in nanoscience and nanotechnology." *J. Polym. Sci. Pol. Chem.* **2003**, *41*, 3713-3725.

(32) W. Lu and C. M. Lieber "Nanoelectronics from the bottom up." *Nat. Mater.* **2007**, *6*, 841-850.

(33) S. Nayak and L. A. Lyon "Soft nanotechnology with soft nanoparticles." *Angew. Chem.-Int. Edit.* **2005**, *44*, 7686-7708.

(34) C. A. Mirkin, R. L. Letsinger, R. C. Mucic and J. J. Storhoff "A DNA-based method for rationally assembling nanoparticles into macroscopic materials." *Nature* **1996**, *382*, 607-609.

(35) M. Shimomura and T. Sawadaishi "Bottom-up strategy of materials fabrication: a new trend in nanotechnology of soft materials." *Curr. Opin. Colloid Interface Sci.* **2001**, *6*, 11-16.

(36) A. K. Gupta and M. Gupta "Synthesis and surface engineering of iron oxide nanoparticles for biomedical applications." *Biomaterials* **2005**, *26*, 3995-4021.

(37) L. R. MacGillivray and J. L. Atwood "A chiral spherical molecular assembly held together by 60 hydrogen bonds." *Nature* **1997**, *389*, 469-472.

(38) S. C. Zimmerman, F. W. Zeng, D. E. C. Reichert and S. V. Kolotuchin "Self-assembling dendrimers." *Science* **1996**, *271*, 1095-1098.

(39) A. Mehdi, C. Reye and R. Corriu "From molecular chemistry to hybrid nanomaterials. Design and functionalization." *Chem. Soc. Rev.* **2011**, *40*, 563-574.

(40) M. Fujita "Metal-directed self-assembly of two- and three-dimensional synthetic receptors." *Chem. Soc. Rev.* **1998**, *27*, 417-425.

(41) P. J. Stang and B. Olenyuk "Self-assembly, symmetry, and molecular architecture: Coordination as the motif in the rational design of supramolecular metallacyclic polygons and polyhedra." *Acc. Chem. Res.* **1997**, *30*, 502-518.

(42) F. Caruso, H. Lichtenfeld, M. Giersig and H. Mohwald "Electrostatic self-assembly of silica nanoparticle - Polyelectrolyte multilayers on polystyrene latex particles." *J. Am. Chem. Soc.* **1998**, *120*, 8523-8524.

(43) G. M. Whitesides and B. Grzybowski "Self-assembly at all scales." *Science* **2002**, *295*, 2418-2421.

(44) P. W. K. Rothemund "Folding DNA to create nanoscale shapes and patterns." *Nature* **2006**, *440*, 297-302.

(45) P. W. K. Rothemund, A. Ekani-Nkodo, N. Papadakis, A. Kumar, D. K. Fygenson and E. Winfree "Design and characterization of programmable DNA nanotubes." *J. Am. Chem. Soc.* **2004**, *126*, 16344-16352.

(46) L. Grill, M. Dyer, L. Lafferentz, M. Persson, M. V. Peters and S. Hecht "Nano-architectures by covalent assembly of molecular building blocks." *Nat. Nanotechnol.* **2007**, *2*, 687-691.

(47) C. J. Hawker and K. L. Wooley "The convergence of synthetic organic and polymer chemistries." *Science* **2005**, *309*, 1200-1205.

(48) J. M. Lehn "Toward self-organization and complex matter." *Science* **2002**, *295*, 2400-2403.

(49) A. Firouzi, D. Kumar, L. M. Bull, T. Besier, P. Sieger, Q. Huo, S. A. Walker, J. A. Zasadzinski, C. Glinka, J. Nicol, D. Margolese, G. D. Stucky and B. F. Chmelka "Coperative organization of inorganic-surfactant and biomimetic assemblies." *Science* **1995**, *267*, 1138-1143.

(50) F. M. Menger and C. A. Littau "Gemini surfactants - a new class of self-assembling molecules." *J. Am. Chem. Soc.* **1993**, *115*, 10083-10090.

(51) H. Yan, S. H. Park, G. Finkelstein, J. H. Reif and T. H. LaBean "DNA-templated self-assembly of protein arrays and highly conductive nanowires." *Science* **2003**, *301*, 1882-1884.

(52) J. W. Kelly "The alternative conformations of amyloidogenic proteins and their multi-step assembly pathways." *Curr. Opin. Struct. Biol.* **1998**, *8*, 101-106.

(53) E. Winfree, F. R. Liu, L. A. Wenzler and N. C. Seeman "Design and self-assembly of two-dimensional DNA crystals." *Nature* **1998**, *394*, 539-544.

(54) C. D. Mao, T. H. LaBean, J. H. Reif and N. C. Seeman "Logical computation using algorithmic self-assembly of DNA triple-crossover molecules." *Nature* **2000**, *407*, 493-496.

(55) J. D. Hartgerink, E. Beniash and S. I. Stupp "Self-assembly and mineralization of peptide-amphiphile nanofibers." *Science* **2001**, *294*, 1684-1688.

(56) S. G. Zhang "Fabrication of novel biomaterials through molecular self-assembly." *Nat. Biotechnol.* **2003**, *21*, 1171-1178.

(57) S. Vauthey, S. Santoso, H. Y. Gong, N. Watson and S. G. Zhang "Molecular self-assembly of surfactant-like peptides to form nanotubes and nanovesicles." *Proc. Natl. Acad. Sci. U. S. A.* **2002**, *99*, 5355-5360.

(58) D. J. Pochan, Z. Y. Chen, H. G. Cui, K. Hales, K. Qi and K. L. Wooley "Toroidal triblock copolymer assemblies." *Science* **2004**, *306*, 94-97.

(59) H. G. Cui, Z. Y. Chen, S. Zhong, K. L. Wooley and D. J. Pochan "Block copolymer assembly via kinetic control." *Science* **2007**, *317*, 647-650.

(60) D. E. Discher and A. Eisenberg "Polymer vesicles." *Science* **2002**, *297*, 967-973.

(61) L. F. Zhang and A. Eisenberg "Multiple morphologies of crew-cut aggregates of polystyrene-b-poly(acrylic acid) block copolymers." *Science* **1995**, *268*, 1728-1731.

(62) Z. B. Li, E. Kesselman, Y. Talmon, M. A. Hillmyer and T. P. Lodge "Multicompartment micelles from ABC miktoarm stars in water." *Science* **2004**, *306*, 98-101.

(63) G. Riess "Micellization of block copolymers." *Prog. Polym. Sci.* **2003**, *28*, 1107-1170.

(64) K. Kataoka, A. Harada and Y. Nagasaki "Block copolymer micelles for drug delivery: design, characterization and biological significance." *Adv. Drug Deliv. Rev.* **2001**, *47*, 113-131.

(65) P. Alexandridis and T. A. Hatton "Poly(ethylene oxide)-poly(propylene oxide)-poly(ethylene oxide) block-copolymer surfactants in aqueous-solutions and at interfaces - thermodynamics, structure, dynamics, and modeling." *Colloid Surf. A-Physicochem. Eng. Asp.* **1995**, *96*, 1-46.

(66) Z. Y. Chen, H. G. Cui, K. Hales, Z. B. Li, K. Qi, D. J. Pochan and K. L. Wooley "Unique toroidal morphology from composition and sequence control of triblock copolymers." *J. Am. Chem. Soc.* **2005**, *127*, 8592-8593.

(67) S. Zhong, H. G. Cui, Z. Y. Chen, K. L. Wooley and D. J. Pochan "Helix self-assembly through the coiling of cylindrical micelles." *Soft Matter* **2008**, *4*, 90-93.

(68) M. F. Zhang and A. H. E. Müller "Cylindrical polymer brushes." *J. Polym. Sci. Pol. Chem.* **2005**, *43*, 3461-3481.

(69) S. S. Sheiko, B. S. Sumerlin and K. Matyjaszewski "Cylindrical molecular brushes: Synthesis, characterization, and properties." *Prog. Polym. Sci.* **2008**, *33*, 759-785.

(70) T. Yokozawa and A. Yokoyama "Chain-growth polycondensation: The living polymerization process in polycondensation." *Prog. Polym. Sci.* **2007**, *32*, 147-172.

(71) W. A. Braunecker and K. Matyjaszewski "Controlled/living radical polymerization: Features, developments, and perspectives." *Prog. Polym. Sci.* **2007**, *32*, 93-146.

(72) C. W. Bielawski and R. H. Grubbs "Living ring-opening metathesis polymerization." *Prog Polym Sci* **2007**, *32*, 1-29.

(73) S. Penczek, M. Cypryk, A. Duda, P. Kubisa and S. Slomkowski "Living ring-opening polymerizations of heterocyclic monomers." *Prog. Polym. Sci.* **2007**, *32*, 247-282.

(74) E. J. Goethals and F. Du Prez "Carbocationic polymerizations." *Prog. Polym. Sci.* **2007**, *32*, 220-246.

(75) D. Baskaran and A. H. E. Müller "Anionic vinyl polymerization - 50 years after Michael Szwarc." *Prog. Polym. Sci.* **2007**, *32*, 173-219.

(76) D. Neugebauer, Y. Zhang, T. Pakula and K. Matyjaszewski "Heterografted PEO-PnBA brush copolymers." *Polymer* **2003**, *44*, 6863-6871.

(77) M. F. Zhang, T. Breiner, H. Mori and A. H. E. Müller "Amphiphilic cylindrical brushes with poly(acrylic acid) core and poly(n-butyl acrylate) shell and narrow length distribution." *Polymer* **2003**, *44*, 1449-1458.

(78) B. S. Sumerlin, D. Neugebauer and K. Matyjaszewski "Initiation efficiency in the synthesis of molecular brushes by grafting from via atom transfer radical polymerization." *Macromolecules* **2005**, *38*, 702-708.

(79) H. G. Böner, K. Beers, K. Matyjaszewski, S. S. Sheiko and M. Möller "Synthesis of molecular brushes with block copolymer side chains using atom transfer radical polymerization." *Macromolecules* **2001**, *34*, 4375-4383.

(80) H. G. Böner, D. Duran, K. Matyjaszewski, M. da Silva and S. S. Sheiko "Synthesis of molecular brushes with gradient in grafting density by atom transfer polymerization." *Macromolecules* **2002**, *35*, 3387-3394.

(81) C. Cheng, K. Qi, E. Khoshdel and K. L. Wooley "Tandem synthesis of core-shell brush copolymers and their transformation to peripherally cross-linked and hollowed nanostructures." *J. Am. Chem. Soc.* **2006**, *128*, 6808-6809.

(82) K. Matyjaszewski, S. H. Qin, J. R. Boyce, D. Shirvanyants and S. S. Sheiko "Effect of initiation conditions on the uniformity of three-arm star molecular brushes." *Macromolecules* **2003**, *36*, 1843-1849.

(83) H. F. Gao and K. Matyjaszewski "Synthesis of molecular brushes by "grafting onto" method: Combination of ATRP and click reactions." *J. Am. Chem. Soc.* **2007**, *129*, 6633-6639.

(84) D. Lanson, M. Schappacher, R. Borsali and A. Deffieux "Synthesis of (poly(chloroethyl vinyl ether)-g-polystyrene)comb-b-(poly(chloropyran ethoxy vinyl ether)-g-polyisoprene)comb copolymers and study of hyper-branched micelle formation in dilute solutions." *Macromolecules* **2007**, *40*, 5559-5565.

(85) B. Helms, J. L. Mynar, C. J. Hawker and J. M. J. Frechét "Dendronized linear polymers via "click chemistry"." *J. Am. Chem. Soc.* **2004**, *126*, 15020-15021.

(86) A. Muehlebach and F. Rime "Synthesis of well-defined macromonomers and comb copolymers from polymers made by atom transfer radical polymerization." *J. Polym. Sci. Pol. Chem.* **2003**, *41*, 3425-3439.

(87) G. H. Deng and Y. M. Chen "Preparation of novel macromonomers and study of their polymerization." *J. Polym. Sci. Pol. Chem.* **2004**, *42*, 3887-3896.

(88) H. I. Lee, W. Jakubowski, K. Matyjaszewski, S. Yu and S. S. Sheiko "Cylindrical core-shell brushes prepared by a combination of ROP and ATRP." *Macromolecules* **2006**, *39*, 4983-4989.

(89) H. I. Lee, K. Matyjaszewski, S. Yu-Su and S. S. Sheiko "Hetero-grafted block brushes with PCL and PBA side chains." *Macromolecules* **2008**, *41*, 6073-6080.

(90) C. Cheng, E. Khoshdel and K. L. Wooley "One-pot tandem synthesis of a core - Shell brush copolymer from small molecule reactants by ring-opening metathesis and reversible addition-fragmentation chain transfer (co)polymerizations." *Macromolecules* **2007**, *40*, 2289-2292.

(91) A. Nese, Y. Kwak, R. Nicolay, M. Barrett, S. S. Sheiko and K. Matyjaszewski "Synthesis of Poly(vinyl acetate) Molecular Brushes by a Combination of Atom Transfer Radical Polymerization (ATRP) and Reversible Addition-Fragmentation Chain Transfer (RAFT) Polymerization." *Macromolecules* **2010**, *43*, 4016-4019.

(92) K. Ishizu, J. Satoh and A. Sogabe "Architecture and solution properties of AB-type brush-block-brush amphiphilic copolymers via ATRP techniques." *J. Colloid Interface Sci.* **2004**, *274*, 472-479.

(93) O. W. Webster "Living polymerization methods." *Science* **1991**, *251*, 887-893.

(94) N. Hadjichristidis, H. Iatrou, S. Pispas and M. Pitsikalis "Anionic polymerization: High vacuum techniques." *J. Polym. Sci. Pol. Chem.* **2000**, *38*, 3211-3234.

(95) C. J. Hawker, A. W. Bosman and E. Harth "New polymer synthesis by nitroxide mediated living radical polymerizations." *Chem. Rev.* **2001**, *101*, 3661-3688.

(96) D. Benoit, V. Chaplinski, R. Braslau and C. J. Hawker "Development of a universal alkoxyamine for "living" free radical polymerizations." *J. Am. Chem. Soc.* **1999**, *121*, 3904-3920.

(97) T. Fukuda, T. Terauchi, A. Goto, K. Ohno, Y. Tsujii, T. Miyamoto, S. Kobatake and B. Yamada "Mechanisms and kinetics of nitroxide-controlled free radical polymerization." *Macromolecules* **1996**, *29*, 6393-6398.

(98) K. Matyjaszewski and J. H. Xia "Atom transfer radical polymerization." *Chem. Rev.* **2001**, *101*, 2921-2990.

(99) J. S. Wang and K. Matyjaszewski "Controlled living radical polymerization - atom-transfer radical polymerization in the presence of transition-metal complexes." *J. Am. Chem. Soc.* **1995**, *117*, 5614-5615.

(100) M. Kamigaito, T. Ando and M. Sawamoto "Metal-catalyzed living radical polymerization." *Chem. Rev.* **2001**, *101*, 3689-3745.

(101) M. Sawamato and M. Kamigaito "Transition-metal-catalyzed living-radical polymerization." *Chemtech* **1999**, *29*, 30-38.

(102) G. Moad, E. Rizzardo and S. H. Thang "Living radical polymerization by the RAFT process." *Aust. J. Chem.* **2005**, *58*, 379-410.

(103) G. Moad, E. Rizzardo and S. H. Thang "Radical addition-fragmentation chemistry in polymer synthesis." *Polymer* **2008**, *49*, 1079-1131.

(104) A. B. Lowe and C. L. McCormick "Reversible addition-fragmentation chain transfer (RAFT) radical polymerization and the synthesis of water-soluble (co)polymers under homogeneous conditions in organic and aqueous media." *Prog. Polym. Sci.* **2007**, *32*, 283-351.

(105) J. Chiefari, Y. K. Chong, F. Ercole, J. Krstina, J. Jeffery, T. P. T. Le, R. T. A. Mayadunne, G. F. Meijs, C. L. Moad, G. Moad, E. Rizzardo and S. H. Thang "Living free-radical polymerization by reversible addition-fragmentation chain transfer: The RAFT process." *Macromolecules* **1998**, *31*, 5559-5562.

(106) D. Pantazis, I. Chalari and N. Hadjichristidis "Anionic polymerization of styrenic macromonomers." *Macromolecules* **2003**, *36*, 3783-3785.

(107) D. Neugebauer, Y. Zhang, T. Pakula, S. S. Sheiko and K. Matyjaszewski "Densely-grafted and double-grafted PEO brushes via ATRP. A route to soft elastomers." *Macromolecules* **2003**, *36*, 6746-6755.

(108) Z. Li, J. Ma, C. Cheng, K. Zhang and K. L. Wooley "Synthesis of hetero-grafted amphiphilic diblock molecular brushes and their self-assembly in aqueous medium." *Macromolecules* **2010**, *43*, 1182-1184.

(109) Z. Li, K. Zhang, J. Ma, C. Cheng and K. L. Wooley "Facile syntheses of cylindrical molecular brushes by a sequential RAFT and ROMP 'grafting-through' methodology." *J. Polym. Sci., Part A: Polym. Chem.* **2009**, *47*, 5557-5563.

(110) M. Buback and F. D. Kuchta "Termination kinetics of free-radical polymerization of styrene over an extended temperature and pressure range." *Macromol. Chem. Phys.* **1997**, *198*, 1455-1480.

(111) M. Kato, M. Kamigaito, M. Sawamoto and T. Higashimura "Polymerization of methyl-methacrylate with the carbon-tetrachloride dichlorotris(triphenylphosphine)ruthenium(II) methylaluminum bis(2,6-di-tert-butylphenoxide) initiating system - possibility of living radical polymerization." *Macromolecules* **1995**, *28*, 1721-1723.

(112) O. Coulembier, A. P. Dove, R. C. Pratt, A. C. Sentman, D. A. Culkin, L. Mespouille, P. Dubois, R. M. Waymouth and J. L. Hedrick "Latent, thermally activated organic catalysts for the on-demand living polymerization of lactide." *Angew. Chem.-Int. Edit.* **2005**, *44*, 4964-4968.

(113) F. Nederberg, E. F. Connor, M. Moller, T. Glauser and J. L. Hedrick "New paradigms for organic catalysts: The first organocatalytic living polymerization." *Angew. Chem.-Int. Edit.* **2001**, *40*, 2712-2715.

(114) Y. Xia, J. A. Kornfield and R. H. Grubbs "Efficient Synthesis of Narrowly Dispersed Brush Polymers via Living Ring-Opening Metathesis Polymerization of Macromonomers." *Macromolecules* **2009**, *42*, 3761-3766.

(115) Y. Xia, B. D. Olsen, J. A. Kornfield and R. H. Grubbs "Efficient synthesis of narrowly dispersed brush copolymers and study of their assemblies: the importance of side-chain arrangement." *J. Am. Chem. Soc.* **2009**, *131*, 18525-18532.

(116) A. J. Boydston, T. W. Holcombe, D. A. Unruh, J. M. J. Fréchet and R. H. Grubbs "A Direct Route to Cyclic Organic Nanostructures via Ring-Expansion Metathesis Polymerization of a Dendronized Macromonomer." **2009**, *131*, 5388-5389.

(117) R. R. Schrock, J. S. Murdzek, G. C. Bazan, J. Robbins, M. Dimare and M. Oregan "Synthesis of molybdenum imido alkylidene complexes and some reations involving acyclic olefins." *J. Am. Chem. Soc.* **1990**, *112*, 3875-3886.

(118) P. Schwab, R. H. Grubbs and J. W. Ziller "Synthesis and applications of RuCl2(=CHR')(PR(3))(2): The influence of the alkylidene moiety on metathesis activity." *J. Am. Chem. Soc.* **1996**, *118*, 100-110.

(119) M. Scholl, S. Ding, C. W. Lee and R. H. Grubbs "Synthesis and activity of a new generation of ruthenium-based olefin metathesis catalysts coordinated with 1,3-dimesityl-4,5-dihydroimidazol-2-ylidene ligands." *Org. Lett.* **1999**, *1*, 953-956.

(120) G. C. Vougioukalakis and R. H. Grubbs "Ruthenium-based olefin metathesis catalysts coordinated with unsymmetrical N-heterocyclic carbene ligands: Synthesis, structure, and catalytic activity." *Chem.-Eur. J.* **2008**, *14*, 7545-7556.

(121) J. A. Love, J. P. Morgan, T. M. Trnka and R. H. Grubbs "A practical and highly active ruthenium-based catalyst that effects the cross metathesis of acrylonitrile." *Angew. Chem.-Int. Edit.* **2002**, *41*, 4035-4037.

Chapter 2

Homo-grafted molecular brushes

[Portions of this work have been published previously as Zhou Li, Ke Zhang, Jun Ma, Chong Cheng, and Karen L. Wooley, *J. Polym. Sci., Part A: Polym. Chem.* **2009,** *47*, 5557-5563]

Part I. Facile syntheses of molecular brushes by a sequential RAFT and ROMP "grafting-through" methodology

ABSTRACT

The orthogonality of RAFT and ROMPolymerization chemistries are exploited for a highly efficient "grafting through" strategy to afford cylindrical molecular brushes. The ROMP of α-norbornenyl-functionalized poly(*t*-butyl acrylate) macroRAFT chain transfer agents, catalyzed by Grubbs' 3rd generation catalyst, achieved completion in minutes under air. Following hydrolysis, functionalizable water-soluble poly(acrylic acid) molecular brushes were afforded.

INTRODUCTION

Of significant interest is the development of synthetic methodologies to prepare complex macromolecular structures that contain functionalities, allowing for stimuli-responsive characteristics and further chemical modifications.(1-3) The cylindrical molecular brush, which is composed of many side chain polymers distributed densely along a backbone, has attracted much attention because its chemical composition, size and morphology can be controlled precisely by choosing appropriate monomers and tuning the lengths of the backbone and side chains.(4, 5) To prepare such structures, three synthetic strategies are often employed: "grafting onto"(6, 7) (grafting side chains onto a pre-established multifunctional backbone by coupling reactions), "grafting from"(8-10) (growth of side chains from a multifunctionalized initiating backbone) and "grafting through"(11-15) (polymerization of previously synthesized side chains through their terminal groups). Previously, our laboratory has demonstrated the compatibility of the three primary living radical polymerizations (nitroxide mediated radical polymerization (NMRP), atom transfer radical polymerization (ATRP) and reversible addition-fragmentation chain transfer (RAFT) polymerization) together with ring-opening metathesis polymerization (ROMP) in the "grafting from" method.(9, 16, 17) Our interest has focused recently on the "grafting through" method, because it provides exceptional control over the grafting density, the length of the backbone, and the length of the side chains, each independently.

Although the "grafting through" approach offers versatility in the construction of complex macromolecular systems, it is likely to encounter steric hindrance during the polymerization of high molecular weight or sterically-bulky macromonomers.(4, 5) To overcome this issue, ROMP has often been used, which is driven by the release of

enthalpy from cyclic monomer structures and affords a polymer backbone with a relatively loose grafting density. For example, the syntheses of molecular brushes have been reported using ROMP from norbornene-terminated poly(ethylene oxide),(13) polystyrene,[12] polyphosphazene,(11) poly(ε-caprolactone),(15) and polylactide,(14) macromonomers synthesized mainly from anionic polymerization or ring opening polymerization. NMRP, ATRP and RAFT are controlled radical polymerization techniques that allow for the preparation of well-defined polymers from vinylic monomers, which can be converted into ROMP-based macromonomers. Grubbs recently reported an elegant combination of ATRP, click chemistry and ROMP to produce narrowly-dispersed brush polymers, whereby the termini of ATRP-generated poly(*tert*-butyl acrylate), poly(methyl acrylate) and polystyrene were converted to norbornenyl groups *via* click chemistry, and those norbornenyl groups were then utilized for "grafting-through" growth of the final brush polymers.(18) In this study, we also take advantage of the reactivity and control of ROMP in "grafting-through" polymerizations, but we obtain the norbornenyl-functionalized macromonomers directly from RAFT(19) of *t*-butyl acrylate using a dual-functionality small molecule that serves as a RAFT agent and carries the norbornene unit. The selectivity of RAFT for the polymerization of *t*-butyl acrylate in the presence of the norbornenyl group allows this chemistry to be used to prepare α-norbornenyl-functionalized poly(*t*-butyl acrylate). Subsequent ROMP of the resulting macromonomer then achieves brush synthesis. A kinetic study of this polymerization showed that it was extremely quick and air-insensitive, using the 3rd generation Grubbs' catalyst. Furthermore, the poly(*t*-butyl acrylate) side chains were

converted to poly(acrylic acid)s, affording water-soluble functional nanoparticles, which are pH-responsive and are readied for future chemical modifications.

RESULTS AND DISCUSSION

The dual ROMP-active and RAFT chain transfer agent containing both a norbornene and a trithiocarbonate functionality, NB-TTC, was prepared in 89% yield by esterification of *exo*-5-norbornene-2-methanol[3] (1.0 equiv.) and S-1-dodecyl-S'-(R,R'-dimethyl-R"-acetic acid)trithiocarbonate. ^{1}H NMR spectroscopy showed a series of characteristic resonances, including those of the norbornene alkenyl protons at 6.05 ppm, C***H*****$_2$**OC(O) at 4.17 and 3.92 ppm, C***H*****$_2$**SC(S)S at 3.25 ppm and the terminal C***H*****$_3$** group at 0.85 ppm, whose integrations agreed with the theoretical ratios.

The chain transfer agent was then used in the polymerization of *t*-butyl acrylate to afford the NB-P*t*BA macromonomers (**Scheme 2-1**). An undesirable amount of the norbornenyl groups participated in the RAFT polymerization in our first trials, as was confirmed by both gel permeation chromatography (GPC), which gave unsymmetrical peaks, and ^{1}H NMR spectroscopy, which revealed partial reduction of the norbornene alkenyl proton resonance intensities. To suppress the norbornenyl group radical polymerization, a series of experiments was conducted to optimize the polymerization conditions. Ultimately, the polymerization was performed in 2-butanone (50% v/v) with 0.05 equiv. AIBN at 51 ^{o}C and quenched at 40% conversion by freezing the reaction mixture in a liquid nitrogen bath. By this method, the RAFT polymerization was controlled, as indicated by retention of both the norbornenyl terminus and the trithiocarbonate terminus in the resulting

macromonomer. The ^{1}H NMR spectrum showed good agreement between the resonance intensities for the protons from the norbornenyl double bond at 6.05-6.10 ppm and the protons from the C***H*****$_2$**SC(S)S group resonating at 3.30-3.40 ppm. GPC analysis of the macromonomer showed a symmetric peak with a polydispersity index (PDI) of 1.16, also demonstrating that the polymerization was well controlled. The M_n obtained from ^{1}H NMR spectroscopy (17.3 kDa) agreed with the M_n value from GPC (16.9 kDa, relative to polystyrene standards). Overall, the involvement of norbornenyl groups in RAFT was suppressed and a linear NB-terminated poly(*t*-butyl acrylate) was synthesized, which could then serve as a macromonomer and/or a macroRAFT chain transfer agent.

The brush synthesis was achieved by ROMP of the terminal norbornenyl group of the NB-P*t*BA macromonomer (**Scheme 2-1**), using the modified second generation Grubbs' catalyst.[17] ROMP of bulky macromonomers using the 1st and 2nd generations Grubbs' catalysts generally require longer reaction times than those of small monomers.(14, 17, 20) The 3rd generation Grubbs' catalyst exhibits fast initiation and propagation,(20) suggesting that it could be an ideal catalyst for the ROMP of bulky macromonomers. Therefore, a kinetic study was performed for the ROMP of the norbornenyl-terminated poly(*t*-butyl acrylate) using 320 equiv. of P*t*BA macromonomer relative to catalyst at room temperature in CH_2Cl_2. The polymerization was conducted in air without Ar protection. At increasing time intervals, an aliquot of the reaction mixture was collected, quenched by ethyl vinyl ether and analyzed by GPC (Fig. 1). At 1 min, *ca*. 75% conversion was achieved and the reaction had reached completion at 2 min. GPC analysis showed that the macromonomer peak at 21.4 min had nearly disappeared and a peak for the molecular brush appeared at 17.4 min. By ^{1}H NMR spectroscopy, the

characteristic protons resonating at 6.05-6.10 ppm and 2.60-2.00 ppm disappeared, supporting complete consumption of the norbornenyl groups. Conducting the reaction in open air or under argon protection showed no discernible difference by GPC and NMR. Even when left for 12 h, no deleterious side reactions were observed. After quenching with ethyl vinyl ether and isolation by precipitation into a H_2O: methanol mixture (1:5, v:v), the molecular brushes were obtained in >90% yield with well-defined molecular weight and composition.

As observed by GPC, the P*t*BA molecular brushes had uniform size distribution, with a PDI of 1.20, similar to that of the macromonomer (**Figure 2-1**). By comparison of their relative areas of integration, *ca*. 93% of the macromonomer had been incorporated into the final brush structure. Within all the experiments, however, there remained a small peak at 21.4 min elution time in the GPC chromatograms of the products, which is believed to be due to the presence of residual macromonomer. One possible explanation is that these macromonomers lacked a norbornenyl end group, due to the mechanism of RAFT and the potential for a portion of the *t*BA chains to be initiated by AIBN during the macromonomer synthesis.

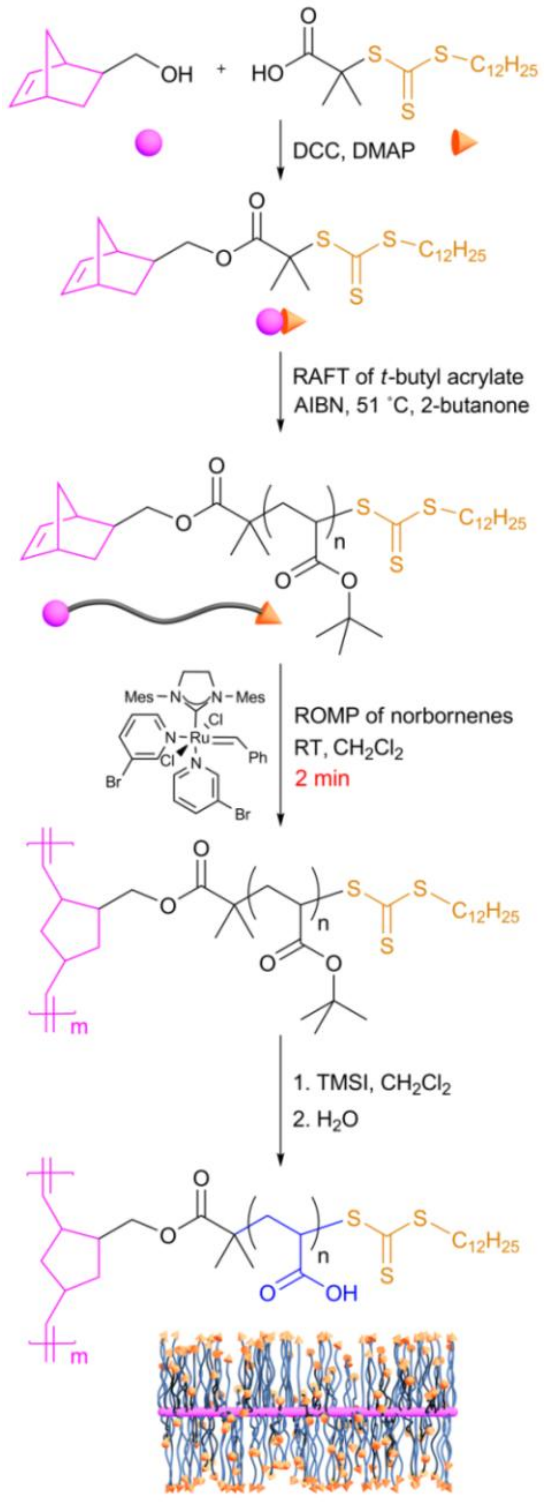

Scheme 2-1. The RAFT-ROMP "grafting through" synthetic route to molecular brushes bearing poly(acrylic acid) side chains.

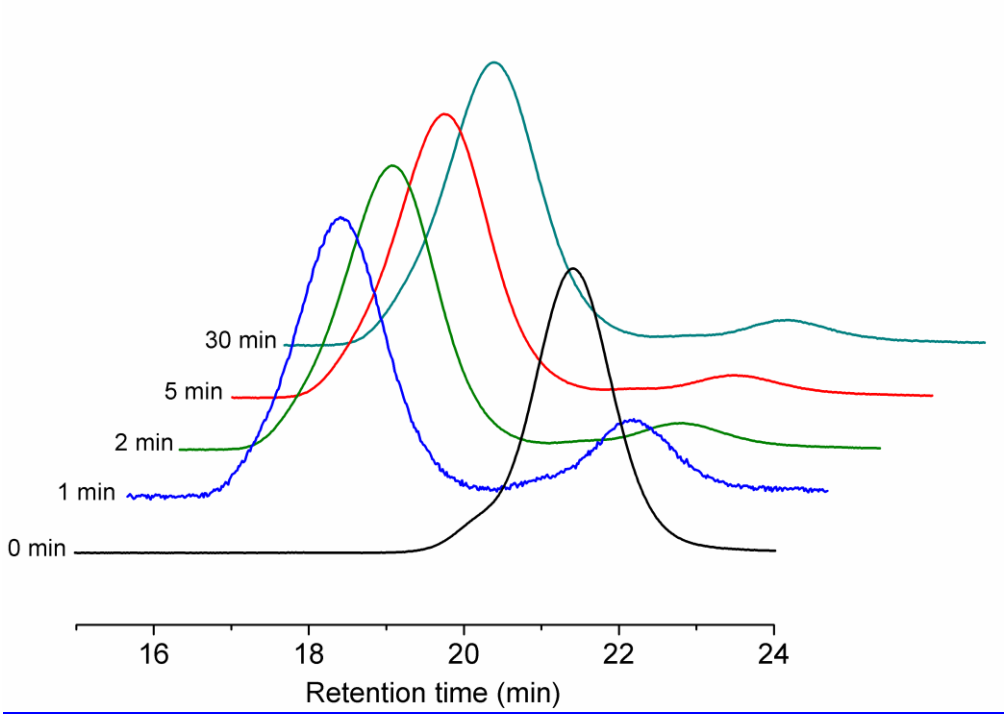

Figure 2-1. GPC curves from the ROMP kinetic study of α-norbornenyl-functionalized P*t*BA.

To afford water-soluble poly(acrylic acid) (PAA) brushes, the *t*-butyl groups were cleaved by reaction with trimethylsilyl iodide (TMSI), followed by hydrolysis of the intermediate silyl esters. Treatment of the P*t*BA molecular brush with TMSI in CH_2Cl_2 at room temperature for 90 min, concentration under reduced pressure, dissolution into THF, decoloration with sodium thiosulfate, dialysis against water, and lyophilization gave the PAA molecular brush structure. The deprotection was confirmed by expected characteristic absorption bands in the IR spectra, and by the loss of *t*-butyl protons (1.50 ppm) in the ^{1}H NMR spectrum and the loss of *t*-butyl carbons (29.0 and 81.1 ppm) in the ^{13}C NMR spectrum, each obtained in DMSO-d_6. For each molecular brush, the resonances corresponding to the protons of the double bonds along the backbone were

not discerned, in any solvent, suggesting that there is limited solvent access to the most internal regions of the molecular brush frameworks and/or limited mobility for the central norbornenyl backbone.

Differential scanning calorimetry (DSC) analysis indicated that there was no observable difference between the thermal transition temperatures for the linear *vs*. brush structure, suggesting that the apparent mobility differences were either not present in the bulk state or were too subtle to be observed by the relatively insensitive DSC technique. Both the P*t*BA macromonomer and the resulting molecular brush showed a T_g at 43 ^oC, which is typical for P*t*BA. Upon removal of the *t*BA protecting groups, the T_g of the PAA molecular brush had increased to 101 °C. Collecting accurate T_g values for PAA is complicated by many factors,(21) including the extent of hydration; the thermal history has a significant impact, therefore, the second heating run was used for determination of the T_g value.

The solution-state sizes of the P*t*BA and PAA molecular brushes were determined by dynamic light scattering (DLS) in THF and water, respectively. The average diameters of the P*t*BA brush were 17 ± 2 nm by number averaging, 19 ± 2 nm by volume averaging and 24 ± 2 nm by intensity averaging. Solvation of the PAA brushes into DMSO and dialysis against nanopure water allowed for measurement of the hydrodynamic diameter, D_h, of the PAA brushes. The aqueous solution after dialysis had a pH of 4. At this pH, the particles showed an apparent diameter of *ca*. 340 nm, which was much larger than that of the P*t*BA brush, indicating intermolecular aggregation in the aqueous solution. Given the fact that the pKa of acrylic acid units is around 4.0-4.5,(22) the pH of the solution was then increased. Initially, titration with NaOH to pH 9 gave a decrease in the

D_h to 36 ± 10 nm (number averaged), falling into a reasonable range of the size of a single PAA brush if hydration is considered, in comparison with the P*t*BA brushes in THF solution. Further increase of pH to 14 showed similar results as those at pH 9. When the solution was titrated back to pH 0 using HCl, aggregates reformed, having an initial number-average diameter of *ca*. 1028 nm, and macroscopic precipitation occurred overnight.

The PAA brushes were also studied by atomic force microscopy (AFM) (**Figure 2-2(A)** and **2-2(B)**). The images from the PAA solution at pH 4 showed collapsed globular structures, whose height was *ca*. 1.5 nm and diameter was *ca*. 32 nm. The size was much smaller than the hydrodynamic size of the aggregates measured by DLS at pH 4, but similar to that of individual PAA brushes at pH 9. Disassembly of aggregates and conformational reorganization within the macromolecular structures may have occurred when the particles were adsorbed onto the mica surface, suggesting that the intermolecular attractive forces were relatively weak and the structures were quite flexible. The images from PAA brushes deposited from a solution at pH 9 showed particles with rod-like morphology, whose height was again *ca*. 1.5 nm but length was about 58 nm, suggesting a more extended conformation at elevated pH. A similar phenomenon was also reported previously.(23) The average norbornenyl unit length (0.18 nm) calculated from the AFM image collected from the pH 9 sample preparation suggested that the backbone was not fully extended (0.5 nm per norbornenyl repeat unit). Similarly, in the work by Fréchet and Grubbs,(24) nanorings from ROMP of sterically-bulky dendritic macromonomers also did not adopt fully extended conformations, rather they had an average backbone unit length of *ca*. 0.25 nm.

Transmission electron microscopy (TEM) was also used to study the size and morphology of the PAA brushes (**Figure 2-2(C)** and **(D)**). The TEM images were quite difficult to obtain and are challenging to interpret. Some particle-particle interactions are

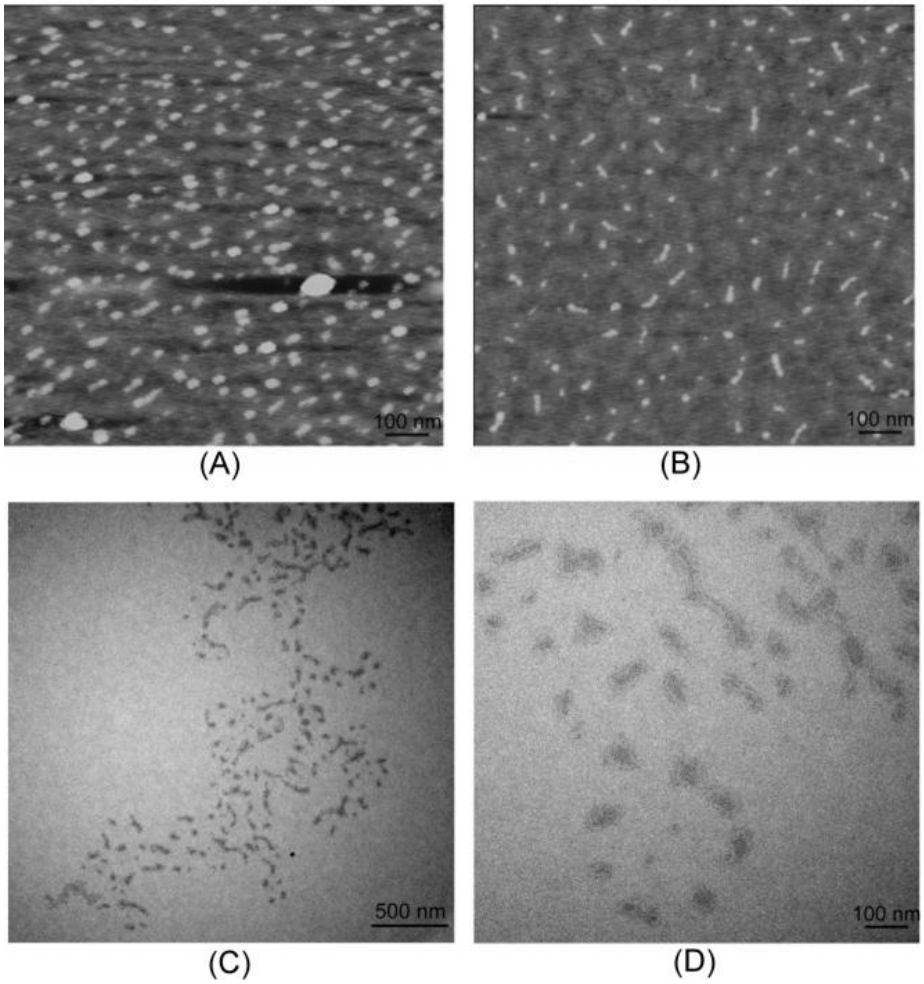

Figure 2-2. Tapping-mode AFM images of PAA brushes on mica after being spin-coated from aqueous solutions (2 μL) at pH 4 (A) and pH 9 (B) onto freshly-cleaved mica and allowed to dry under ambient conditions; TEM images of PAA brushes on a carbon-coated copper grid after being deposited from aqueous solution at pH 4, staining with uranyl acetate solution (1% wt.) (pH = 4), removal of the excess solution and allowing to dry under ambient conditions, collected at different magnifications (C, D).

captured, but individual particles could be selected out and counted to calculate the average particle size, which was *ca.* 68 nm. This value fell into a reasonable range,

compared with the sizes measured by DLS and AFM. As was observed by AFM, most of the molecular brushes deposited at pH 4 were seen as globular structures, although a few elongated images are discernible.

In conclusion, the present study has introduced a methodology for the synthesis of cylindrical molecular brushes with low polydispersity, well defined side chain and chain end structures, and well controlled grafting density. This synthetic strategy is accomplished by combining RAFT and ROMP in a "grafting through" methodology. The practical advantages of this strategy include time efficiency and air insensitivity. Because the ROMP-active norbornenyl group is introduced into the initial RAFT chain transfer agents, the final brush polymer structures retain the trithiocarbonate end groups, so that it would be possible to follow with further "grafting from" chain growth. The brushes bearing carboxylic acid groups also may be used for further chemical modifications, in addition to their observed pH-responsive transformations.

Part II. Other homo-grafted molecular brushes synthesized by the "grafting-through" methodology

The "grafting-through" strategy we developed is versatile and a variety of functional groups can be incorporated into the molecular brush architectures by this method. As we have discussed in the **Introduction** chapter, the ruthenium-based metathesis catalysts are tolerant with various functional groups due to the low oxophilicity of late transition metals. **Figure 2-3** showed a library of homo-grafted molecular brushes that have been synthesized successfully by the "grafting-through" strategy. It includes poly(*t*-butyl

acrylate), poly(methyl acrylate), poly(t-butyl methacrylate), poly(methyl methacylate), polystyrene, poly(4-acetoxystyrene), polypentafluorostyrene, polylactide and polyhedral oligomeric silsesquioxane. Using the modified 2nd generation catalyst as the initiator, ROMP of macromonomers with norbornenyl terminus can afford the resulting molecular brush structure in minutes, just like what we did with poly(t-butyl acrylate) in Part I. Based on the nature of the monomers, the respective macromonomers can be prepared from a wide range of small monomers or precursory polymers by appropriate methods, including RAFT polymerization, ATRP, ROP and chain end modification. The detailed synthesis of the macromonomers and molecular brushes can be found in the following chapters.

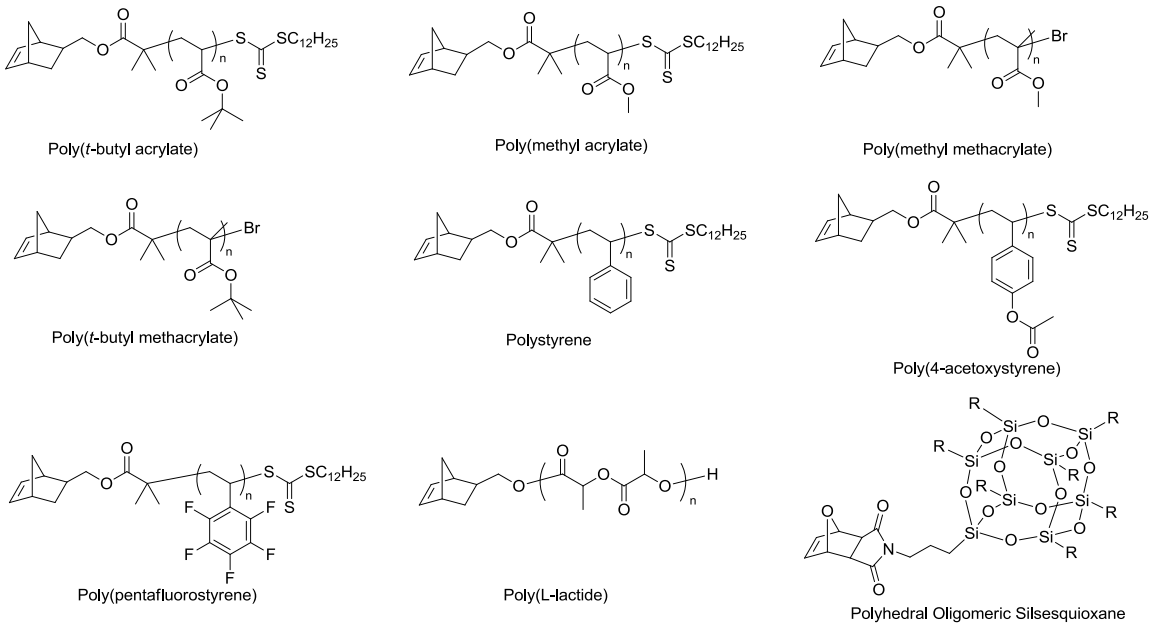

Figure 2-3. A library of macromonomers that have been tested by the "grafting-through" strategy.

EXPERIMENTAL

Measurements.

Infrared spectra were obtained on a Perkin-Elmer Spectrum BX FT-IR system using diffuse reflectance sampling accessories. ^{1}H-NMR spectra were recorded at 300 MHz on solutions in $CDCl_3$, DMSO-d_6, or CD_2Cl_2 on a Varian Mercury 300 spectrometer with the solvent proton signal as standard. ^{13}C-NMR spectra were recorded at 75.4 MHz on solutions in $CDCl_3$, DMSO-d_6, or CD_2Cl_2 on a Varian Mercury 300 spectrometer with the solvent carbon signal as standard.

Gel permeation chromatography (GPC) was conducted on a Waters 1515 HPLC (Waters Chromatography, Inc.) equipped with a Waters 2414 differential refractometer and a three-column series PL gel 5μm Mixed C, 500 Å, and 10^4 Å, 300 × 7.5 mm columns (Polymer Laboratories Inc.). The system was equilibrated at 35 °C in anhydrous THF, which served as the polymer solvent and eluent with a flow rate of 1.0 mL/min. Polymer solutions were prepared at a known concentration (*ca.* 3 mg/mL) and an injection volume of 200 μL was used. Data collection and analysis were performed, respectively, with Precision Acquire software and Discovery 32 software (Precision Detectors, Inc.). The system was calibrated by a nearly monodispersed polystyrene standard (Pressure Chemical Co., M_p = 90 kDa, M_w/M_n < 1.04). The differential refractometer was calibrated with standard polystyrene reference material (SRM 706 NIST), of known specific refractive index increment dn/dc (0.184 mL/g).

DLS analysis was performed using a Brookhaven Instruments Co. (Holtsville,NY) system consisting of a model BI-200SM goniometer, a model EMI-9865 photomultiplier, and a model BI-9000AT digital correlator. Incident light was provided by a model 95-2 Ar^+ laser (Lexel Corp., Palo Alto, CA) operated at 514.5 nm. All measurements were made at 20 ± 1 °C in solvents. Prior to analysis, solutions were filtered through 0.2 μm poly(ether sulfone) membrane syringe filters (Gelman Laboratory, Pall Corporation, Ann Arbor, MI) to remove dust particles. Scattered light was collected at 90° angle. The digital correlator was operated with 522 channels, a dual sampling time of 100 ns, a 5s ratio channel spacing, and a duration time of 6 min. A photomultiplier aperture of 400 μm was used, and the incident laser intensity was adjusted to obtain a photon counting rate between 200 to 300 kcps. Only measurements in which the measured and calculated baselines of the intensity autocorrelation function agreed to with 0.1% were used to calculate the particle size. The calculation of the particle size distribution and distribution averages was performed with the ISDA software package (Brookhaven Instruments Co., Holstville, NY), which employed double exponential fitting, cumulants analysis, NNLS, and CONTIN particle size distribution analysis routines.

Samples for AFM imaging were prepared by spin-casting *ca.* 2.0 μL of the sample solution onto freshly cleaved mica plates (Ruby clear mica, New York Mica Co.). AFM instrumentation was a Nanoscope IIIa system (Digital Instruments, Santa Barbara, CA), equipped with a J-type vertical engage piezoelectric scanner and operated in a tapping mode in air. Tapping-mode imaging was carried out with high resolution probes (DP14/HI'RES/Al BS, from μmash: L, 125 μm; normal spring constant, 5.0 N/m;

resonance frequency, 160 kHz). The average height and average diameter values were determined by section analysis, using the Nanoscope III software package.

Glass transition temperature (T_g) determinations were performed by using differential scanning calorimetry (DSC) on a DSC822$_e$ instrument (Mettler-Toledo, Inc.) in a temperature range of −50-200 °C with a heating rate of 10 °C/min under nitrogen. The data were acquired and analyzed with STAR$_e$ software (Mettler-Toledo, Inc.). The T_g values were taken at the midpoint of the inflection tangent, upon the third heating scans.

Materials.

Unless otherwise noted, all solvents and reagents were purchased from Aldrich Chemical Co. (St. Louis, MO) and used as received. *tert*-Butyl acrylate (*t*BA, 98%) and dichloromethane (CH_2Cl_2, 99+%) were distilled over CaH_2 before use. The norbornenyl-functionalized alcohol (17) ,S-1-dodecyl-S'-(R,R'-dimethyl-R"-acetic acid)trithiocarbonate (25) and Grubbs' 3rd generation catalyst(20) were prepared following literature methods.

Synthesis of ROMP-active RAFT chain transfer agent, with norbornenyl (NB) and trithiocarbonate (TTC) units (NB-TTC)

Into a 500 mL RB flask with a stir bar were placed *exo*-5-norbornene-2-methanol (2.52 g, 20.7 mmol), S-1-dodecyl-S'-(R,R'-dimethyl-R"-acetic acid)trithiocarbonate (8.93 g, 24.5 mmol), *N*,*N*'-dicyclohexylcarbodiimide (5.31 g, 25.7 mmol), and 4-(dimethylamino)pyridine (0.98 g, 8.1 mmol). Dry CH_2Cl_2 (220 mL) was then injected into the flask to dissolve all the reagents. The reaction was allowed to stir at room temperature for 60 h, at which time, TLC showed complete conversion of the alcohol. After filtration through fluted filter paper, concentration *in vacuo* and flash chromatography eluting with 10% ethyl acetate-hexane the product NB-TTC was afforded as an orange-colored oil. Yield: 89%. IR: 3059, 2925, 2853, 1735, 1569, 1465, 1378, 1361, 1324, 1253, 1154, 1126, 1066, 998, 971, 904, 816, 750, 706 cm^{-1}; ^1H NMR (300 MHz, $CDCl_3$, ppm) δ 6.05 (br s, 2H, norbornenyl alkenyl protons), 4.17 (dd, J = 7 and 11 Hz, 1H, C***H*****$_2$**OC(O)), 3.92 (dd, J = 10 and 10 Hz, 1H, C***H*****$_2$**OC(O)), 3.25 (t, J = 7 Hz, 2H, C***H*****$_2$**SC(S)S), 2.80 (s, 1H, allylic proton of norbornenyl group), 2.65 (s, 1H, allylic proton of norbornenyl group), 1.50-1.80 (br m, 10H, C(O)C(C***H*****$_3$)$_2$S, one bridge proton of norbornenyl group, C***H***$CH_2OC(O)$ and SCH_2C***H*****$_2C_{10}H_{23}$) 1.00-1.50 (br m, 21H, aliphatic protons), 0.85 (ill-defined t, 3H, $C(S)SCH_2C_{10}H_{20}C$***H*****$_3$**); ^{13}C NMR (125 MHz, $CDCl_3$, ppm) 14.37, 22.93, 25.63, 25.68, 28.16, 29.15, 29.34, 29.58, 29.66, 29.68, 29.80, 29.86, 32.15, 37.07, 37.93, 41.85, 43.91, 45.17, 56.22, 70.30, 136.55, 137.08, 173.24, 221.65.

RAFT-based synthesis of α-norbornenyl poly(*t*-butyl acrylate) macromonomer

To a 50 mL Schlenk flask with a stir bar, NB-TTC (0.1031 g, 0.2203 mmol) and *t*-butyl acrylate (10.0 mL, 68.3 mmol) were added, followed by the addition of AIBN (as a freshly-prepared stock solution in 2-butanone, 0.20 mg/mL, 10 mL, 5 mol%). After 4 cycles of freeze-pump-thaw, the polymerization was conducted in a 51 ^{o}C oil bath. At every hour, an aliquot was withdrawn and analyzed by ^{1}H-NMR spectroscopy to determine the extent of monomer conversion. At 3 h, the reaction was quenched by freezing the reaction mixture in a liquid nitrogen bath. The reaction mixture was then precipitated in 20% H_2O-methanol 3 times and the polymer (NB-P*t*BA macromonomer) was collected. Yield: 1.23 g, 45%. M_n^{NMR} = 17.3 kDa, M_n^{GPC} = 16.9 kDa, M_w/M_n = 1.16; T_g = 43 ^{o}C; IR: 2977, 2932, 1727, 1479, 1448, 1392, 1367, 1338, 1257, 1148, 1035, 908, 845, 751, 705, 637, 471, 428 cm^{-1}; ^{1}H NMR (300 MHz, $CDCl_3$, ppm) δ 6.05-6.10 (norbornenyl alkene), 4.60-4.72 (C***H***SC(S)S), 3.80-4.20 (C***H*****$_2$**OC(O)), 3.30-3.40 (C***H*****$_2$**SC(S)S), 2.60-2.90 (allylic protons of norbornenyl groups), 2.05-2.40 (polymer backbone protons) 1.00-1.95 (*t*-butyl protons and C(S)SCH_2C_{10}***H*****$_{20}$**CH_3), 0.80-0.90 (C(S)S$CH_2C_{10}H_{20}$C***H*****$_3$**); ^{13}C NMR (75 MHz, $CDCl_3$, ppm) 28.0-28.2, 35.7-37.3, 41.5-43.5, 80.2, 174.3.

ROMP-based synthesis of molecular brushes bearing poly(*t*-butyl acrylate) side chains

To a solution of Grubbs' catalyst in CH_2Cl_2 (8.4×10^{-3} mg/mL, 100 μL, 1 equiv.) under argon in a scintillation vial capped with a septum was added the NB-P*t*BA

macromonomer (102.3 mg, 320 equiv.) in CH_2Cl_2 (1.0 mL) *via* syringe. The reaction was allowed to stir at room temperature for 4 h, and was then quenched by addition of ethyl vinyl ether (a few drops) *via* syringe. The final P*t*BA brush product was obtained after precipitating the reaction mixture in 20% H_2O-methanol. It was later found that the reaction could be performed under air. T_g=43 ^oC; IR: 2977, 2931, 1728, 1479, 1448, 1392, 1367, 1256, 1148, 1035, 845, 751, 632, 471 cm^{-1}; ^1H NMR (300 MHz, CD_2Cl_2, ppm) δ 4.60-4.72 (C***H***SC(S)S), 3.80-4.20 (C***H*****$_2$**OC(O)), 3.30-3.40 (C***H*****$_2$**SC(S)S), 2.05-2.40 (grafted chain backbone protons) 0.70-1.95 (*t*-butyl protons and C(S)SCH_2C_{11}***H*****$_{23}$**); ^{13}C NMR (75 MHz, CD_2Cl_2, ppm) 28.0-28.2, 35.7-38.3, 41.0-43.7, 80.2, 175.9.

Conversion of *t*-butyl groups to acrylic acid groups

P*t*BA brush (23.6 mg) was loaded into a vial and dissolved in CH_2Cl_2 (5.0 mL). A solution of trimethylsilyl iodide (400 μL, diluted by 1.0 mL CH_2Cl_2) was added. After 90 min, the excess solvent and reagent were removed *in vacuo*. The residue was then redissolved in THF and decolorized by addition of $Na_2S_2O_3$ to afford a colorless solution. Dialysis of the solution against nanopure water for 5 days cleaved the silyl ester bonds and gave the final PAA brush product, which was collected after removal of water by lyophilization. T_g= 101 ^oC; at pH 4, H_{av}^{AFM} = 1.5 nm; L_{av}^{AFM} = 32 nm; at pH 9, H_{av}^{AFM} = 1.5 nm; L_{av}^{AFM} = 58 nm; D_{av}^{TEM} = 68 nm; IR: 2917, 2849, 1718, 1560, 1542, 1458, 1259, 1195, 1131, 1076, 800 cm^{-1}; ^1H NMR (300 MHz, DMSO-d_6, ppm) δ 14.10-15.70 (COO***H***), 4.60-4.72 (C***H***SC(S)S), 3.80-4.20 (C***H*****$_2$**OC(O)), 3.30-3.40 (C***H*****$_2$**SC(S)S), 2.05-

2.40 (polymer backbone protons), 0.70-1.95 (polymer backbone protons and C(S)SCH$_2$C$_{11}$***H$_{23}$***); ^{13}C NMR (75 MHz, DMSO-*d$_6$*, ppm) 35.0-39.0, 41.3-43.5, 176.2.

RAFT-based synthesis of α-norbornenyl poly(methyl acrylate) macromonomer

To a 25 mL Schlenk flask with a stir bar, NB-TTC (0.3750 g, 0.801 mmol) and methyl acrylate (5.0 mL, 55 mmol) were added, followed by the addition of AIBN (as a freshly-prepared stock solution in 2-butanone, 1.3 mg/mL, 5.0 mL, 0.040 mmol). After 4 cycles of freeze-pump-thaw, the polymerization was conducted in a 51 ^{o}C oil bath. At every hour, an aliquot was withdrawn and analyzed by ^{1}H-NMR spectroscopy to determine the extent of monomer conversion. At 7 h, the reaction was quenched by freezing the reaction mixture in a liquid nitrogen bath. The reaction mixture was then precipitated in pentane 3 times and the polymer (NB-PMA macromonomer) was collected. Yield: 1.2 g, (85% based on the conversion of MA). M_n^{NMR} = 2618 Da, M_n^{GPC} = 2420 Da, M_w/M_n = 1.11; T_g = 5 ^{o}C.

RAFT-based synthesis of α-norbornenyl polystyrene macromonomer, NB-PS, 2. To a 10 mL Schlenk flask with a stir bar, NB-CTA (0.2070 g, 0.442 mmol), followed by the addition of AIBN (as a freshly-prepared stock solution in styrene, 2.5 mg/mL, 5.0 mL, 6 mol%). After 4 cycles of freeze-pump-thaw, the polymerization was conducted in an oil bath at 50 ^{o}C. After 18 hours, the reaction was quenched by freezing the reaction mixture in a liquid nitrogen bath. The reaction mixture was then precipitated in methanol 3 times and the polymer (NB-PS macromonomer) was collected. Yield: 1.6 g. M_n^{NMR} = 4630 Da, M_n^{GPC} = 4560 Da, M_w/M_n = 1.08; T_g: 93 ^{o}C; IR: 3082, 3059, 3025, 3001, 2924, 2851,

1943, 1869 1802, 1725, 1601, 1583, 1541, 1493, 1452, 1371, 1266, 1181, 1154, 1110, 1068, 1028, 906, 757, 698, 667 cm^{-1}; ^1H NMR (300 MHz, CD_2Cl_2, ppm) δ 6.36-7.50 (styrenyl protons), 6.00-6.10 (norbornenyl alkene), 4.60-4.90 (C***H***SC(S)S), 3.50-3.80 (C***H₂***OC(O)), 3.30-3.40 (C***H₂***SC(S)S), 2.60-2.90 (allylic protons of norbornenyl groups), 1.12-2.40 (backbone protons and $C(S)SCH_2C_{10}$***H₂₀***CH_3), 0.80-0.90 (backbone protons and $C(S)SCH_2C_{10}H_{20}C$***H₃***); ^{13}C NMR (75 MHz, CD_2Cl_2, ppm) δ 145, 128, 126, 42.5-46.0, 40.0-41.8. Elemental analysis. Anal. Calcd for $C_{344}H_{362}O_2S_3$, C, 89.4; H, 7.8; O, 0.7; S, 2.1. Found, C, 89.4; H, 7.8; O, 0.7; S, 2.0.

ATRP-based synthesis of α-norbornenyl poly(methyl methacrylate) macromonomer

NB-ATRP (0.5463 g, 2.000 mmol), methyl methacrylate (20.0 mL, 194 mmol), CuCl (0.200g, 2 mmol) and 20 mL anisole were added to a 100 mL flask. After freezing the solution by liquid nitrogen, $CuCl_2$ (13.6 mg, 0.1 mmol) and TMEDA (0.65 mL, 4.3 mmol) were added. Five cycles of freeze-pump-thaw were performed to remove oxygen and the polymerization was conducted in a 60 ^oC oil bath. An aliquot was withdrawn during the polymerization and analyzed by ^1H-NMR spectroscopy to determine the extent of monomer conversion. At 14 h, the reaction was quenched by freezing the reaction mixture in a liquid nitrogen bath when the monomer conversion was 20%. The reaction mixture was then precipitated in pentane 3 times and the polymer (NB-PMMA macromonomer) was collected. Yield: 3.1 g (79% based on the conversion of the monomer). M_n^{NMR} = 3950 Da, M_n^{GPC} = 3420 Da, M_w/M_n = 1.24.

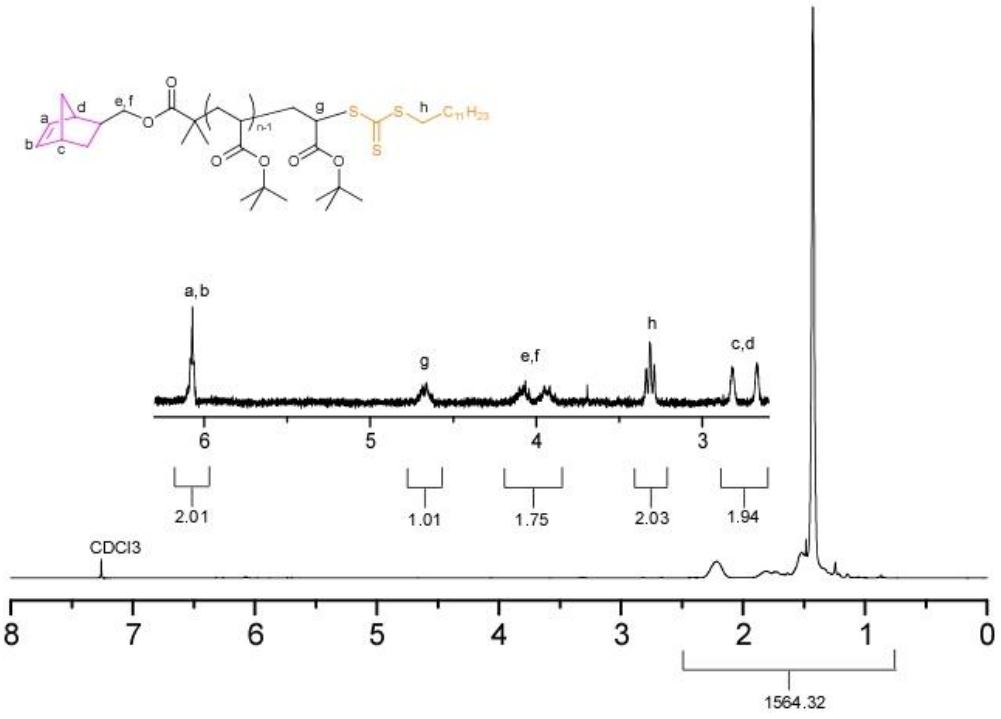

Figure 2-4. ^{1}H-NMR spectrum of P*t*BA macromonomer.

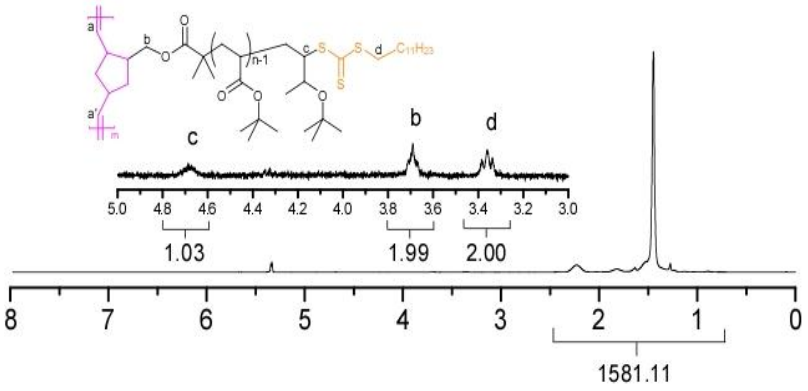

Figure 2-5. ^{1}H-NMR spectrum of P*t*BA molecular brush.

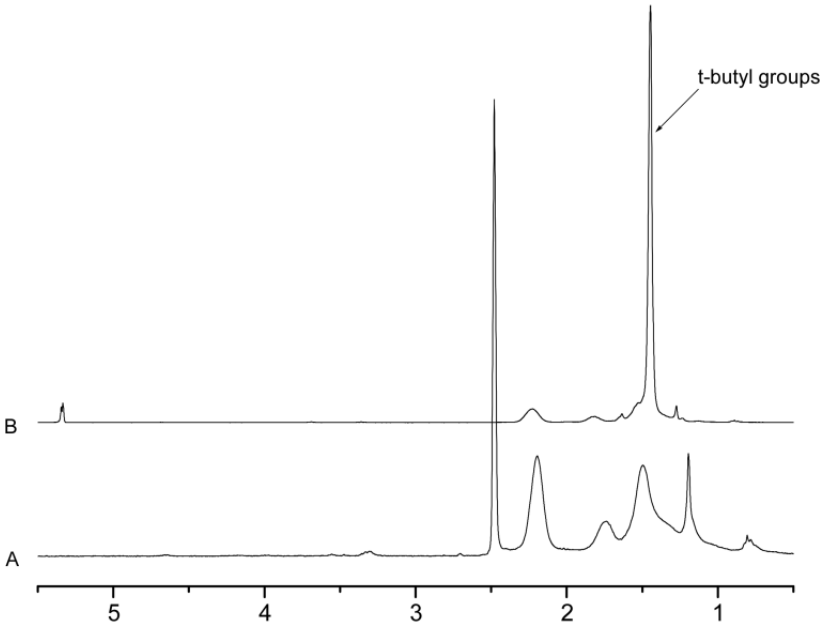

Figure 2-6. ^{1}H-NMR spectrum of molecular brushes before (B) and after (A) hydrolysis.

References

(1) L. Gu, C. Feng, D. Yang, Y. Li, J. Hu, G. Lu and X. Huang "PPEGMEA-b-PDEAEMA: Double hydrophilic double-grafted copolymer stimuli-responsive to both pH and salinity." **2009**, *47*, 3142-3153.

(2) J. K. Oh, F. Perineau, B. Charleux and K. Matyjaszewski "AGET ATRP in water and inverse minemulsion: A facile route for prepration of high-molecular-weight biocompatible brush-like polymers." **2009**, *47*, 1771-1781.

(3) J. T. Wiltshire and G. G. Qiao "Degradable Star Polymers with High "Click" Functionality." **2009**, *47*, 1485-1498.

(4) S. S. Sheiko, B. S. Sumerlin and K. Matyjaszewski "Cylindrical molecular brushes: Synthesis, characterization, and properties." *Prog. Polym. Sci.* **2008**, *33*, 759-785.

(5) M. F. Zhang and A. H. E. Müller "Cylindrical polymer brushes." *J. Polym. Sci. Pol. Chem.* **2005**, *43*, 3461-3481.

(6) H. F. Gao and K. Matyjaszewski "Synthesis of molecular brushes by "grafting onto" method: Combination of ATRP and click reactions." *J. Am. Chem. Soc.* **2007**, *129*, 6633-6639.

(7) M. Schappacher and A. Deffieux "Synthesis of macrocyclic copolymer brushes and their self-assembly into supramolecular tubes." *Science* **2008**, *319*, 1512-1515.

(8) H. G. Börner, K. Beers, K. Matyjaszewski, S. S. Sheiko and M. Moller "Synthesis of molecular brushes with block copolymer side chains using atom transfer radical polymerization." *Macromolecules* **2001**, *34*, 4375-4383.

(9) C. Cheng, E. Khoshdel and K. L. Wooley "One-pot tandem synthesis of a core - Shell brush copolymer from small molecule reactants by ring-opening metathesis and reversible addition-fragmentation chain transfer (co)polymerizations." *Macromolecules* **2007**, *40*, 2289-2292.

(10) M. F. Zhang, T. Breiner, H. Mori and A. H. E. Müller "Amphiphilic cylindrical brushes with poly(acrylic acid) core and poly(n-butyl acrylate) shell and narrow length distribution." *Polymer* **2003**, *44*, 1449-1458.

(11) H. R. Allcock, C. R. de Denus, R. Prange and W. R. Laredo "Synthesis of norbornenyl telechelic polyphosphazenes and ring-opening metathesis polymerization reactions." *Macromolecules* **2001**, *34*, 2757-2765.

(12) S. Breunig, V. Heroguez, Y. Gnanou and M. Fontanille "Ring-opening metathesis polymerization of omega-norbornenyl polystyrene macromonomers and characterization of the corresponding structures." **1995**151-166.

(13) V. Heroguez, S. Breunig, Y. Gnanou and M. Fontanille "Synthesis of alpha-norbornenylpoly(ethylene oxide) macromonomers and their ring-opening metathesis polymerization." *Macromolecules* **1996**, *29*, 4459-4464.

(14) S. Jha, S. Dutta and N. B. Bowden "Synthesis of ultralarge molecular weight bottlebrush polymers using Grubbs' catalysts." *Macromolecules* **2004**, *37*, 4365-4374.

(15) D. Mecerreyes, D. Dahan, P. Lecomte, P. Dubois, A. Demonceau, A. F. Noels and R. Jérôme "Ring-opening metathesis polymerization of new alpha-norbornenyl poly(epsilon-caprolactone) macromonomers." *J. Polym. Sci. Pol. Chem.* **1999**, *37*, 2447-2455.

(16) C. Cheng, E. Khoshdel and K. L. Wooley "Facile one-pot synthesis of brush polymers through tandem catalysis using Grubbs' catalyst for both ring-opening metathesis and atom transfer radical polymerizations." *Nano Lett.* **2006**, *6*, 1741-1746.

(17) C. Cheng, K. Qi, E. Khoshdel and K. L. Wooley "Tandem synthesis of core-shell brush copolymers and their transformation to peripherally cross-linked and hollowed nanostructures." *J. Am. Chem. Soc.* **2006**, *128*, 6808-6809.

(18) Y. Xia, J. A. Kornfield and R. H. Grubbs "Efficient Synthesis of Narrowly Dispersed Brush Polymers via Living Ring-Opening Metathesis Polymerization of Macromonomers." **2009**, *ASAP*,

(19) G. Moad, E. Rizzardo and S. H. Thang "Living radical polymerization by the RAFT process." *Aust. J. Chem.* **2005**, *58*, 379-410.

(20) T. L. Choi and R. H. Grubbs "Controlled living ring-opening-metathesis polymerization by a fast-initiating ruthenium catalyst." *Angew. Chem.-Int. Edit.* **2003**, *42*, 1743-1746.

(21) J. J. Maurer, D. J. Eustace and C. T. Ratcliffe "Thermal Characterization of Poly(acrylic acid)." **1987**, *20*, 196-202.

(22) Pradip, C. Maltesh, P. Somasundaran, R. A. Kulkarni and S. Gundiah "Polymer-polymer complexation in dilute aqueous-solutions - poly(acrylic acid)-poly(ethylene oxide) and poly(acrylic acid)-poly(vinylpyrrolidone)." *Langmuir* **1991**, *7*, 2108-2111.

(23) H. I. Lee, J. R. Boyce, A. Nese, S. S. Sheiko and K. Matyjaszewski "pH-induced conformational changes of loosely grafted molecular brushes containing poly(acrylic acid) side chains." *Polymer* **2008**, *49*, 5490-5496.

(24) A. J. Boydston, T. W. Holcombe, D. A. Unruh, J. M. J. Fréchet and R. H. Grubbs "A Direct Route to Cyclic Organic Nanostructures via Ring-Expansion Metathesis Polymerization of a Dendronized Macromonomer." **2009**, *131*, 5388-5389.

(25) J. T. Lai, D. Filla and R. Shea "Functional polymers from novel carboxyl-terminated trithiocarbonates as highly efficient RAFT agents." *Macromolecules* **2002**, *35*, 6754-6756.

Chapter 3

Hetero-grafted diblock molecular brushes

[Portions of this work have been published previously as Zhou Li, Jun Ma, Chong Cheng, Ke Zhang, and Karen L. Wooley, *Macromolecules*, **2010**, *43*(3), 1182-1184.]

Synthesis of hetero-grafted amphiphilic diblock molecular brushes and their self assembly in aqueous medium

ABSTRACT

A facile and efficient "grafting through" strategy was developed to synthesize hetero-grafted diblock molecular brushes with precisely controlled structure, by utilizing the orthogonality and livingness of ROMP and RAFT polymerizations. These diblock molecular brushes were chemically transformed to amphiphilic nanostructures, whose aqueous solution self-assembly were studied. Characterizations of both preliminary and secondary nanostructures revealed that ca. 60-80 unimers were assembled to a more complicated nanostructure.

INTRODUCTION

Self assembly of synthetic macromolecules, inspired by the organization of biomolecules in nature, is a powerful approach for fabricating novel nanostructures, whose potential applications in nanomedicine are of significant interest.[1, 2] Using amphiphilic linear copolymers as building blocks, various supramolecular architectures have been constructed, whose compositions, sizes and morphologies are all tunable.[3-5] In spite of that, those nanostructures, made from synthetic macromolecules, are still primitive, compared with those from biomolecules, which exhibit high complexity developed by evolution for millions of years. Our interest to attain nanostructures with higher complexities, approaching those of biological systems, drives our design of more types and sizes of macromolecular and nanoscopic building blocks, extending beyond simple linear block copolymers.

RESULTS AND DISCUSSION

Our initial targets are hetero-grafted diblock molecular brushes,[6, 7] in which two different types of polymeric side chains are grafted sequentially along a backbone. These structures are designed as nanoscopic molecular frameworks having defined three-dimensional shape and control over the entire compositional profile, to mimic some features of the globular shape and compositional heterogeneities of protein building blocks. Hetero-grafted diblock molecular brushes may be synthesized by "grafting from" and "grafting onto" strategies.[8-11] Although effective, these two strategies suffer from significant steric effects, leading to side reactions and less control over the structures.(6)

The "grafting through" strategy,(12-15) in which pre-synthesized side chains with polymerizable chain ends are polymerized to afford the final brush structure, can eliminate these side reactions and thus provide better structure control. To polymerize the highly-diluted chain end groups of the side chains, ring opening metathesis polymerization (ROMP) is often applied.(12, 15) Herein, by exploiting the orthogonality and livingness of reversible addition-fragmentation chain transfer (RAFT) polymerization[16] and ROMP,[17-19] we have developed a facile and efficient "grafting through" strategy to synthesize hetero-grafted diblock molecular brushes with precisely-controlled architecture. These structures were transformed into amphiphilic diblock molecular brushes, which were then investigated as nanoscopic building blocks for the assembly of supramolecular nanostructures in aqueous medium.

The amphiphilic hetero-grafted diblock molecular brush was produced by a highly efficient, one-pot "grafting-through" process, involving the sequential ROMP of norbornenyl-terminated macromonomers, followed by a deprotection reaction (**Scheme 3-1**). α-Norbornenyl poly(*t*-butyl acrylate) (NB-P*t*BA) (**1**) and α-norbornenyl polystyrene (NB-PS) (**2**) macromonomers were first synthesized by selective RAFT polymerizations of *t*-butyl acrylate and styrene, respectively, from a norbornenyl-functionalized chain transfer agent (NB-CTA).[12] In order to suppress reaction of the NB group, reduce bi-radical coupling and control the RAFT polymerizations, moderate temperature (50 ºC) and low feed amount of the radical initiator, 2,2-azobisisobutyronitrile (AIBN) ($[NB\text{-}CTA]_0/[AIBN]_0 = 20 : 1$) were employed. The well-defined structures of **1** and **2** were verified by ^1H NMR spectroscopy and gel permeation chromatography (GPC). Little to no side reaction of the NB group during the RAFT

polymerizations was confirmed by ^{1}H NMR spectroscopy, based on the integral ratio of the NB alkenyl protons (6.02-6.10 ppm) to the RAFT agent chain end C***H*****$_2$**SC(S)S methylene protons (3.33-3.53 ppm) being *ca.* 1 : 1. As analyzed by GPC, both **1** and **2** had mono-modal molecular weight distributions with polydispersities (PDIs) less than 1.12. The number-averaged molecular weights (Mn) calculated from ^{1}H NMR spectroscopy (Mn^{NMR}) agreed well with those from GPC (Mn^{GPC}) (**1**, Mn^{NMR} = 4950 Da, Mn^{GPC} = 4670 Da; **2**, Mn^{NMR} = 4630 Da, Mn^{GPC} = 4560 Da), further supporting the controlled nature of the selective RAFT polymerizations.

These α-norbornenyl-functionalized macromonomers, NB-P*t*BA (**1**) and NB-PS (**2**), were readily used to synthesize hetero- grafted diblock molecular brushes (**3**) by sequential ROMP. We and Grubbs' group[12, 15] have reported that the modified 2nd generation Grubbs' catalyst[20] is highly efficient for the synthesis of i homo-grafted molecular brushes by ROMP using the "grafting through" strategy. In this study, we further explored the utilization of this Grubbs' catalyst in the sequential ROMP to synthesize hetero-grafted molecular brushes. As shown in **Scheme 3-1**, brush copolymer PNB-*g*-P*t*BA was synthesized by ROMP of **1** in CH_2Cl_2. Without purification, a solution of **2** was added into the living PNB-*g*-P*t*BA polymerization mixture to afford the diblock brush copolymer P(NB-*g*-P*t*BA)-*b*-P(NB-*g*-PS), 3, with regio-selective grafts. During ROMP, small aliquots were withdrawn and measured by GPC. As shown in **Scheme 3-1**, nearly quantitative conversions of NB-P*t*BA and NB-PS were observed, with little residual macromonomer at each stage of the ROMP process. The well-defined structures

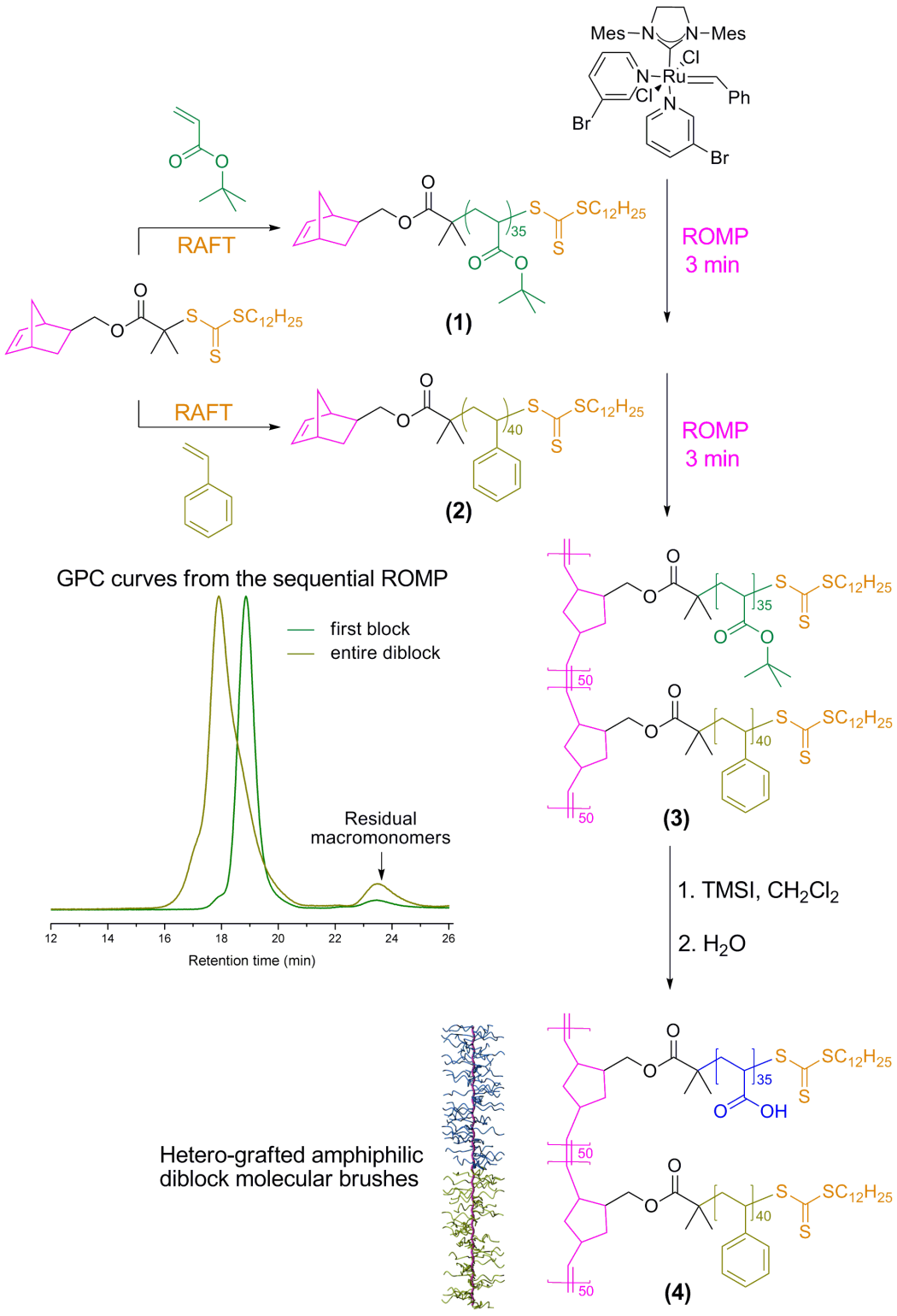

Scheme 3-1. The 'grafting through' synthetic route to hetero-grafted amphiphilic diblock molecular brushes by combined RAFT, ROMP, and chemical transformation.

of both PNB-*g*-P*t*BA and P(NB-*g*-P*t*BA)-*b*-P(NB-*g*-PS) were supported by GPC, with mono-modal molecular weight distributions and narrow PDIs (<1.20). The successful incorporation of **2** to produce an overall diblock backbone structure is reflected by evolution of the GPC curve after the second ROMP reaction. Synthesis of the diblock molecular brushes was accomplished in 6 min (3 min for growth of each block), indicating the fast and efficient ROMP reactions.(21) The amphiphilic diblock molecular brush P(NB-*g*-PAA)-*b*-P(NB-*g*-PS) (**4**) was obtained after deprotection of **3** with trimethylsilyl iodide (TMSI) and hydrolysis of the intermediate TMS-esters.

Supramolecular assembly of the nanoscopic, amphiphilic block graft copolymers was investigated by using phase-segregation micellization methods that are traditional for linear block copolymers.[22] Dissolution of **4** in a common solvent for the entire

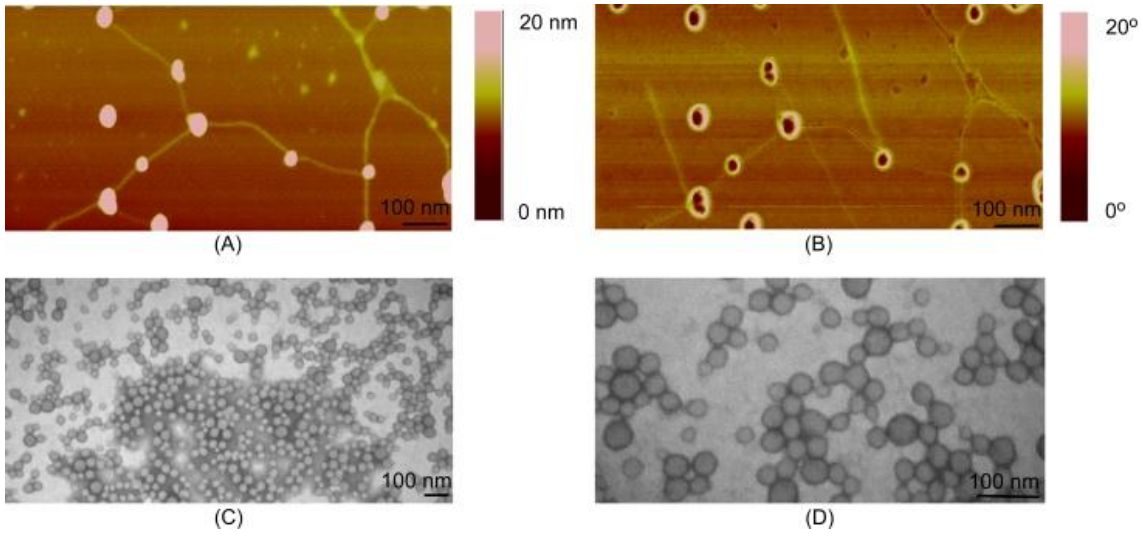

Figure 3-1. Images of the supramolecular micelles. (A) Tapping-mode AFM height image; (B) Tapping-mode AFM phase image; (C) TEM image (80k×); (D) TEM image (200k×).

framework, *N,N*-dimethylformamide (DMF), was followed by dialysis against nanopure water to afford the aqueous micelle solution **5**. The assemblies were characterized by dynamic light scattering (DLS), atomic force microscopy (AFM) and transmission electron microscopy (TEM).

The data from DLS, TEM and AFM were compared and contrasted to evaluate the nature of the supramolecular structures **5**, from the aqueous assembly of **4**. The number-averaged hydrodynamic diameter ($D_{h,n}$) of 5 was 48 ± 5 nm, according to DLS, which, when compared with the size of the unimers 4 in DMF ($D_{h,n}$ = 11 ± 2 nm), suggested aggregation of *ca.* 80 units of **4** to form supramolecular structures in water. Similarly-sized aggregates of globular shape were observed by both TEM and tapping-mode AFM. The TEM diameter of **5** was measured as 43 ± 7 nm; the unimers **4** were not observed well. By AFM, however, two populations were observed from spin coating of an aqueous solution of **5** onto mica: an aggregate having an average diameter (D_{afm}) of 73 ± 8 nm (not corrected for tip effects) and average height of 28 ± 8 nm, together with what appeared to be unimers having an average diameter of 47 ± 5 nm and average height of 1.9 ± 0.4 nm. The average diameter and height of unimers, obtained by spin coating a DMF solution of **4** onto mica, were 53 ± 5 nm and 1.6 ± 0.3 nm (**Figure 3-1**), respectively. Taking into account the diameter as measured by TEM and the height as measured by AFM, the supramolecular assemblies underwent only low degrees of shape deformation upon adsorption onto the solid substrates. If it is assumed that the AFM tip diameter is the difference between the TEM- and AFM-measured diameters, *ca.* 30 nm, then the diameter of the unimers was *ca.* 20 nm, giving an aggregation number of *ca.* 60 of **4** within the assembled structures **5**. This aggregation number is in agreement with

that estimated from the DLS data, and is smaller than that of micelles typically from linear amphiphilic copolymers (usually a few hundred[22]). It should be noted that both AFM and TEM showed that **5** had a broad size distribution, which may be explained by the large size of the building blocks relative to the assembled structure.

In summary, we have demonstrated the synthesis of hetero-grafted diblock molecular brushes *via* a "grafting through" strategy, based on the orthogonality of ROMP and RAFT polymerizations. These diblock molecular brushes were converted to amphiphilic nanostructures, whose aqueous solution self-assembly behaviors were studied. Further work ongoing in our group and the laboratory of Robert H. Grubbs (we acknowledge clever designs of block brush copolymers under study by Grubbs' group(23)) is expected to lead to advanced macromolecular-based building blocks that are capable of hierarchical supramolecular assembly into complex, functional nano- and microscopic objects.

EXPERIMENTAL

Characterizations.

Infrared spectra were obtained on a Perkin-Elmer Spectrum BX FT-IR system using diffuse reflectance sampling accessories. ^{1}H NMR spectra were recorded at 300 MHz on solutions in $CDCl_3$, DMSO-d_6, CD_2Cl_2, or THF-d_8 on a Varian Mercury 300 spectrometer with the solvent proton signals as standard. ^{13}C NMR spectra were

recorded at 75 MHz on solutions in $CDCl_3$, DMSO-d_6, CD_2Cl_2 or THF-d_8 on a Varian Mercury 300 spectrometer with the solvent carbon signals as standard.

Gel permeation chromatography (GPC) was conducted on a Waters 1515 HPLC (Waters Chromatography, Inc.) equipped with a Waters 2414 differential refractometer and a three-column series PL gel 5μm Mixed C, 500 Å, and 104 Å, 300 × 7.5 mm columns (Polymer Laboratories Inc.). The system was equilibrated at 25 °C in anhydrous THF, which served as the polymer solvent and eluent with a flow rate of 1.0 mL/min. Polymer solutions were prepared at a known concentration (*ca.* 3 mg/mL) and an injection volume of 200 μL was used for every sample. Data collection and analysis were performed, respectively, with Precision Acquire software and Discovery 32 software (Precision Detectors, Inc.). The system was calibrated by a nearly monodispersed polystyrene standard (Pressure Chemical Co., $Mw/Mn < 1.04$). The differential refractometer was calibrated with standard polystyrene reference material (SRM 706 NIST), of known specific refractive index increment dn/dc (0.184 mL/g).

Dynamic light scattering (DLS) analysis was performed using a Brookhaven Instruments Co. (Holtsville, NY) system consisting of a model BI-200SM goniometer, a model EMI-9865 photomultiplier, and a model BI-9000AT digital correlator. Incident light was provided by a model 95-2 Ar^+ laser (Lexel Corp., Palo Alto, CA) operated at 514.5 nm. All measurements were made at 20 ± 1 °C in solvents. Scattered light was collected at 90° angle. The digital correlator was operated with 522 channels, a dual sampling time of 100 ns, a 5 s ratio channel spacing, and a duration time of 6 min. A photomultiplier

aperture of 400 μm was used, and the incident laser intensity was adjusted to obtain a photon counting rate between 200 to 300 kcps. Only measurements in which the measured and calculated baselines of the intensity autocorrelation function agreed to with 0.1% were used to calculate the particle size. The calculation of the particle size distribution and distribution averages was performed with the ISDA software package (Brookhaven Instruments Co., Holstville, NY), which employed double exponential fitting, cumulants analysis, NNLS, and CONTIN particle size distribution analysis routines.

Samples for atomic force microscopy (AFM) imaging were prepared by spin-casting *ca.* 2.0 μL of the sample solution onto freshly cleaved mica plates (Ruby clear mica, New York Mica Co.). AFM instrumentation was a Nanoscope IIIa system (Digital Instruments, Santa Barbara, CA), equipped with a J-type vertical engage piezoelectric scanner and operated in a tapping mode in air. Tapping-mode imaging was carried out with high resolution probes (DP14/HI'RES/Al BS, from μmash: L, 125 μm; normal spring constant, 5.0 N/m; resonance frequency, 160 kHz). The average height and average diameter values were determined by section analysis, using the Nanoscope III software package.

Elemental analysis was carried out by Midwest Microlabs, LLC.

Samples for transmission electron microscopy (TEM) imaging were prepared by placing a 5μL drop of aqueous solution containing micelles (*ca*. 0.2 mg/mL) and allowing it to

incubate for 5 min on a carbon-coated copper grid. After blotting off the extra solution, an equal volume of 1.0 wt % of phosphotungstic acid (PTA, a negative stain) was used to stain the grid for 1 min. TEM imaging was performed on a Hitachi H-7500 TEM.

Glass transition temperature (T_g) determinations were performed by using differential scanning calorimetry (DSC) on a DSC822e instrument (Mettler-Toledo, Inc.) in a temperature range of −50 - 200 °C with a heating rate of 10 °C/min under nitrogen. The data were acquired and analyzed with STARe software (Mettler-Toledo, Inc.). The T_g values were taken at the midpoint of the inflection tangent, upon the third heating scans.

Materials

Unless otherwise noted, all solvents and reagents were purchased from Sigma-Aldrich Chemical Co. (St. Louis, MO) and used as received. Dichloromethane (CH_2Cl_2, 99+%) were distilled over CaH_2 before use. *tert*-Butyl acrylate (*t*BA, 98%), styrene (S, 99%) were passed through a neutral alumina column before polymerization. The norbornenyl-functionalized RAFT chain transfer agent (NB-CTA) (Li, Z.; Zhang, K.; Ma, J.; Cheng, C.; Wooley, K. L. *J. Polym. Sci. Part A Polym. Chem.* **2009**, *47*, 5557-5563.) and the Grubb's catalyst (Choi, T. L.; Grubbs, R. H. *Angew. Chem. Int. Edit.* **2003**, *42*, 1743-1746.) were prepared respectively following literature methods.

Synthesis

RAFT-based synthesis of α-norbornenyl poly(*t*-butyl acrylate) macromonomer, NB-P*t*BA, 1. To a 50 mL Schlenk flask with a stir bar, NB-CTA (0.6481 g, 1.38 mmol) and

t-butyl acrylate (10.0 mL, 68.3 mmol) were added, followed by the addition of AIBN (as a freshly-prepared stock solution in 2-butanone, 1.10 mg/mL, 10 mL, 5 mol%). After 4 cycles of freeze-pump-thaw, the polymerization was conducted in an oil bath at 51 ^{o}C. At time intervals, an aliquot was withdrawn and analyzed by ^{1}H NMR spectroscopy to determine the extent of monomer conversion. After 310 min, the reaction was quenched by freezing the reaction mixture in a liquid nitrogen bath. The reaction mixture was then precipitated in 20% H_2O-methanol 3 times and the polymer (NB-P*t*BA macromonomer) was collected. Yield: 2.3 g. M_n^{NMR} = 4950 Da, M_n^{GPC} = 4670 Da, M_w/M_n = 1.11; T_g: 43 ^{o}C; IR: 2977, 2932, 1727, 1479, 1448, 1392, 1367, 1338, 1257, 1148, 1035, 908, 845, 751, 705, 637, 471, 428 cm^{-1}; ^{1}H NMR (300 MHz, $CDCl_3$, ppm) δ 6.05-6.10 (norbornenyl alkene), 4.60-4.72 (C***H***SC(S)S), 3.80-4.20 (C***H*****$_2$**OC(O)), 3.30-3.40 (C***H*****$_2$**SC(S)S), 2.60-2.90 (allylic protons of norbornenyl groups), 2.05-2.40 (polymer backbone protons) 1.00-1.95 (*t*-butyl protons, polymer backbone protons and C(S)SCH$_2$C$_{10}$***H*****$_{20}$**CH$_3$), 0.80-0.90 (C(S)SCH$_2$C$_{10}$H$_{20}$C***H*****$_3$**); ^{13}C NMR (75 MHz, $CDCl_3$, ppm) δ 174.3, 80.2, 41.5-43.5, 35.7-37.3, 28.0-28.2. Elemental analysis. Anal. Calcd for $C_{269}H_{462}O_{72}S_3$, C, 65.4; H, 9.4; O, 23.3; S, 2.0. Found, C, 65.5; H, 9.1; O, 23.4; S, 2.1.

RAFT-based synthesis of α-norbornenyl polystyrene macromonomer, NB-PS, 2. To a 10 mL Schlenk flask with a stir bar, NB-CTA (0.2070 g, 0.442 mmol), followed by the addition of AIBN (as a freshly-prepared stock solution in styrene, 2.5 mg/mL, 5.0 mL, 6 mol%). After 4 cycles of freeze-pump-thaw, the polymerization was conducted in an oil bath at 50 ^{o}C. After 18 hours, the reaction was quenched by freezing the reaction mixture in a liquid nitrogen bath. The reaction mixture was then precipitated in methanol 3 times

and the polymer (NB-PS macromonomer) was collected. Yield: 1.6 g. M_n^{NMR} = 4630 Da, M_n^{GPC} = 4560 Da, M_w/M_n = 1.08; T_g: 93 ^oC; IR: 3082, 3059, 3025, 3001, 2924, 2851, 1943, 1869 1802, 1725, 1601, 1583, 1541, 1493, 1452, 1371, 1266, 1181, 1154, 1110, 1068, 1028, 906, 757, 698, 667 cm^{-1}; ^1H NMR (300 MHz, CD_2Cl_2, ppm) δ 6.36-7.50 (styrenyl protons), 6.00-6.10 (norbornenyl alkene), 4.60-4.90 (C***H***SC(S)S), 3.50-3.80 (C***H*****$_2$**OC(O)), 3.30-3.40 (C***H*****$_2$**SC(S)S), 2.60-2.90 (allylic protons of norbornenyl groups), 1.12-2.40 (backbone protons and C(S)SCH$_2$C$_{10}$***H*****$_{20}$**CH$_3$), 0.80-0.90 (backbone protons and C(S)SCH$_2$C$_{10}$H$_{20}$C***H*****$_3$**); ^{13}C NMR (75 MHz, CD_2Cl_2, ppm) δ 145, 128, 126, 42.5-46.0, 40.0-41.8. Elemental analysis. Anal. Calcd for $C_{344}H_{362}O_2S_3$, C, 89.4; H, 7.8; O, 0.7; S, 2.1. Found, C, 89.4; H, 7.8; O, 0.7; S, 2.0.

Sequential ROMP-based synthesis of hetero-grafted diblock molecular brush, P(NB-*g*-P*t*BA)-*b*-P(NB-*g*-PS), 3. To a solution of Grubbs' catalyst in CH_2Cl_2 (4.1 mg/mL, 100 μL, 1 equiv.) under argon in a scintillation vial capped with a septum was added a CH_2Cl_2 solution of **1** (104.1 mg/mL, 1000 μL, 50 equiv.) *via* an argon-flushed syringe. The reaction was allowed to stir at room temperature for 3 min, and an aliquot of the reaction mixture (100 μL) was withdrawn (for the analysis of the first block). After that, a CH_2Cl_2 solution of **2** (100.1 mg/mL, 900 μL, 50 equiv.) was added to the living polymerization mixture immediately to allow for the second ROMP reaction. Another 3 min later, the polymerization was quenched by addition of a small amount of ethyl vinyl ether. The final diblock molecular brush was obtained after precipitating the reaction mixture in methanol. Yield: 178.1 mg. M_n^{GPC}(RI) = 197.8 kDa; T_g: 41 ^oC and 91 ^oC; IR: 3081, 3059, 3025, 2919, 2853, 1943, 1871 1802, 1732, 1601, 1583, 1542,

1493, 1479, 1453, 1392, 1367 , 1258, 1152, 1070, 1030, 966, 907, 854, 813, 738, 698, 539 cm^{-1}; ^1H NMR (300 MHz, CD_2Cl_2, ppm) δ 6.36-7.50 (styrenyl protons), 4.60-4.72 (C***H***SC(S)S), 3.30-3.40 (C***H*****$_2$**SC(S)S), 2.05-2.40 (grafted chain backbone protons), 0.70-2.00 (grafted chain backbone protons, *t*-butyl protons and C(S)SCH_2C_{11}***H*****$_{23}$**); ^{13}C NMR (75 MHz, CD_2Cl_2, ppm) δ 174, 145, 128, 126, 80.6, 40.5-47.5, 35.5-38.5, 28.0-30.0. Elemental analysis. Anal. Calcd for $C_{613}H_{824}O_{74}S_6$, C, 77.0; H, 8.6; O, 12.4; S, 2.0. Found, C, 77.3; H, 8.4; O, 12.5; S, 2.0.

Synthesis of amphiphilic diblock molecular brush, P(NB-*g*-PAA)-*b*-P(NB-*g*-PS), 4. Polymer **3** (20.1 mg, 7.34×10^{-2} mmol of *t*-butyl group) was dissolved in CH_2Cl_2 (5.0 mL) in a vial. A solution of trimethylsilyl iodide (400 μL, 2.81 mmol, diluted by 1.0 mL CH_2Cl_2) was added. The reaction was stirred at room temperature for 90 min, followed by the removal of the excess solvent and reagent under reduced pressure. The residue was redissolved in THF and decolorized by the addition of $Na_2S_2O_3$ (10 wt. %) aqueous solution. The solution was then dialyzed against nanopure water for 5 days, followed by lyophilization to afford the final amphiphilic hetero-grafted diblock molecular brushes. Yield: 13.7 mg; T_g: 93 ^oC; IR: 3432, 3081, 3059, 3025, 2924, 2851, 1723, 1600, 1492, 1452, 1366, 1255, 1168, 1026, 843, 757, 698, 666 cm^{-1}; ^1H NMR (300 MHz, THF-d_8, ppm) δ 9.00-10.70 (COO***H***), 6.36-7.50 (styrenyl protons), 2.15-2.60 (grafted chain backbone protons), 0.70-2.00 (grafted chain backbone protons, and C(S)SCH_2C_{11}***H*****$_{23}$**); ^{13}C NMR (75 MHz, THF-d_8, ppm) δ 176, 144, 128, 126, 41.5-47.5, 33.5-37.5.

Preparation of micelle solution, 5. Amphiphilic hetero-grafted diblock molecular brush **4** (4.7 mg) was dissolved in DMF (10 mL) and stirred at room temperature for 1 hour, and then dialyzed against nanopure water for 5 days, to afford a clear solution **5** (0.13 mg/mL).

DLS results

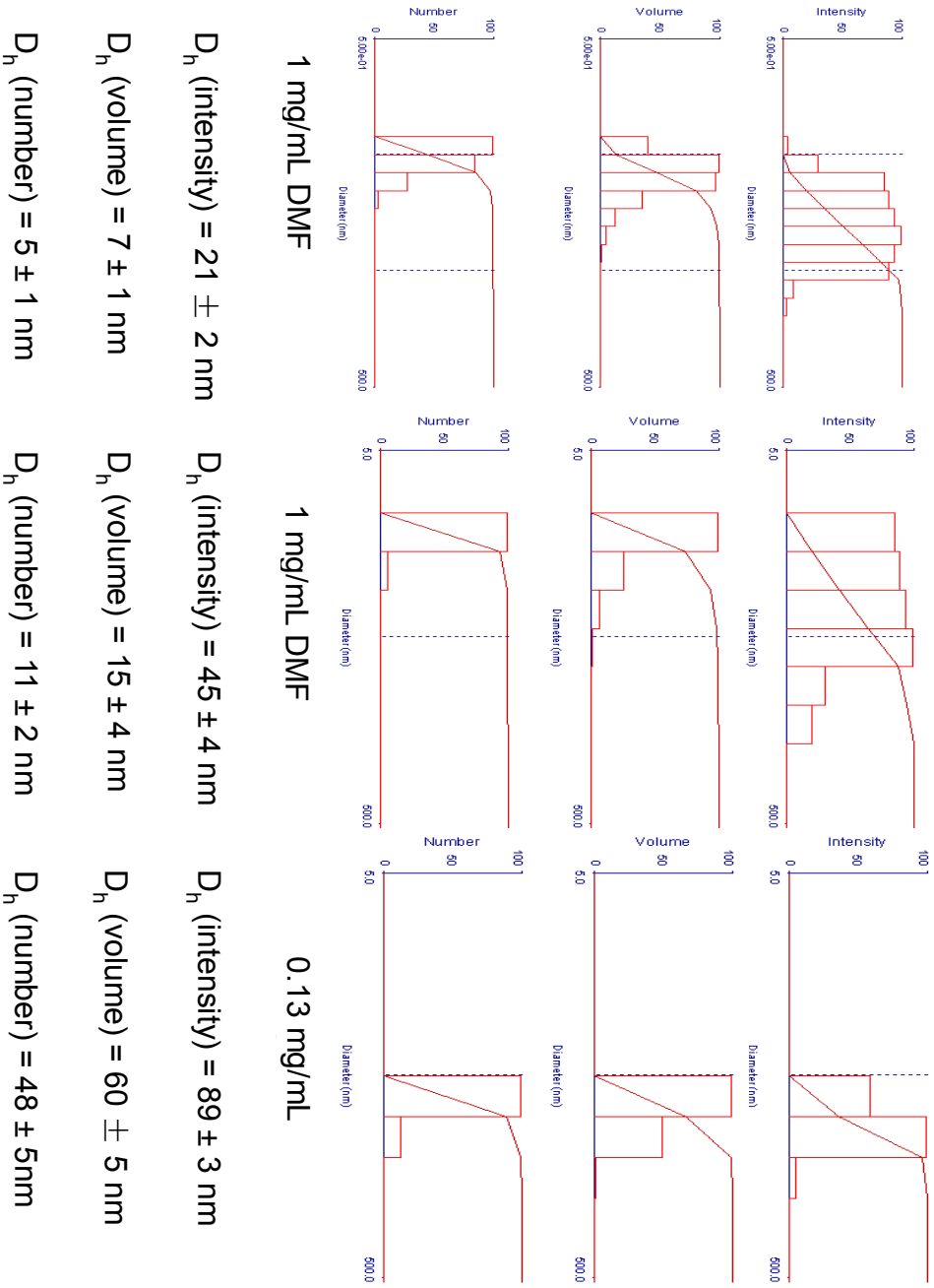

Figure 3-2. Dynamic light scattering results of nanoparticles. P(NB-*g*-P*t*BA)-*b*-P(NB-*g*-PS), **3 (left)**; P(NB-*g*-PAA)-*b*-P(NB-*g*-PS), **4 (middle)**; micelles, **5 (right).**

AFM results

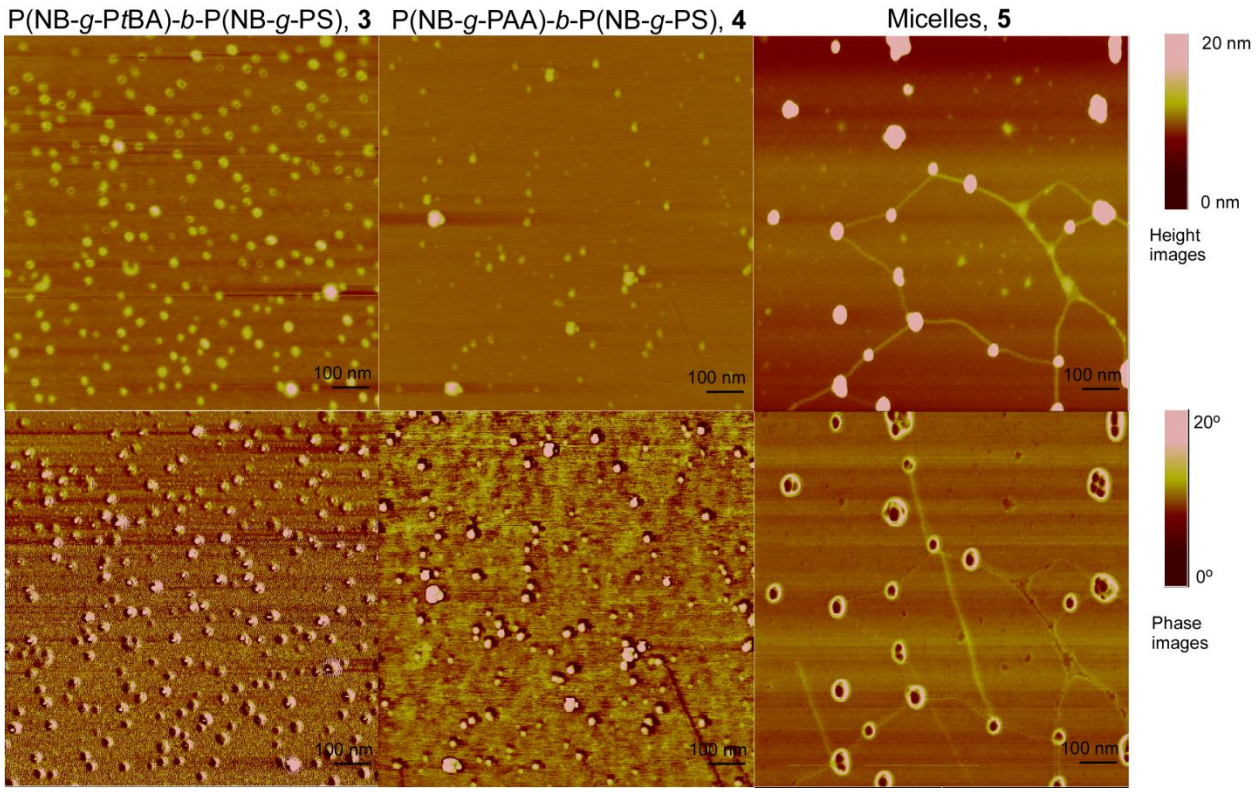

Figure 3-3. AFM images of nanoparticles. P(NB-*g*-P*t*BA)-*b*-P(NB-*g*-PS), **3 (left)**; P(NB-*g*-PAA)-*b*-P(NB-*g*-PS), **4 (middle)**; micelles, **5 (right)**. Samples were prepared by spin-casting *ca.* 2.0 μL of the sample solution onto freshly cleaved mica plates. The solutions were 0.02 mg/mL **3** in $CHCl_3$, 0.04 mg/mL **4** in DMF and 0.13 mg/mL **5** in water, respectively.

The aggregation number of unimers per micelle was calculated based on the following equation:

$$\mathbf{N}=\left(\frac{R1}{R2}\right)^2 \times \frac{H1}{H2}$$

Where R1 is the average radius of the micelles (21 nm), R2 is the average radius of the unimers (10 nm), H1 is the average height of the micelles (28 nm), and H2 is the average height of the unimers (2 nm).

REFERENCE

(1) V. Wagner, A. Dullaart, A. K. Bock and A. Zweck "The emerging nanomedicine landscape." *Nat. Biotechnol.* **2006**, *24*, 1211-1217.

(2) G. M. Whitesides and B. Grzybowski "Self-assembly at all scales." *Science* **2002**, *295*, 2418-2421.

(3) D. J. Pochan, Z. Y. Chen, H. G. Cui, K. Hales, K. Qi and K. L. Wooley "Toroidal triblock copolymer assemblies." *Science* **2004**, *306*, 94-97.

(4) L. F. Zhang, K. Yu and A. Eisenberg "Ion-induced morphological changes in "crew-cut" aggregates of amphiphilic block copolymers." *Science* **1996**, *272*, 1777-1779.

(5) Z. Li, E. Kesselman, Y. Talmon, M. A. Hillmyer and T. P. Lodge "Multicompartment micelles from ABC miktoarm stars in water." *Science* **2004**, *306*, 98-101.

(6) S. S. Sheiko, B. S. Sumerlin and K. Matyjaszewski "Cylindrical molecular brushes: Synthesis, characterization, and properties." *Prog. Polym. Sci.* **2008**, *33*, 759-785.

(7) M. F. Zhang and A. H. E. Müller "Cylindrical polymer brushes." *J. Polym. Sci., Part A: Polym. Chem.* **2005**, *43*, 3461-3481.

(8) K. Ishizu, J. Satoh and A. Sogabe "Architecture and solution properties of AB-type brush-block-brush amphiphilic copolymers via ATRP techniques." *J. Colloid Interf. Sci.* **2004**, *274*, 472-479.

(9) H. I. Lee, K. Matyjaszewski, S. Yu-Su and S. S. Sheiko "Hetero-grafted block brushes with PCL and PBA side chains." *Macromolecules* **2008**, *41*, 6073-6080.

(10) L. Zhao, M. Byun, J. Rzayev and Z. Lin "Polystyrene-Polylactide Bottlebrush Block Copolymer at the Air/Water Interface." *Macromolecules* **2009**, *ASAP*,

(11) J. Rzayev "Synthesis of Polystyrene - Polylactide Bottlebrush Block Copolymers and Their Melt Self-Assembly into Large Domain Nanostructures." *Macromolecules* **2009**, *42*, 2135-2141.

(12) Z. Li, K. Zhang, J. Ma, C. Cheng and K. L. Wooley "Facile syntheses of cylindrical molecular brushes by a sequential RAFT and ROMP ldquografting-throughrdquo methodology." *J. Polym. Sci., Part A: Polym. Chem.* **2009**, *47*, 5557-5563.

(13) A. Nyström, M. Malkoch, I. Furó, D. Nyström, K. Unal, P. Antoni, G. Vamvounis, H. C., K. L. Wooley, E. Malmström and A. Hult "Characterization of Poly(norbornene) Dendronized Polymers Prepared by Ring-Opening Metathesis Polymerization of Dendron Bearing Monomers." *Macromolecules* **2006**, *39*, 7241–7249.

(14) S. Rajaram, T. L. Choi, M. Rolandi and J. M. J. Fréchet "Synthesis of Dendronized Diblock Copolymers via Ring-Opening Metathesis Polymerization and Their Visualization Using Atomic Force Microscopy." *J. Am. Chem. Soc.* **2007**, *129*, 9619-1621.

(15) Y. Xia, J. A. Kornfield and R. H. Grubbs "Efficient Synthesis of Narrowly Dispersed Brush Polymers via Living Ring-Opening Metathesis Polymerization of Macromonomers." *Macromolecules* **2009**, *42*, 3761-3766.

(16) G. Moad, E. Rizzardo and S. H. Thang "Living radical polymerization by the RAFT process." *Aust. J. Chem.* **2005**, *58*, 379-410.

(17) C. Cheng, K. Qi, E. Khoshdel and K. L. Wooley "Tandem synthesis of core-shell brush copolymers and their transformation to peripherally cross-linked and hollowed nanostructures." *J. Am. Chem. Soc.* **2006**, *128*, 6808-6809.

(18) J. A. Love, M. S. Sanford, M. W. Day and R. H. Grubbs "Synthesis, structure, and activity of enhanced initiators for olefin metathesis." *J. Am. Chem. Soc.* **2003**, *125*, 10103-10109.

(19) T. M. Trnka, J. P. Morgan, M. S. Sanford, T. E. Wilhelm, M. Scholl, T. L. Choi, S. Ding, M. W. Day and R. H. Grubbs "Synthesis and activity of ruthenium alkylidene complexes coordinated with phosphine and N-heterocyclic carbene ligands." *J. Am. Chem. Soc.* **2003**, *125*, 2546-2558.

(20) T. L. Choi and R. H. Grubbs "Controlled living ring-opening-metathesis polymerization by a fast-initiating ruthenium catalyst." *Angew. Chem. Int. Edit.* **2003**, *42*, 1743-1746.

(21) Here, the synthesized molecular brush bears a 50:50 backbone. It should be pointed out that molecular brushes with longer diblock backbones can also be synthesized, using similar techniques. The longest diblock backbones so far is 100: 100.

(22) G. Riess "Micellization of block copolymers." *Prog. Polym. Sci.* **2003**, *28*, 1107-1170.

(23) Y. Xia and R. H. Grubbs *Personal Communication* **2009**

Chapter 4

Side chain block molecular brushes

[Portions of this work have been published previously as Zhou Li, Jun Ma, Nam S. Lee and Karen L. Wooley, *J. Am. Chem. Soc.*, **2011**, *133(5)*, 1228-1231.]

Dynamic Cylindrical Assembly of Triblock Copolymers by a Hierarchical Process of Covalent and Supramolecular Interactions

ABSTRACT

We have developed a hierarchical process that combines linear triblock copolymers into concentric globular sub-units through strong chemical bonds and is followed by their supramolecular assembly *via* weak non-covalent interactions to afford one-dimensionally-assembled, dynamic cylindrical nanostructures. The molecular brush architecture forces triblock copolymers to adopt some intramolecular interactions within confined framework and then drives their intermolecular interactions in the mixtures of organic solvent and water. In contrast, the triblock copolymers, when not pre-connected into the molecular brush architectures, organize only into globular assemblies.

INTRODUCTION

Nature has evolved a complicated process to create sophisticated functional materials through hierarchical self assembly of simple nanoscale motifs.(1-3) With the broader development of nanotechnologies, much effort has been made to understand and mimic this process to construct artificial nanostructures from synthetic molecules in the laboratory. Molecules with selective physical or chemical interactions are designed to drive the assembly processes, and various nanostructures with different functions have been obtained by tuning the properties of the synthetic molecules.(4-17) Among those molecules, block copolymers are of great interest.(4, 5, 8, 13, 16, 18) However, the complexities of nanostructures derived from block copolymers remain lower than those from Nature, possibly because their structures are usually simpler than those originating from biomolecules. Herein, we demonstrate that dynamic hierarchical cylindrical assembly of triblock copolymers is achieved by stepwise application of covalent bonds and supramolecular interactions. Linear ABC triblock copolymers were initially prepared, then linked together by selective reaction through a single chain end site on each polymer chain, to establish a covalent molecular brush architecture. This process was followed by multi-molecular supramolecular assembly in water to afford dynamic nanocylindrical assemblies, whereas the linear triblock copolymer precursor was incapable of producing such a unique morphology.

RESULTS AND DISCUSSION

Molecular brushes are non-linear macromolecules, in which many polymeric side chains are distributed along a backbone.(19, 20) Generally, there are three strategies to synthesize molecular brushes: “grafting-from” (polymerization of side chains from

initiating groups along a backbone),(21-23) "grafting-onto" (addition of previously synthesized side chains to a backbone),(24) and "grafting-through" (polymerization of the chain end groups of previously synthesized macromonomers).(25-28) Although molecular brushes with long backbones have been synthesized by "grafting-from" and "grafting-onto" approaches, it has been difficult to control the side chain grafting density and ensure control over the final compositions by these two strategies, due to steric effects in the reactions involving multiple reactive sites in proximity.(19, 20) The "grafting-through" strategy is favored for good control over both grafting density and side chain structures and has, in our research, allowed for dense grafting of well-defined triblock copolymers onto a central backbone chain

The "grafting-through" strategy is a highly-efficient process to synthesize block copolymer-based molecular brushes, for which we have developed a special case that combines four different polymer compositions, organized topologically within the macromolecular framework, by two controlled polymerization techniques: Reversible addition-fragmentation chain transfer (RAFT) polymerization and ring opening metathesis polymerization (ROMP).(25, 28-30) A molecular brush with polystyrene, poly(methyl acrylate) and poly(acrylic acid) triblock side chains grafted along a polynorbornene backbone was synthesized in three steps, including RAFT, ROMP and deprotection (**Figure 4-1.A**).

In the first step, the triblock macromonomer, α-norbornenyl polystyrene-*b*-poly(methyl acrylate)-*b*-poly (*t*-butyl acrylate) (NB-PS-*b*-PMA-*b*-P*t*BA), was synthesized from a norbornene-functionalized chain transfer agent (NB-CTA) by sequential RAFT polymerizations. Placement of the polymerizable norbornenyl unit at the polystyrene

chain terminus was done so that its polymerization into a molecular brush would present the hydrophobic materials within the inner region of the final supramolecularly-assembled structures, after converting the *t*-butyl acrylate portion of the polyacrylate chain segments to poly(acrylic acid). However, the reinitiation of polymerization is usually disfavored when growing polyacrylates from polystyrene macroCTAs. Another challenge in this step is the participation of norbornenyl groups in the multiple radical polymerizations, which would destroy the defined macromolecular architecture and prevent later conversion into the molecular brush topology. Therefore, the polymerization conditions (temperature, solvent, monomer conversion and initiator feed ratio) were tuned carefully.

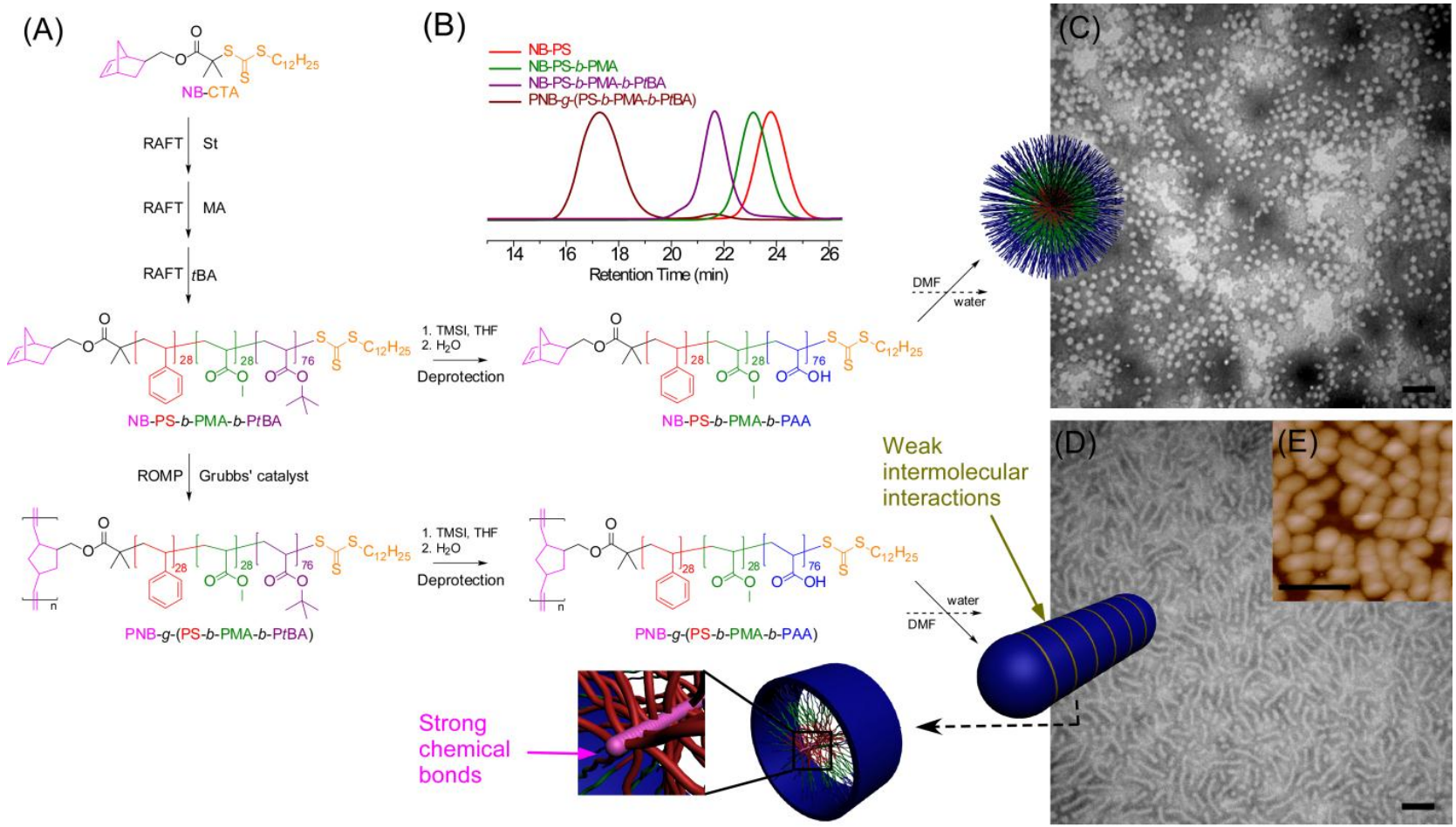

Figure 4-1. (A) Synthesis and self assembly of concentrically-amphiphilic molecular brushes, having triblock PS-*b*-PMA-*b*-PAA side chains, and linear amphiphilic PS-*b*-PMA-*b*-PAA triblock copolymers. (B) gel permeation chromatography profiles of NB-PS, NB-PS-*b*-PMA, NB-PS-*b*-PMA-*b*-P*t*BA and PNB-*g*-(PS-*b*-PMA-*b*-P*t*BA). (C) TEM image of the nanostructures self assembled from linear NB-PS-*b*-PMA-*b*-PAA triblock copolymers in solution and then cast onto a carbon-coated copper grid. (D) TEM image of the hierarchical cylindrical nanostructures comprised of PNB-*g*-(PS-*b*-PMA-*b*-PAA) self assembled in solution and then cast onto a carbon-coated copper grid. (E) AFM image of the hierarchical cylindrical nanostructures comprised of PNB-*g*-(PS-*b*-PMA-*b*-PAA) self assembled in solution and then cast onto a mica substrate. Scale bar: 100 nm.

The well-controlled structure of the macromonomer was confirmed by both ^{1}H NMR spectroscopy and gel permeation chromatography (GPC), as shown in **Figure 4-1.B**. Obvious peak position shifts were observed after each chain extension and the corresponding peaks were all symmetric, indicating mono-modal molecular weight distributions with low polydispersity indices (PDIs). The final macromonomer (NB-PS-*b*-PMA-*b*-P*t*BA) had a molecular weight of 15,900 Da with a PDI of 1.20.

The backbone of the overall molecular brush (PNB-*g*-(PS-*b*-PMA-*b*-P*t*BA)) was grown in the second step, by ROMP of the chain end norbornenyl groups of NB-PS-*b*-PMA-*b*-P*t*BA. ROMP has been widely used to polymerize bulky macromonomers to afford densely grafted polymers.(25-28, 31-34) As shown in the GPC trace (**Figure 4-1.B**), a peak shift to lower retention time was observed with over 95% conversion of the macromonomers to brush structures and a residual peak at 21 – 22 min.(25, 28) The resulting molecular brushes had a molecular weight of 1.52×10^{6} Da with narrow molecular weight distribution (PDI = 1.15), which, by the nature of the "grafting-through" procedure, had an even grafting density of side chains along the backbone. Finally, PNB-*g*-(PS-*b*-PMA-*b*-P*t*BA) was then converted to the concentrically-amphiphilic block brush copolymer PNB-*g*-(PS-*b*-PMA-*b*-PAA) by deprotection of the acrylic acid groups by acidolysis of the *t*-butyl acrylate repeat units.

In addition to providing control over the molecular brush structure and composition, the "grafting-through" strategy also offered the opportunity to isolate exact structural and compositional analogs of the linear triblock copolymer side chains. By deprotecting the acrylic acid repeat units of NB-PS-*b*-PMA-*b*-P*t*BA, NB-PS-*b*-PMA-*b*-PAA was obtained, whose composition is consistent with the side chains of the molecular brush. The

solution-state assembly behaviors of these two amphiphilic macromolecules—one being a complex molecular brush architecture and the other being a linear polymer chain—were then investigated and compared.

When transitioned from *N*,*N*-dimethylformamide into water, the nanostructures from the triblock molecular brush copolymer and linear copolymer amphiphiles exhibited different morphologies, regardless of their compositional consistency. As shown in the transmission electron microscopy (TEM) images, the linear amphiphilic macromolecules gave globular nanoscopic morphologies with overall diameters of 21 ± 2 nm (**Figure 4-1.E**); while the molecular brushes exhibited cylindrical morphologies with diameters of 18 ± 2 nm and lengths of 92 ± 21 nm (**Figure 4-1.C**). The diameter of the cylinders was close to the diameter of the globules, suggesting that the core-shell micellar arrangement of PS-*b*-PMA-*b*-PAA polymer side chains in the molecular brushes was similar to that of those polymers, not connected by covalent bonds. Under imaging by atomic force microscopy (AFM), it is obvious that the cylindrical nanoassemblies were composed of individual globular structures, presumably individual molecular brushes, arranged by a one dimensional assembly (**Figure 4-1.D** and **Figure 4-4**). Assuming that the individual brushes were globular and their sizes did not change significantly when they were assembled, the average number of brushes per cylinder was around four-to-five.

It was hypothesized that within the molecular brush framework, the rigid polynorbornene backbone limited the conformational freedom of the triblock copolymer grafted side chains, providing opportunities for interactions uni-directionally between individual molecular brushes, especially by interactions at the backbone chain ends where the density of chains would be minimized. The linear amphiphilic triblock copolymer

requires multi-molecular interactions to remain as stable dispersions in water. When confined through covalent bonds within the molecular brush architecture, aqueous dispersions of the discrete triblock copolymers would be stabilized by the PAA segments of surrounding chains, but only to a limited extent. The extent of solution-state stabilization was not expected to be equal among the triblock copolymer side chains distributed along the polynorbornene backbone – those grafted at the ends of the backbone would be less stabilized because the chain packing density is expected to be lower than for those along the backbone. Assembly through contacts between the hydrophobic interior (PS and PMA) counterparts from multiple molecular brushes would reduce the intrinsic energy and, thereby, retain their multi-molecular assembly tendency. By having lower density, less well stabilized and active end caps on the molecular brushes, one-dimensional assembly would be promoted, to afford the cylindrical nanostructures as observed.

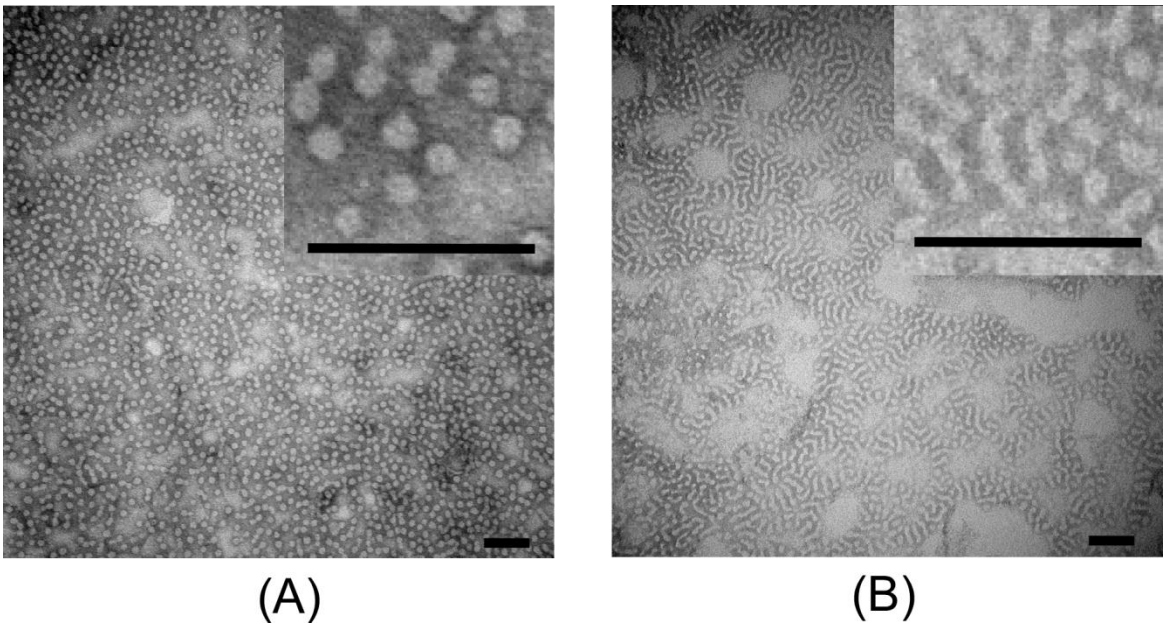

Figure 4-2. (A) TEM images of the disassembled nanostructures after heating the aqueous solution of PNB-g-(PS-b-PMA-b-PAA) at 70 oC for 3 h. (B) TEM images of the partially reassembled nanostructures after adding an equivalent volume of THF to the heated PNB-g-(PS-b-PMA-b-PAA) aqueous solution. Scale bar: 100 nm.

To further study this proposed mechanism, the aqueous solution was heated at 70 ^{o}C for 3 h. Upon heating, it was found that the cylindrical morphologies were replaced by globular entities with a number-averaged diameter of 19 ± 2 nm, as observed by TEM, suggesting that disassembly of the cylindrical nanostructures into individual brushes had occurred (**Figure 4-2.A**). The disassembly was further confirmed by dynamic light scattering (DLS) analysis of the PNB-*g*-(PS-*b*-PMA-*b*-PAA) aqueous solutions at different temperatures, which showed that the hydrodynamic sizes of the nanostructures decreased when the temperature was increased from 25 ^{o}C to 70 ^{o}C (**Figure 4-6**). The disassembly can be explained by analyzing the forces in the cylindrical structures to bring the triblock copolymer chains together. There were two interactions involved in the cylindrical nanostructures: One was the strong covalent bonds which held the amphiphilic triblock copolymer onto the polynorbornene backbone; the other was the

weak intermolecular non-covalent interactions that assembled individual brushes into cylindrical structures. Heating the solution provided sufficient energy to break the weak intermolecular interactions, but the strong covalent bonds were still conserved by this process. The disassembly confirmed that the cylindrical nanostructures resulted from the self assembly of the amphiphilic molecular brushes *via* intermolecular interactions.

Interestingly, cooling the heated solution at room temperature could not reproduce the cylindrical structures, even after concentrating the solution ten-fold to increase the frequency of intermolecular collisions between molecular brushes. This result suggested that the interaction between the hydrophobic core domains of amphiphilic molecular brushes is a key parameter to their self-organization behaviors. After being disassembled by heat, the individual brushes had to adopt conformations in which the inner hydrophobic cores were fully surrounded by hydrophilic shells to decrease the intrinsic energy. As a result, the cores became inaccessible by other molecules, leading to incapability to interact with each other to reproduce the cylindrical nanostructure.

Changing the environmental medium can change the conformations, conformational degrees of freedom, mobility and dynamics of individual brushes. An equivalent volume of THF was added to the heated micellar solution, from which TEM images showed that shorter cylindrical nanostructures appeared, suggesting that the hydrophobic domains became accessible and interactive again after adding a common solvent, which led to attraction between individual molecular brushes (**Figure 4-2.B**). Furthermore, the heated solution was lyophilized and the resulting powders were dissolved in DMF and dialyzed against water again to reproduce the cylindrical structures (**Figure 4-5**). The results from TEM showed cylindrical structures with similar sizes to the original assemblies prior to

heating. In addition to providing mechanistic insights, the thermally-driven disassembly and solvent-promoted re-assembly are interesting triggers to alter these unique morphologies.

More insights into the mechanism of the self assembly of molecular brushes were obtained by comparing the molecular brush structures in organic solvent and after dialysis into water, to determine whether any pre-assembly occurred prior to the aqueous-promoted assembly process. DLS was used to characterize the samples before and after dialysis in bulk solution state. At 25 °C, the number-averaged hydrodynamic diameter of the molecular brushes in DMF solution before dialysis was 20 ± 6 nm (**Figure 4-7**), while the number-averaged hydrodynamic diameter of the assembled structures after dialysis was 134 ± 38 nm (**Figure 4-6**). These data indicate a transformation from individual molecular brushes in organic solvent to multimolecular assemblies in water. Furthermore, TEM was used to observe their morphologies in dry state, after drop deposition onto a carbon-coated copper grid and drying under ambient conditions (**Figure 4-8** and **Figure 4-9**). To avoid the possible side effects of water from the aqueous staining solution, RuO_4 vapor was used. Surprisingly, it was found that the samples dried from DMF solution showed long cylindrical structures that appeared to be branched and interconnected with each other, while those from the aqueous solution contained shorter, discrete cylinders. When dried on the TEM grids, the highly flexible and mobile characteristics of the molecular brushes in DMF promoted interactions between them that were not necessarily unidirectional. As a result, some branching sites were observed, facilitated by more than two contact points between one molecular brush and its neighbors. Although the images of **Figure 4-8** are essentially drying patterns,

they provide significant information regarding the intermolecular interactions and degrees of flexibility that are possible even for these densely-grafted triblock molecular brush copolymers. In comparison, the dynamically-assembled structures were "frozen" in water after dialysis, as suggested by both DLS and TEM.

Given the observation that the molecular brushes were discrete, individual entities in DMF solution before dialysis, combined with the fact that the separated individual molecular brushes alone could not undergo intermolecular interactions in water, the self-assembled structures were proposed to be created during dialysis, when the flexibilities of the triblock side chains were still in an appropriate range for intermolecular interactions and the mobilities of the molecular brushes were decreased significantly to avoid separation of the assembled structures. Overall, a mechanism of the self assembly of PNB-*g*-(PS-*b*-PMA-*b*-PAA) into dynamic hierarchical cylindrical nanostructures was proposed, as shown in **Figure 4-3**.

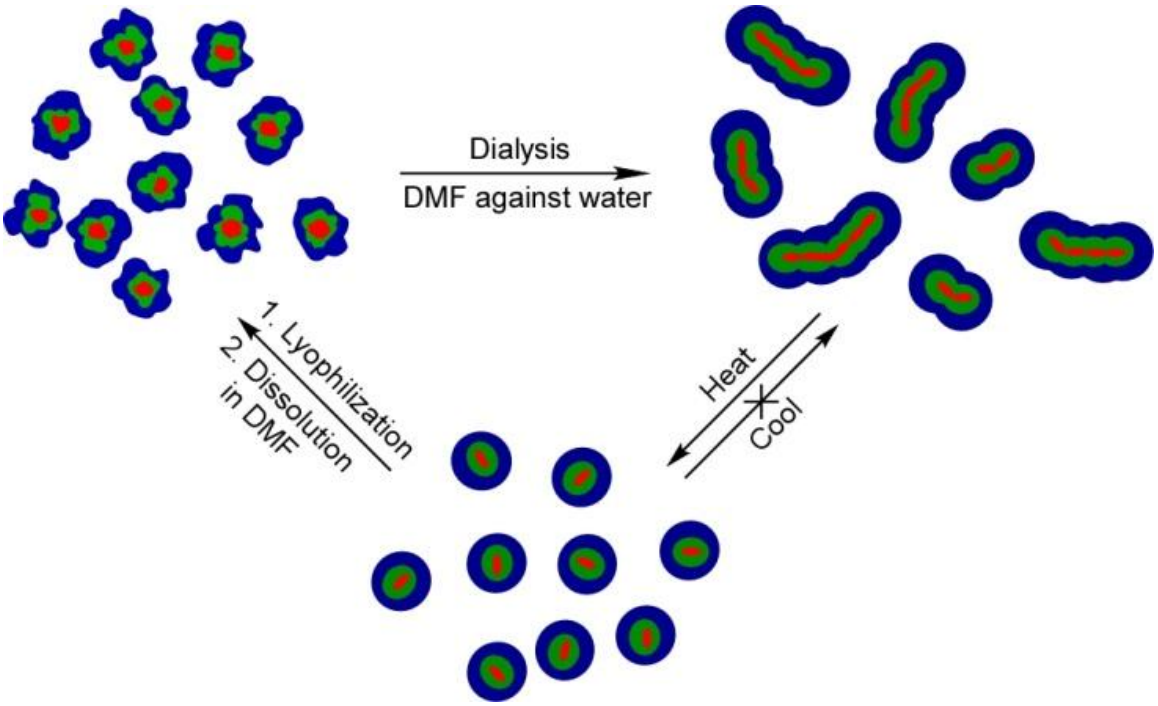

Figure 4-3. Schematic illustrations of the morphologies of the PNB-*g*-(PS-*b*-PMA-*b*-PAA) molecular brushes at different stages. The molecular brushes were more flexible in DMF solution before dialysis, exposing the internal components to participate in intermolecular interactions. The dynamic hierarchical cylindrical structures were "frozen" in aqueous solution after dialysis and they could undergo thermo-driven disassembly. Due to the low degree of the flexibility in water, the disassembled molecular brushes could not re-assemble into cylindrical structures by simply cooling. Reproduction of the hierarchical cylindrical structures was achieved by lyophilizing the disassembled molecular brushes, dissolving them in DMF and dialyzing the solution against water.

The hierarchical process demonstrated here, which is developed from applying covalent and supramolecular interactions stepwise to amphiphilic linear triblock copolymers, has enabled the production of dynamic, one-dimensional, cylindrical assemblies. Although originating from a symmetrical, concentrically-arranged molecular brush block copolymer structure, the relative chain densities along the primary molecular brush backbone provided for differentiation of accessibility to the core chain segments — greater at the backbone ends than the mid-segment, to produce these complex

hierarchically-assembled nanomaterials. With all of the attention that is being placed upon the incorporation of chemically-distinct functionalities within polymer frameworks, this physically-induced asymmetry is an exciting new direction to take as a general methodology toward the preparation of other unique materials. In fact, the combination of recent advances in synthetic polymer chemistry and solution-state assembly can be tuned individually, to influence their intra- and intermolecular interactions, and facilitate the arrangement of polymer building blocks into complex, functional materials, ultimately, approaching the sophistication of Nature.

Acknowledgement.

This research is supported by the National Science Foundation (grant numbers DMR-0906815 and DMR-1032267) and by fellowship support from the McDonnell International Scholars Academy (to Z. L.) The Welch Foundation is gratefully acknowledged for partial support through the W. T. Doherty-Welch Chair in Chemistry, Grant No. A-0001. We also thank the electron microscopy facilities at Washington University in St. Louis, Department of Otolaryngology, Research Center for Auditory and Visual Studies funded by NIH P30 DC004665.

EXPERIMENTAL

Measurements

Proton nuclear magnetic resonance (^{1}H NMR) spectra were recorded at 300 MHz on a Varian Mercury 300 spectrometer with solvent proton resonance as reference. Carbon nuclear magnetic resonance (^{13}C NMR) spectra were recorded at 75 MHz on a Varian Mercury 300 spectrometer with solvent carbon resonance as reference. Infrared spectra were obtained on a Perkin-Elmer Spectrum BX FT-IR system using diffuse reflectance sampling accessories.

Gel permeation chromatograph (GPC) was conducted on a Waters 1515 HPLC (Waters Chromatography, Inc.) equipped with a Waters 2414 differential refractometer and a Model PD2040 dual-angle (15^{o} and 90^{o}) light scattering detector (Precision Detectors, Inc.), and a three-column series PL gel 5μm Mixed C, 500 Å, and 104 Å, 300 × 7.5 mm columns (Polymer Laboratories Inc.). The system was equilibrated at 35 °C in THF, which served as the polymer solvent and eluent with a flow rate of 1.0 mL/min. Polymer solutions were prepared at a known concentration (*ca.* 3 mg/mL) and an injection volume of 200 μL was used. Data collection and analysis were performed, respectively, with Precision Acquire software and Discovery 32 software (Precision Detectors, Inc.). The system was calibrated using polystyrene standards.

Differential scanning calorimetry (DSC) was conducted on a DSC822^{e} instrument (Mettler-Toledo, Inc.) at temperature range of −50 - 200 °C with a heating rate of

10 °C/min under nitrogen. The data were acquired and analyzed with STAR^e software (Mettler-Toledo, Inc.). The Glass transition temperature (T_g) values were taken at the midpoint of the inflection tangent, upon the third heating scans.

Dynamic light scattering (DLS) measurements were conducted using Delsa Nano C (Beckman Coulter, Inc., Fullerton, CA) equipped with a laser diode operating at 658 nm. Size measurements were made in *N*,*N*-dimethylformamide (DMF) (n = 1.4282, η = 0.794 cP at 25 ± 1 °C) or water (n = 1.3329, η = 0.890 cP at 25 ± 1 °C; n = 1.3293, η = 0.547 cP at 50 ± 1 °C; n = 1.3255, η = 0.404 cP at 70 ± 1 °C). Scattered light was detected at 15° angle and analyzed using a log correlator over 70 accumulations for a 0.5 mL of sample in a glass size cell (0.9 mL capacity). The samples in the glass size cell were equilibrated at the desired temperature for 60 minutes before measurements were made. The photomultiplier aperture and the attenuator were automatically adjusted to obtain a photon counting rate of *ca*. 10 kcps. The calculation of the particle size distribution and distribution averages was performed using CONTIN particle size distribution analysis routines. The peak average of histograms from intensity, volume or number distributions out of 70 accumulations was reported as the average diameter of the particles.

Atomic force microscopy (AFM) was conducted on a MFP-3D-BIO system (Asylum Research, Santa Barbara, CA), operated in a tapping mode in air with high resolution probes (DP14/HI'RES/Al BS, from μmash: L, 125 μm; normal spring constant, 5.0 N/m; resonance frequency, 160 kHz). The average height and diameter values were determined by section analysis, using the IGOR Pro software package. Transmission

electron microscopy (TEM) imaging was performed in high-contrast mode with a Hitachi H-7500 at 80 kV accelerating voltage.

Materials

Azobisisobutyronitrile (AIBN, 98%, Aldrich) was recrystallized from methanol before use. *Tert*-butyl acrylate (*t*BA, 98%, Aldrich), methyl acrylate (MA, 99%, Aldrich), styrene (St, 99%, Aldrich), were passed through neutral alumina column before polymerizations. Iodotrimethylsilane (TMSI, 97%, Aldrich) and sodium thiosulfate ($Na_2S_2O_3$, 98.0%, Sigma-Aldrich) were used as received. The Grubbs' catalyst and the norbornenyl-functionalized RAFT chain transfer agent (NB-CTA) were prepared by the methods reported.(19, 20) Spectr/Por® membranes (MWCO 3500 Da, Spectrum Medical Industries, Inc., Laguna Hills, CA) were used for dialysis.

Synthesis of α-norbornenyl polystyrene (NB-PS).

The polymer was prepared from the polymerization mixture of St (18.20 g, 175 mmol), NB-CTA (541 mg, 0.862 mmol), AIBN (1.6 mg, 1.0×10^{-2} mmol) at 50 °C. The polymerization was quenched after 40 h when the monomer conversion was measured to be 10% by ^{1}H NMR spectroscopy (the conversion was calculated by the integration ratio of aromatic protons and one alkenyl proton (6.32-7.40 ppm) to the other two alkenyl protons (5.7 ppm and 5.2 ppm)). The isolated yield was 1.60 g (74 %, based on the conversion of St). M_n^{calc} = 2740 Da, M_n^{GPC} = 3340 Da, PDI = 1.14. T_g: 93 °C. IR (cm^{-1}): 3150-2850 (strong), 1943 (medium-weak), 1869 (medium-weak), 1802 (medium-weak), 1725 (medium-strong), 1601 (medium-strong), 1583 (medium), 1541 (weak), 1493

(strong), 1452 (strong), 1371 (medium), 1266 (medium), 1181 (medium), 1154 (medium), 1110 (medium), 1068 (medium-strong), 1028 (medium-strong), 906 (medium), 757 (strong). ^{1}H NMR (300 MHz, CD_2Cl_2, ppm): δ 0.80-0.90 (-C***H***$_3$ of the RAFT chain end and backbone protons), 1.10-2.50 (alkyl protons of RAFT agent and polystyrene backbone protons), 2.74-2.79 (>C***H***-CH=CH-C***H***<), 3.23-3.50 (-C***H*****$_2$**SC(S)S-), 6.03-6.16 (-C***H***=C***H***-), 6.32-7.40 (aromatic protons). ^{13}C NMR (75 MHz, CD_2Cl_2, ppm): δ 40.0-41.8, 42.5-46.0, 126, 128, 145.

Synthesis of α-norbornenyl polystyrene-*b*-poly(methyl acrylate) (NB-PS-*b*-PMA).

The polymer was prepared from the polymerization mixture of MA (8.60 g, 100 mmol), NB-PS as the macro-CTA (993 mg, 0.297 mmol) and AIBN (0.9 mg, 5.5×10^{-3} mmol) at 50 °C. The polymerization was quenched after 20 h when the monomer conversion was measured to be 8% by ^{1}H NMR spectroscopy. Yield: 1.18 g (70 %, based on the conversion of MA). M_n^{calc} = 5560 Da, M_n^{GPC} = 5580 Da, PDI = 1.15. T_g: 93 ^{o}C, 11 ^{o}C. IR (cm^{-1}): 3100-2850 (medium-strong, multiple peaks), 1802 (weak), 1733 (strong), 1600 (medium-weak), 1541 (weak), 1493 (medium), 1452 (medium-strong), 1388 (medium-weak), 1253 (medium-weak), 1195 (medium), 1164 (medium-strong), 1110 (medium weak), 988 (weak), 906 (weak), 827 (medium-weak), 752 (medium). ^{1}H NMR (300 MHz, CD_2Cl_2, ppm): δ 0.80-0.90 (-C***H***$_3$ of the RAFT chain end and backbone protons), 1.10-2.50 (alkyl protons of RAFT agent and polymer backbone), 2.74-2.79 (>C***H***-CH=CH-C***H***<), 3.23-3.30 (-C***H*****$_2$**SC(S)S-), 3.55-3.75 (-OC***H***$_3$ of MA units), 6.03-6.15 (-

C***H***=C***H***-), 6.30-7.40 (aromatic protons). ^{13}C NMR (75 MHz, CD_2Cl_2, ppm): δ 35.7-37.2, 40.5-46.5, 51.6, 126, 128, 145, 175.

Synthesis of *α*-norbornenyl polystyrene-*b*-poly(methyl acrylate)-*b*-poly(*t*-butyl acrylate) (NB-PS-*b*-PMA-*b*-P*t*BA).

The polymer was prepared from the polymerization mixture of *t*BA (1.94 g, 15.1 mmol), NB-PS-*b*-PMA as the macro-CTA (385 mg, 0.0689 mmol), AIBN (0.6 mg, 3.7×10^{-3} mmol) and 2-butanone (2.0 mL) at 50 °C. The polymerization was quenched after 20 h when the monomer conversion was measured to be 35% by ^{1}H NMR spectroscopy. Yield: 882 mg (83 %, based on the 35% conversion of *t*BA). M_n^{calc} = 15400 Da, M_n^{GPC} = 15900 Da, PDI = 1.20. T_g: 93 ^{o}C, 43 ^{o}C, 11 ^{o}C. IR (cm^{-1}): 3100-2800 (medium-strong, multiple peaks), 1943 (medium-weak), 1738 (strong), 1601 (medium-weak), 1448 (medium-strong), 1371 (strong), 1256 (medium-strong, broad), 1164 (strong), 845 (medium), 757 (medium-weak). ^{1}H NMR (300 MHz, CD_2Cl_2, ppm): δ 0.80-0.90 (-C***H₃*** of the RAFT chain end), 1.10-2.50 (alkyl protons of RAFT agent and polymer backbone, -(C***H₃***)$_3$C of *t*BA units), 2.74-2.79 (>C***H***-CH=CH-C***H***<), 3.23-3.50 (m, -C***H₂***SC(S)S-), 3.65 (-OC***H₃*** of MA units), 6.03-6.15 (-C***H***=C***H***-), 6.30-7.40 (aromatic protons). ^{13}C NMR (75 MHz, CD_2Cl_2, ppm): δ 28.0-29.0, 35.5-38.5, 40.5-47.5, 51.8, 80.4, 126, 128, 145, 174, 176.

ROMP-based synthesis of molecular brushes with triblock side chains (PNB-*g*-(PS-*b*-PMA-*b*-P*t*BA)).

To a solution of Grubbs' catalyst in CH_2Cl_2 (4.2 mg/mL, 100 μL, 1 equiv.) under argon in a scintillation vial capped with a septum was added the NB-PS-*b*-PMA-*b*-P*t*BA solution in CH_2Cl_2 (73.1 mg/mL, 1000 μL, 100 equiv.) *via* a syringe. The reaction was allowed to stir at room temperature for 1 h and the molecular brush product was obtained after quenching the reaction by ethyl vinyl ether (EVE) and precipitating the reaction mixture in methanol. Yield: 69.2 mg (95%). $M_n^{calc} = 1.59\times10^6$ Da, $M_n^{GPC} = 1.51\times10^6$ Da, PDI=1.15. T_g: 93 °C, 43 °C, 11 °C. IR (cm^{-1}): 3100-2800 (medium-strong, broad), 1943 (medium-weak), 1738 (very strong, broad), 1601 (medium-weak), 1448 (medium-strong), 1371 (strong), 1256 (medium-strong), 1164 (strong, broad), 845 (medium), 757 (medium-weak). ^{1}H NMR (300 MHz, CD_2Cl_2, ppm): δ 1.20-2.05 (polymer backbone protons), 1.25-1.60 (-C(C$\boldsymbol{H_3}$)$_3$ of *t*BA), 2.10-2.58 (grafted side chain backbone protons), 3.50-3.66 (-OC$\boldsymbol{H_3}$ of MA), 6.36-7.30 (aromatic protons). ^{13}C NMR (75 MHz, CD_2Cl_2, ppm): δ 28.0-29.0, 35.5-38.5, 40.5-47.5, 51.7, 80.4, 126, 128, 145, 174, 176.

Hydrolysis of NB-PS-*b*-PMA-*b*-P*t*BA to NB-PS-*b*-PMA-*b*-PAA.

NB-PS-*b*-PMA-*b*-PAA (27.8 mg) was loaded into a vial and dissolved in CH_2Cl_2 (5.0 mL). A solution of TMSI (5.0 mL, 2.5 mL TMSI diluted by 15.0 mL CH_2Cl_2) was added. After 90 min, the excess solvent and reagent were removed *in vacuo*. The residue was then redissolved in THF (7 mL) and decolorized by addition of an aqueous solution of $Na_2S_2O_3$ to afford a colorless solution. Dialysis of the solution against nanopure water

for 5 days cleaved the silyl ester bonds and gave the final amphiphilic NB-PS-*b*-PMA-*b*-PAA, which was collected after removal of water by lyophilization. Yield: 17.8 mg (89%). T_g = 93 °C, 11 °C. (T_g for PAA was not observed or overlapped with that of PS.) IR (cm^{-1}): 3500-2750 (very strong, very broad), 1723 (medium), 1601 (medium-strong), 1492 (medium-strong), 1452 (medium-strong), 1368 (medium-weak), 1168 (medium), 1026 (weak), 825 (medium), 698 (medium). ^{1}H NMR (300 MHz, THF-d_8, ppm): δ 1.20-2.58 (polymer backbone protons), 3.50-3.66 (-OC***H*****$_3$** of MA), 6.36-7.40 (aromatic protons), 10.80-11.60 (-COO***H***). ^{13}C NMR (75 MHz, THF-d_8, ppm): δ 33.4-37.5, 40.5-47.5, 51.3, 126, 128, 144, 172, 174.

Hydrolysis of PNB-*g*-(PS-*b*-PMA-*b*-P*t*BA) to PNB-*g*-(PS-*b*-PMA-*b*-PAA).

PNB-*g*-(PS-*b*-PMA-*b*-P*t*BA) (27.4 mg) was loaded into a vial and dissolved in CH_2Cl_2 (5.0 mL). A solution of TMSI (5.0 mL, 2.5mL TMSI diluted by 15.0 mL CH_2Cl_2) was added. After 90 min, the excess solvent and reagent were removed *in vacuo*. The residue was then redissolved in THF (7 mL) and decolorized by addition of an aqueous solution of $Na_2S_2O_3$ to afford a colorless solution. Dialysis of the solution against nanopure water for 5 days cleaved the silyl ester bonds and gave the final amphiphilic PNB-*g*-(PS-*b*-PMA-*b*-PAA), which was collected after removal of water by lyophilization. Yield: 17.2 mg (88%). T_g= 93 °C, 10 °C. IR: 3500-2750 (very strong, very broad), 1723 (medium), 1600 (medium-strong), 1492 (medium-strong), 1452 (medium-strong), 1366 (medium-weak), 1168 (medium), 1026 (weak), 845 (medium), 698 (medium). ^{1}H NMR (300 MHz, THF-d_8, ppm): δ 1.20-2.58 (polymer backbone protons), 3.50-3.66 (-OC***H*****$_3$** of MA), 6.36-

7.38 (aromatic protons), 10.60-11.40 (-COO***H***). ^{13}C NMR (75 MHz, THF-d_8, ppm): δ 33.0-37.5, 40.5-46.8, 51.2, 126, 128, 144, 172, 174.

Self assembly of amphiphilic macromolecules to nanostrcutres.

The general procedure was: PNB-*g*-(PS-*b*-PMA-*b*-PAA) or NB-PS-*b*-PMA-*b*-PAA (10.0 mg) was dissolved in DMF (2.0 mL) to afford a clear solution, which was then dialyzed against nanopure water for 5 days to afford the self assembled nanostructures. Water was changed 3 times a day.

General protocol for sample preparation for AFM imaging.

A drop of the nanostructure solution (2 μL) was deposited directly onto a freshly cleaved mica and allowed to incubate under ambient conditions for 5 min. After the extra solution was blotted off, the mica was dried at room temperature.

General protocol for sample preparation for TEM imaging.

A drop of the nanostructure solution (5 μL) was deposited directly onto a carbon-coated copper TEM grid and allowed to incubate under ambient conditions for 5 min. After the extra solution was blotted off, the grid was dried at room temperature and stained by either 1.0% PTA solution or RuO_4 vapor.

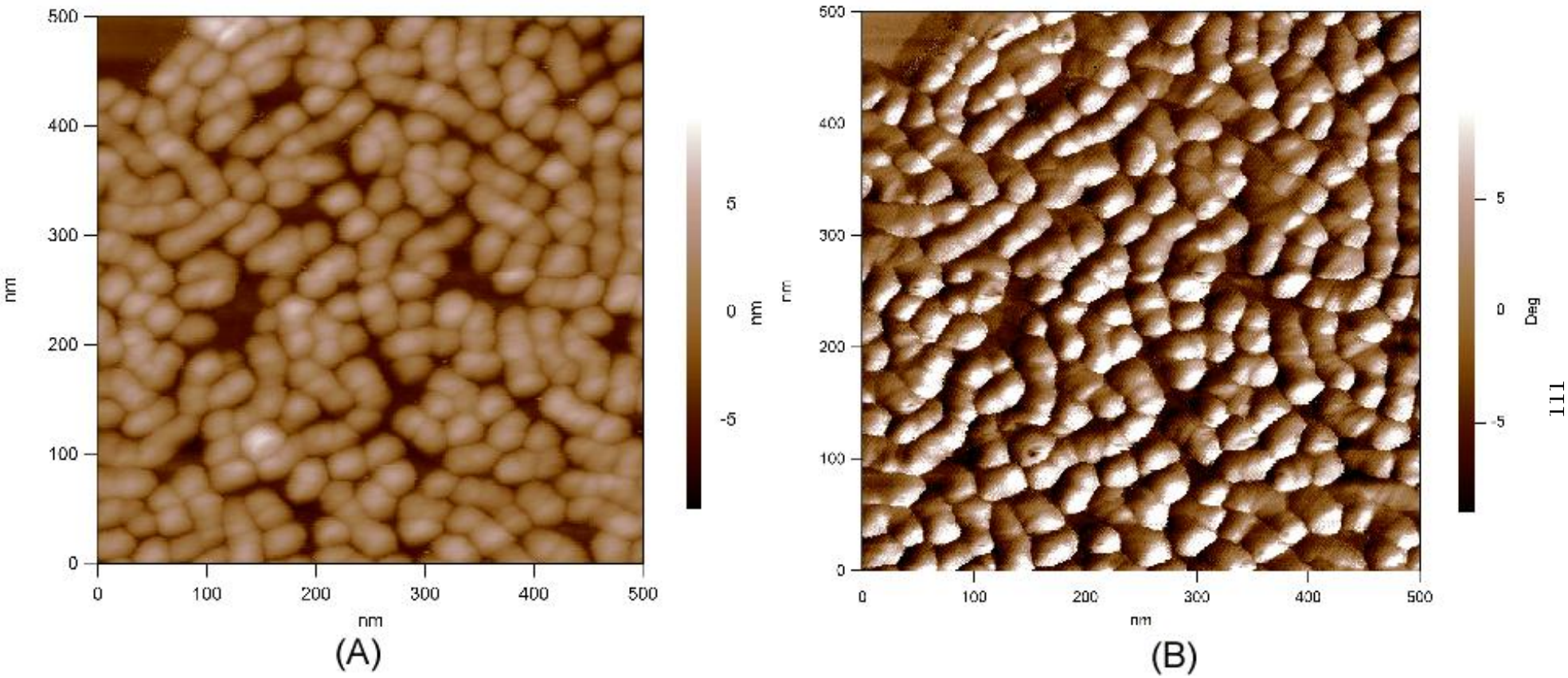

Figure 4-4. AFM images of the hierarchical cylindrical nanostructures from PNB-*g*-(PS-*b*-PMA-*b*-PAA) self-assembled in aqueous solution. (A) Height image. (B) Phase image.

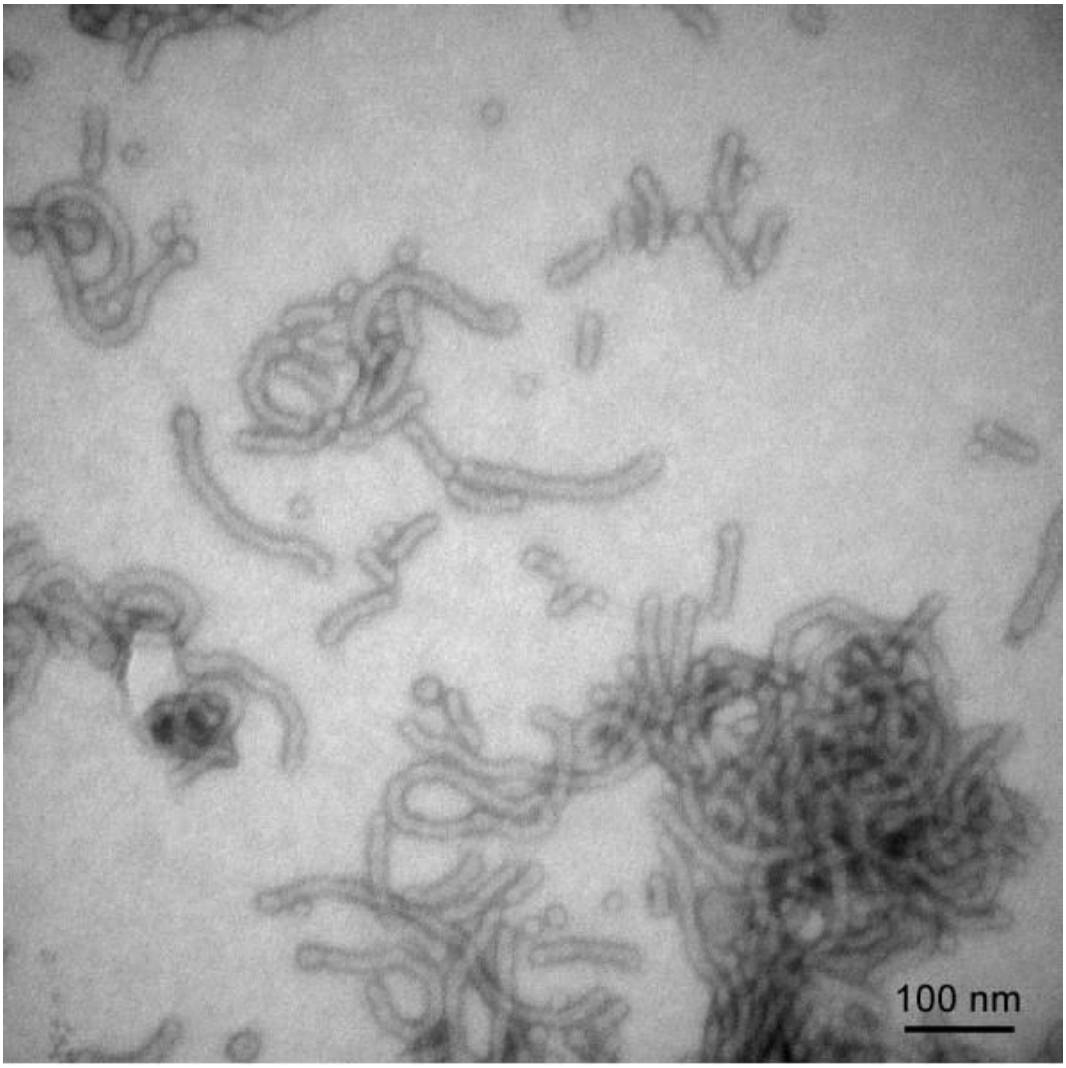

Figure 4-5. TEM image of the re-assembled cylindrical nanostructures. The sample solution was prepared from the disassembled PNB-*g*-(PS-*b*-PMA-*b*-PAA), which was collected by lyophilization and redissolved in DMF, and then dialyzed against water. The sample was stained with 1.0% PTA solution.

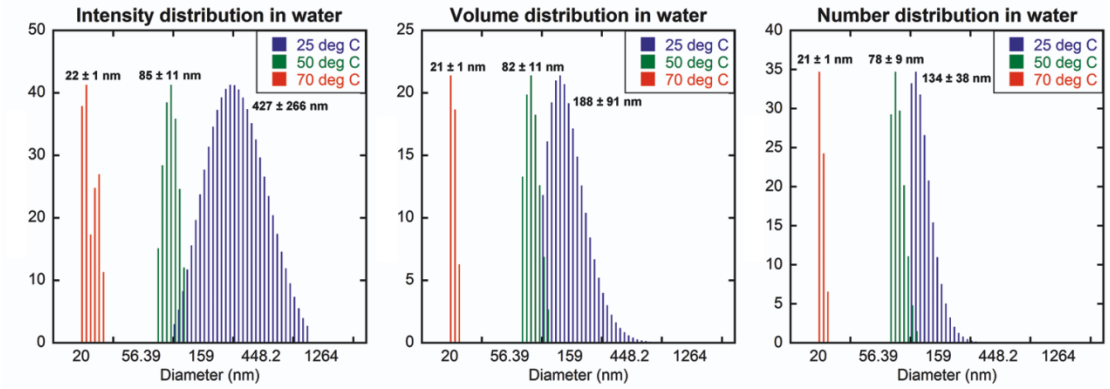

Figure 4-6. DLS histograms of the dynamic hierarchical nanostructures of PNB-*g*-(PS-*b*-PMA-*b*-PAA) in aqueous solutions at different temperatures (blue: 25 ^{o}C, green: 50 ^{o}C, and red: 70 ^{o}C). (All the histograms are normalized and the values along the y axis do not reflect the real physical values).

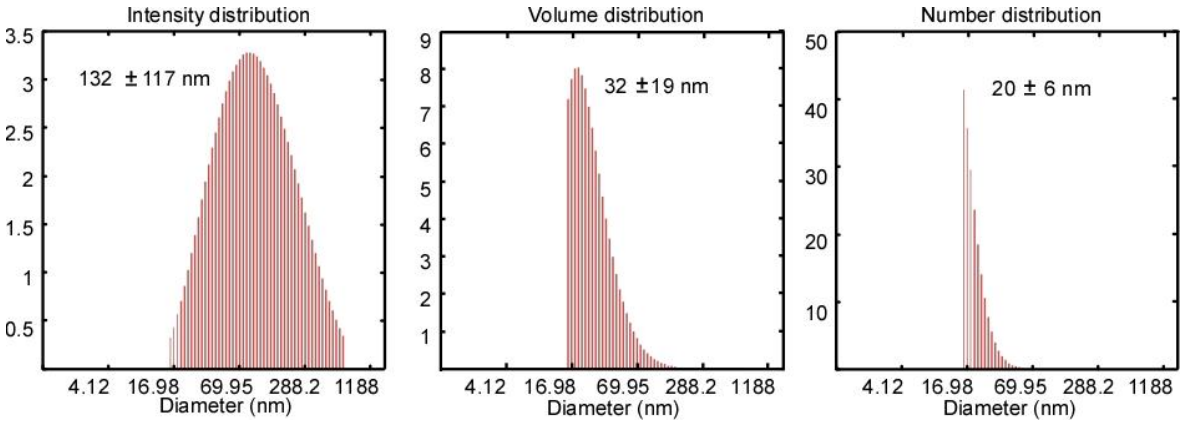

Figure 4-7. DLS histograms of PNB-*g*-(PS-*b*-PMA-*b*-PAA) in DMF solution before dialysis.

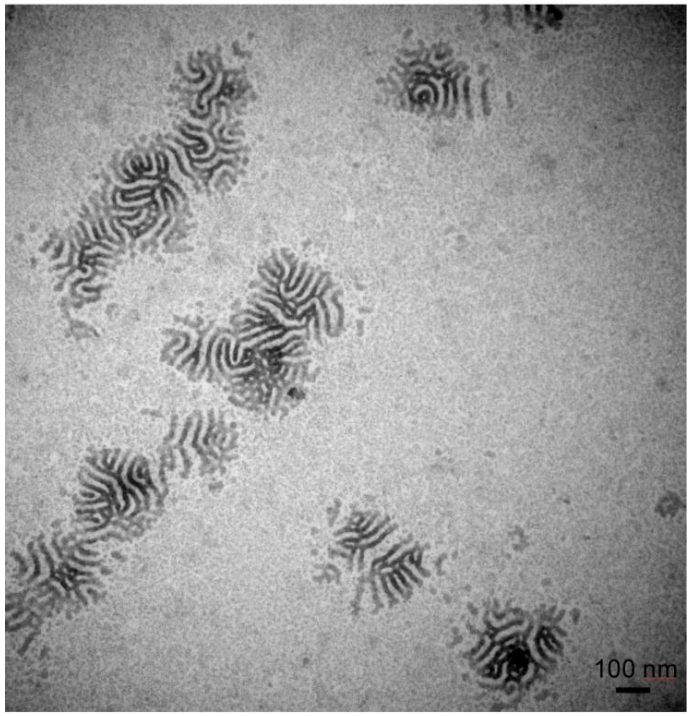

Figure 4-8. TEM image of the patterns dried from the DMF solution of PNB-*g*-(PS-*b*-PMA-*b*-PAA). The sample was stained with RuO_4 vapor.

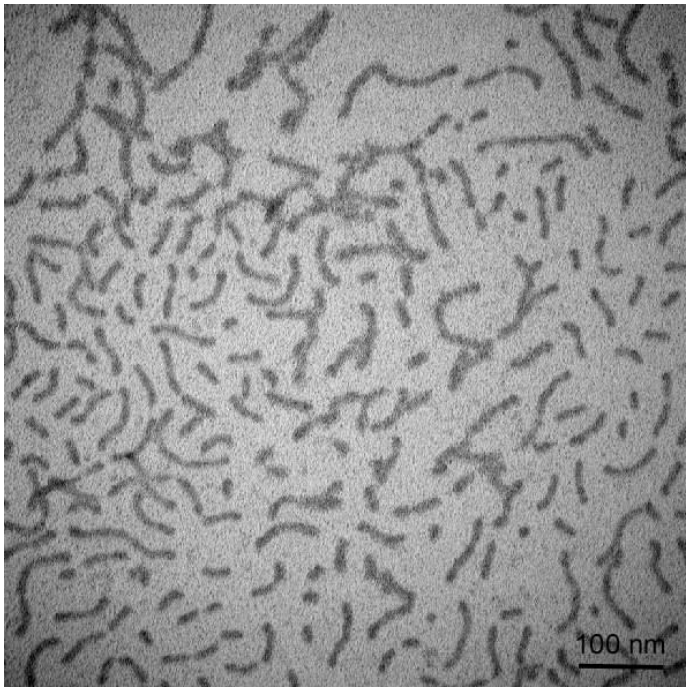

Figure 4-9. TEM image of the hierarchical structures self-assembled from PNB-*g*-(PS-*b*-PMA-*b*-PAA) in aqueous solution. The sample was stained with RuO_4 vapor.

References

(1) G. M. Whitesides and B. Grzybowski "Self-assembly at all scales." *Science* **2002**, *295*, 2418-2421.

(2) C. M. Dobson "Protein folding and misfolding." *Nature* **2003**, *426*, 884-890.

(3) S. G. Zhang "Molecular self-assembly - Another brick in the wall." *Nat. Nanotechnol.* **2006**, *1*, 169-170.

(4) D. J. Pochan, Z. Y. Chen, H. G. Cui, K. Hales, K. Qi and K. L. Wooley "Toroidal triblock copolymer assemblies." *Science* **2004**, *306*, 94-97.

(5) L. F. Zhang and A. Eisenberg "Multiple morphologies of crew-cut aggregates of polysytene-b-poly(acrylic acid) block-copolymers." *Science* **1995**, *268*, 1728-1731.

(6) E. R. Zubarev, M. U. Pralle, E. D. Sone and S. I. Stupp "Self-assembly of dendron rodcoil molecules into nanoribbons." *J. Am. Chem. Soc.* **2001**, *123*, 4105-4106.

(7) C. A. Mirkin, R. L. Letsinger, R. C. Mucic and J. J. Storhoff "A DNA-based method for rationally assembling nanoparticles into macroscopic materials." *Nature* **1996**, *382*, 607-609.

(8) Z. B. Li, E. Kesselman, Y. Talmon, M. A. Hillmyer and T. P. Lodge "Multicompartment micelles from ABC miktoarm stars in water." *Science* **2004**, *306*, 98-101.

(9) P. W. K. Rothemund "Folding DNA to create nanoscale shapes and patterns." *Nature* **2006**, *440*, 297-302.

(10) V. Percec, D. A. Wilson, P. Leowanawat, C. J. Wilson, A. D. Hughes, M. S. Kaucher, D. A. Hammer, D. H. Levine, A. J. Kim, F. S. Bates, K. P. Davis, T. P. Lodge, M. K. Klein, H. DeVane, E. Aqad, B. M. Rosen, A. O. Argintaru, M. J. Sienkowska, K.

Rissanen, S. Nummelin and J. Ropponen "Self-assembly of Janus dendrimers into uniform dendrimersomes and other complex architectures." *Science* **2010**, *328*, 1009-1014.

(11) X. S. Wang, G. Guerin, H. Wang, Y. S. Wang, I. Manners and M. A. Winnik "Cylindrical block copolymer micelles and co-micelles of controlled length and architecture." *Science* **2007**, *317*, 644-647.

(12) A. Walther, M. Drechsler, S. Rosenfeldt, L. Harnau, M. Ballauff, V. Abetz and A. H. E. Müller "Self-Assembly of Janus Cylinders into Hierarchical Superstructures." *J. Am. Chem. Soc.* **2009**, *131*, 4720-4728.

(13) J. Dupont, G. J. Liu, K. Niihara, R. Kimoto and H. Jinnai "Self-assembled ABC triblock copolymer double and triple helices." *Angew Chem Int Ed* **2009**, *48*, 6144-6147.

(14) P. Yin, H. M. T. Choi, C. R. Calvert and N. A. Pierce "Programming biomolecular self-assembly pathways." *Nature* **2008**, *451*, 318-U4.

(15) X. M. Zhu, U. Beginn, M. Möller, R. I. Gearba, D. V. Anokhin and D. A. Ivanov "Self-organization of polybases neutralized with mesogenic wedge-shaped sulfonic acid molecules: An approach toward supramolecular cylinders." *J. Am. Chem. Soc.* **2006**, *128*, 16928-16937.

(16) O. Ikkala and G. ten Brinke "Functional materials based on self-assembly of polymeric supramolecules." *Science* **2002**, *295*, 2407-2409.

(17) A. Böker, Y. Lin, K. Chiapperini, R. Horowitz, M. Thompson, V. Carreon, T. Xu, C. Abetz, H. Skaff, A. D. Dinsmore, T. Emrick and T. P. Russell "Hierarchical nanoparticle assemblies formed by decorating breath figures." *Nat Mater* **2004**, *3*, 302-306.

(18) R. Jones "Why nanotechnology needs better polymer chemistry." *Nat. Nanotechnol.* **2008**, *3*, 699-700.

(19) S. S. Sheiko, B. S. Sumerlin and K. Matyjaszewski "Cylindrical molecular brushes: Synthesis, characterization, and properties." *Prog. Polym. Sci.* **2008**, *33*, 759-785.

(20) M. F. Zhang and A. H. E. Müller "Cylindrical polymer brushes." *J. Polym. Sci., Part A: Polym. Chem.* **2005**, *43*, 3461-3481.

(21) H. G. Börner, K. Beers, K. Matyjaszewski, S. S. Sheiko and M. Möller "Synthesis of molecular brushes with block copolymer side chains using atom transfer radical polymerization." *Macromolecules* **2001**, *34*, 4375-4383.

(22) C. Cheng, K. Qi, E. Khoshdel and K. L. Wooley "Tandem synthesis of core-shell brush copolymers and their transformation to peripherally cross-linked and hollowed nanostructures." *J Am Chem Soc* **2006**, *128*, 6808-6809.

(23) M. F. Zhang, T. Breiner, H. Mori and A. H. E. Müller "Amphiphilic cylindrical brushes with poly(acrylic acid) core and poly(n-butyl acrylate) shell and narrow length distribution." *Polymer* **2003**, *44*, 1449-1458.

(24) H. F. Gao and K. Matyjaszewski "Synthesis of molecular brushes by "grafting onto" method: Combination of ATRP and click reactions." *J. Am. Chem. Soc.* **2007**, *129*, 6633-6639.

(25) Z. Li, J. Ma, C. Cheng, K. Zhang and K. L. Wooley "Synthesis of hetero-grafted amphiphilic diblock molecular brushes and their self-assembly in aqueous medium." *Macromolecules* **2010**, *43*, 1182-1184.

(26) Y. Xia, J. A. Kornfield and R. H. Grubbs "Efficient synthesis of narrowly dispersed brush polymers via living ring-opening metathesis polymerization of macromonomers." *Macromolecules* **2009**, *42*, 3761-3766.

(27) Y. Xia, B. D. Olsen, J. A. Kornfield and R. H. Grubbs "Efficient synthesis of narrowly dispersed brush copolymers and study of their assemblies: the importance of side-chain arrangement." *J. Am. Chem. Soc.* **2009**, *131*, 18525-18532.

(28) Z. Li, K. Zhang, J. Ma, C. Cheng and K. L. Wooley "Facile syntheses of cylindrical molecular brushes by a sequential RAFT and ROMP 'grafting-through' methodology." *J. Polym. Sci., Part A: Polym. Chem.* **2009**, *47*, 5557-5563.

(29) C. W. Bielawski and R. H. Grubbs "Living ring-opening metathesis polymerization." *Prog Polym Sci* **2007**, *32*, 1-29.

(30) G. Moad, E. Rizzardo and S. H. Thang "Living radical polymerization by the RAFT process." *Aust. J. Chem.* **2005**, *58*, 379-410.

(31) A. Nyström, M. Malkoch, I. Furó, D. Nyström, K. Unal, P. Antoni, G. Vamvounis, C. J. Hawker, K. Wooley, E. Malmström and A. Hult "Characterization of poly(norbornene) dendronized polymers prepared by ring-opening metathesis polymerization of dendron bearing monomers." *Macromolecules* **2006**, *39*, 7241-7249.

(32) W. Buchowicz, M. N. Holerca and V. Percec "Self-inhibition of propagating carbenes in ROMP of 7-oxa-bicyclo 2.2,1 hept-2-ene-5,6-dicarboxylic acid dendritic diesters initiated with Ru(=CHPh)Cl-2(PCy3)(1,3-dimesityl-4,5-dihydroimidazol-2-ylidene)." *Macromolecules* **2001**, *34*, 3842-3848.

(33) V. Percec and D. Schlueter "Mechanistic investigations on the formation of supramolecular cylindrical shaped oligomers and polymers by living ring opening

metathesis polymerization of a 7-oxanorbornene monomer substituted with two tapered monodendrons." *Macromolecules* **1997**, *30*, 5783-5790.

(34) C. Cheng and N. L. Yang "Well-Defined Diblock Macromonomer with a Norbornene Group at Block Junction: Anionic Living Linking Synthesis and Ring-Opening Metathesis Polymerization." *Macromolecules* **2010**, *43*, 3153-3155.

Chapter 5

Random-grafted diblock molecular brushes

[Zhou Li, Jun Ma and Karen Wooley, unpublished work]

Synthesis of PPFS-POSS molecular brush copolymers with tunable PPFS/POSS ratios and study of their assemblies

ABSTRACT

We have synthesized a series of 9 PPFS-POSS molecular brush copolymers whose PPFS/POSS ratios are adjusted from 0.1 to 0.9 with an increment of 0.1 by an efficient and facile "grafting through" strategy, and assembled them into complicated nanostructure in 9/1 acetone/methanol. Characterization reveals that PPFS/POSS ratios in molecular brush architecture do not affect the sizes and morphologies of the resulting nanostructures, but can influence their mechanical properties significantly. Decreased amount of PPFS content in molecular brush copolymers leads to flexible and looser nanostructures and increased amount PPFS content leads to rigid and stiff nanostructures. By comparison of nanostructures from molecular brush random copolymers and molecular brush block copolymers, it is found that proper arrangement of PPFS blocks and POSS blocks in the molecular brush architecture may enhance the intermolecular interactions among molecular brushes and leads to stiffer nanostructures.

INTRODUCTION

Well-defined functional nanostructures are of great interest as tailor made materials which are important in many fields like materials science and biomedicine.(1-10) Polymers have been used to construct nanostructures whose physical properties can be adjusted to meet the practical requirements in various circumstances. By tuning the polymer compositions and self assembly conditions, a variety of nanostructures with different properties have been prepared and studied.(11-14) Among all the interesting properties of nanostructures, mechanical properties such as rigidity and flexibility have been rarely studied.

Polyhedral oligomeric silsequioxanes (POSS) is regarded generally as the smallest possible silica nanoparticle with a diamter around 1.5 nm.(15, 16) As an organic-inorganic hybrid compound, POSS materials have been widely used to improve the mechanical and thermal properties of polymers and found wide applications in space shuttles, coatings, nanocomposities.(17-19) Fluorine-containing polymers are important materials for anti-fouling applications as bulk surface materials and as discreate nanoscale objects.(20-25) In this study, we have prepared a series of PPFS-POSS molecular brush copolymers with different PPFS/POSS ratios, and studied the mechanical properties of their nanostructures.

RESULTS AND DISCUSSION

The macromonomers (NB-PPFS and NB-POSS) were synthesized by RAFT polymerization (26, 27) and chain end modification respectively. Their well-controlled structures were confirmed by both ^{1}H NMR spectroscopy and gel permeation

chromatography (GPC). In ^{1}H NMR spectrum of NB-PPFS, the integral ratio of the norbornene alkenyl protons (6.02-6.10 ppm) to the RAFT agent chain end C***H*****$_2$**SC(S)S methylene protons (3.30-3.56 ppm) was 1:1.03, suggesting the suppression of participation of norbornene groups in radical polymerization. GPC analysis revealed that NB-PPFS had mono-modal molecular weight distributions with polydispersity (PDI) of 1.12. In ^{1}H NMR spectrum of NB-POSS, the signal that corresponds to alkenyl protons in maleimide moiety (6.68 ppm) almost disappeared and a new peak at 6.51 ppm showed up, which is assigned to oxo-norbornene alkenyl protons. The ratio of these two peaks is 0.02:1 in the product, indicating 98% incorporation efficiency of ROMP active functional groups to POSS macromonomers.

Various PPFS-POSS molecular brush copolymers were synthesized parallelly from NB-PPFS and NB-POSS macromonomers by copolymerizing them using ring opening metathesis polymerization (ROMP).(28-32) The molar ratios of POSS to PPFS in the molecular brush architectures can be tuned easily from 0.1 to 0.9 with an increment of 0.1 (**Figure 5-1.A**) by changing the feeding amounts of macromonomers in the polymerization while keeping all the other reaction conditions the same. The molar raio of NB-POSS in the molecular brush is defined as *x*. Within a hour, nine different PPFS-POSS molecular brush copolymers were synthesized. **Figure 5-2.B** shows the GPC profile from the synthesis of the PPFS-POSS molecular brush copolymers in which PPFS/POSS ratio was 3/7. The macromonomer peaks at 23.5 -26.0 min were decreased and a new peak appeared at the low retention time region with PDI of 1.23, indicating that lmost all the macromonomers were converted into the molecular brush structure.

The residual peaks at 23.5 -26.0 min in the moleuclar brushe product can be explained by incomplete functionalization of macromonomers. Some of the polymer chains were capped by moieties from the cleaved AIBN initiators in RAFT polymerization and the formation of oxo-norbornene functionalities by [4+2] cycloaddition from maleimide is not 100% quantitative.

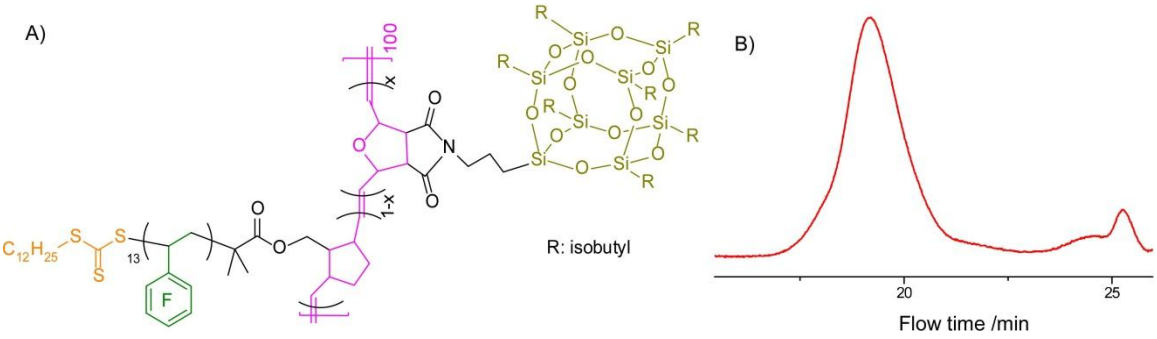

Figure 5-1. A) Structures of PPFS-POSS molecular brush copolymers where x varies from 0.1 to 0.9 with an increment of 0.1. B) GPC profile of $[(PNB\text{-}g\text{-}PPFS)_{0.3}\text{-}co\text{-}(PNB\text{-}g\text{-}POSS)_{0.7}]_{100}$ molecular brush copolymer.

The solution state self assembly behavior of the nine PPFS-POSS molecular brush copolymers was studied in 9/1 acetone/methanol, which is a good solvent for PPFS block but a nonsolvent for POSS block. All of the nanostructures exhibited globular morphology under transmission electron microscopy (TEM). Their size distribution is broader than those nanostructures self-assembled from linear copolymers due to the relatively larger sizes of the building blocks. The comparison of the diameters of these nanostructures indicates that their size difference is within their size variation range. In the 9 PPFS-POSS molecular brush architectures, the lengths of PPFS and POSS blocks

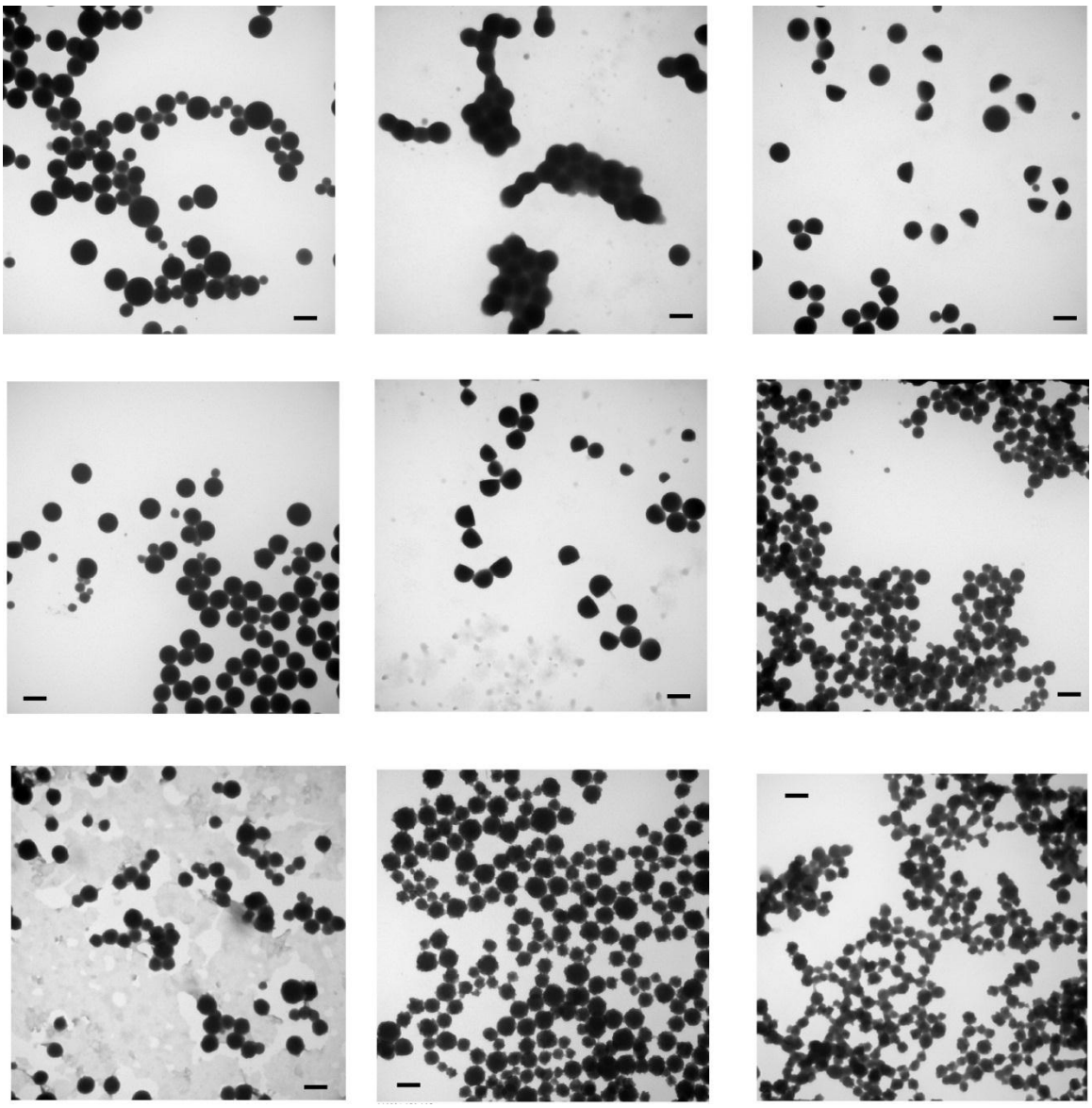

Figure 5-2. TEM images of nanostructures self assembled from various PPFS-POSS molecular brush copolymers. From left to right, at the upper row, x = 0.1, 0.2 and 0.3; at the middle row, x= 0.4, 0.5 and 0.6; at the bottom row, x = 0.7, 0.8 and 0.9. Scale bar: 500 nm.

are unchanged while their relative volumes are altered. The TEM observation agrees with the micellization theory that the size and morphologies of the self assembled nanostructures indicates that their size difference is within their size variation range.(33) In the 9 PPFS-POSS molecular brush architectures, the lengths of PPFS an POSS blocks are unchanged while their relative volumes are altered. The TEM observation agrees with the micellization theory that the size and morphologies of the self assembled nanostructures are controlled mainly by the lengths of the homopolymer sub-units in the linear block copolymers. The geometric regularity of those nanostructures reveals some information regarding to their intrinsic mechanical properties. It was found that those nanostructures made from molecular brushes bearing high PPFS content tends to exhibits perfect spherical curvatures (x = 0.1 - 0.5). When PPFS content of the molecular brush is lowered, irregular and uneven structures will dominate (x = 0.7 -0.9). For example, "flower-like" nanostructures can be found in the sample where x =0.8.

Several possible explanations can be proposed for this phenomenon. First, π-π stacking of PPFS blocks may be the primary interactions which stabilize molecular brushes within the nanostructure framework, thus lowering the PPFS content decreases the interactions among molecular brushes and makes the structures loose. Second, the low surface energy character of PPFS blocks may lead to strong expulsive forces between nanoparticles and the TEM grid surfaces, which is weakened by lowering PPFS content. Therefore, the low PPFS nanostructures are attached to the surface more attractively and deformation may occur to yield irregular structures.

More insights regarding to the mechanical properties of the self assembled nanostructures can be provided by other features that were captured by TEM, along with the nano-

spheres in Figure 5-2. Some "cup-like" nanostructures were noticed in TEM images of the samples prepared from PPFS-POSS molecular brush copolymer where x = 0.4 (**Figure 5-3.A**). Similar structures were also noticed in the samples in which x = 0.3 and 0.5. Those "cup-like" structures may be from the fall-over of the nano-sphere particles, which were absorbed onto the grid surface initially. During sample preparation, they may take a tumble and the previous contact surface of the nano-spheres and grid surface were exposed to form the "cup-like" structures (**Figure 5-3.C**). TEM samples where x =

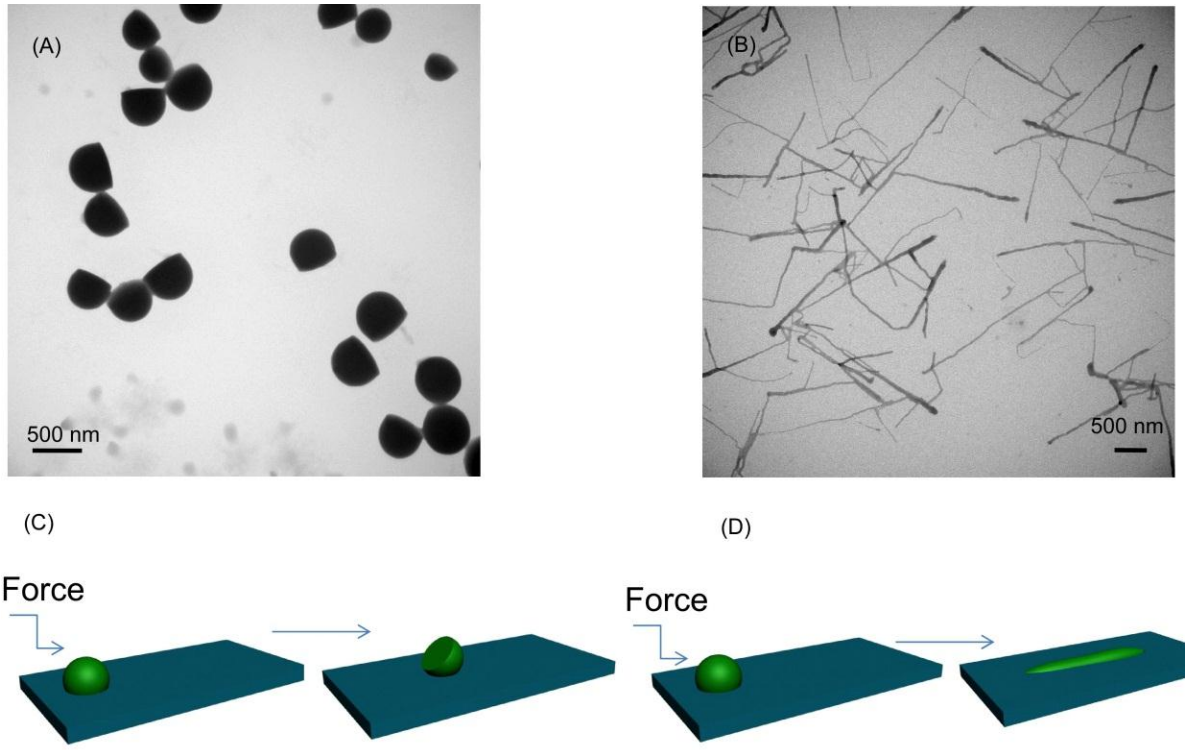

Figure 5-3. A) "Cup-like" features observed on the TEM images of nanostructures self assembled $[(\text{PNB-}g\text{-PPFS})_{0.6}\text{-}co\text{-}(\text{PNB-}g\text{-POSS})_{0.4}]_{100}$ molecular brush copolymers. B) "Fiber-like" features observed on the TEM images of nanostructures self assembled $[(\text{PNB-}g\text{-PPFS})_{0.1}\text{-}co\text{-}(\text{PNB-}g\text{-POSS})_{0.9}]_{100}$ molecular brush copolymers. C) Illustration of the formation of "cup-like" features. D). illustration of the formation of "fiber-like" features.

0.9 exhibited some "fiber-like" features with uneven characteristics (**Figure 5-3.B**), whose one end is darker and thicker than the other. After being attached to the grid surface, nano-spheres moved a few micrometers from one location to another and left a trace while the nanostructures were deformed. These phenomena indicated that the stiffness of the nanoparticles is highly influenced by the PPFS/POSS ratio and nanostructure with higher PPFS content is difficult to be destructed by external forces. Lower ratio of PPFS leads to looser nanostructures which can be deformed by the stronger nanostructure-surface attractive interactions.

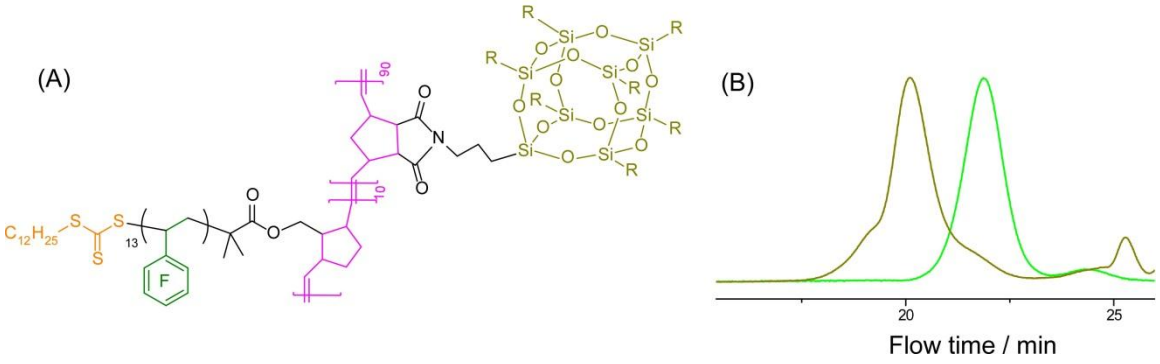

Figure 5-4. A) Structures of [PNB-*g*-PPFS]$_{10}$-*b*-[PNB-*g*-POSS]$_{90}$ hetero-grafted diblock molecular brushes. B) GPC profiles from the synthesis of [PNB-*g*-PPFS]$_{10}$-*b*-[PNB-*g*-POSS]$_{90}$ (green: the first block of the molecular brushes; yellow: the total diblock molecular brushes).

It is interesting to change the arrangement of PPFS and POSS side chains in the molecular brush architecture and study their self assembly behaviors. To achieve this goal, hetero-grafted diblock molecular brushes were synthesized, in which the NB-PPFS and NB-POSS macromonomers were distributed sequentially along the backbone

(**Figure 5-4**). Like the procedure that has been described in Chapter 3, brush copolymer PNB_{10}-*g*-PPFS was synthesized by ROMP of NB-PPFS in CH_2Cl_2 first, followed by addition of a solution NB-POSS into the living polymerization mixture without purification to afford the diblock brush copolymer $[PNB\text{-}g\text{-}PPFS]_{10}$-*b*-$[PNB\text{-}g\text{-}POSS]_{90}$ with regio-selective grafts. During ROMP, small aliquots were withdrawn and measured by GPC. As shown in **Figure 5-4.B**, nearly quantitative conversions of NB-PPFS was observed during the construction of the first block of the brush polymer structure. More NB-POSS macromonomer residuals were left after the second step ROMP, due to the high steric effect from the bulky POSS side chains. Both PNB_{10}-*g*-PPFS and $[PNB\text{-}g\text{-}PPFS]_{10}$-*b*-$[PNB\text{-}g\text{-}POSS]_{90}$ have mono-modal molecular weight distributions and narrow PDIs (<1.20). NB-POSS was introduced successfully to produce an overall diblock backbone structure, as demonstrated by the evolution peak shift by GPC. The resulting hetero-grafted molecular brushes were assembled into nanostructures by the same technique used to assemble PPFS-POSS molecular brush copolymers before. In comparison with nanostructures made from $[(PNB\text{-}g\text{-}PPFS)_{0.1}\text{-}co\text{-}(PNB\text{-}g\text{-}POSS)_{0.9}]_{100}$ molecular brush copolymers, those from $[PNB\text{-}g\text{-}PPFS]_{10}$-*b*-$[PNB\text{-}g\text{-}POSS]_{90}$ hetero-grafted diblock molecular brushes have more regular geometry (**Figure 5-5**) and no "fiber-like" features were observed, suggesting that proper arrangement of PPFS and POSS blocks enhanced the intermolecular interactions among molecular brushes and leads to stiffer nanostructures. When PPFS/POSS ratio is low and PPFS side chains are distributed randomly in molecular brush architecture, it is different for molecular brushes to interpenetrate with each other so that all PPFS side chains encounter counterparts. Selectively accumulating PPFS block in specific regions of molecular brush architecture

increases this possibility and thus lead to strong intermolecular interactions among molecular brushes.

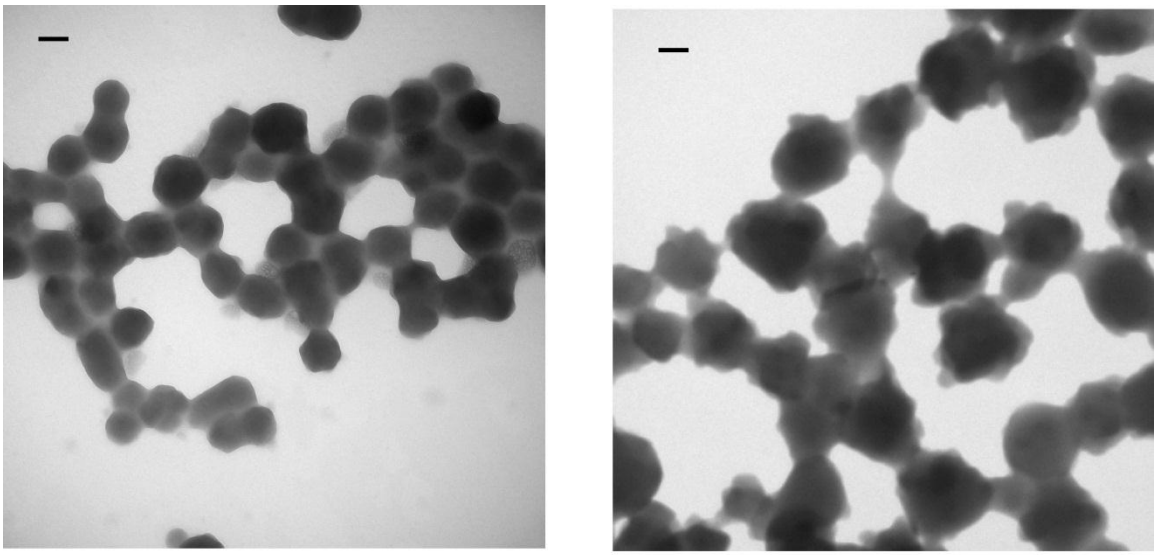

Figure 5-5. A) TEM image of nanostructures self assembled from [PNB-*g*-PPFS]$_{10}$-*b*-[PNB-*g*-POSS]$_{90}$ hetero-grafted diblock molecular brushes. B) TEM image of nanostructures self assembled from [(PNB-*g*-PPFS)$_{0.1}$-*co*-(PNB-*g*-POSS)$_{0.9}$]$_{100}$ molecular brush copolymers. Scale bar: 100 nm.

In conclusion, a series of PPFS-POSS molecular brush copolymers have been synthesized by an efficient and facile "grafting through" strategy, by which the PPFS/POSS ratio of the molecular brushes is adjusted simply by changing the feeding amounts of macromonomers. Nanostructures built from these molecular brushes exhibited similar sizes and morphologies; however their mechanical properties varied with the PPFS/POSS

ratio. Lower PPFS ratio leads to flexible and looser assembled nanostructures, while higher PPFS ratio leads to rigid and stiffer nanostructures. At lower PPFS ratio, proper arrangement of PPFS and POSS blocks in the architecture may enhance the rigidity and stiffness of the nanostructures.

EXPERIMENTAL

Materials

POSS® Maleimide Isobutyl was purchased from Hybrid Plastics. Azobisisobutyronitrile (AIBN, 98%, Sigma-Aldrich) was recrystallized from methanol before use. 2,3,4,5,6-Pentafluorostyrene (PFS, 99%, Sigma-Aldrich), was passed through neutral alumina column before polymerizations. The Grubbs' catalyst and the norbornenyl-functionalized RAFT chain transfer agent (NB-CTA) were prepared by the methods reported.(28, 29)

Synthesis of α-norbornenyl polypentafluorostyrene (NB-PPFS).

The polymer was prepared from the polymerization mixture of PFS (14.06 g, 72.4 mmol), NB-CTA (682.3 mg, 1.448 mmol), AIBN (11.2 mg, 6.8×10^{-2} mmol) at 55 °C. The polymerization was quenched after 20 h when the monomer conversion was measured to be 30% by ^{1}H NMR spectroscopy. The final polymer was isolated by precipitating the polymer solution into methanol and washed by methanol three times. The isolated yield was 3.12 g (74 %, based on the conversion of PFS). M_n^{calc} = 3382 Da, M_n^{GPC} = 2800 Da, PDI = 1.12. IR (cm^{-1}): 2932, 2857, 2640, 2360, 2340, 1725, 1652, 1519, 1504, 1461, 1418, 1367, 1304, 1219, 1132, 1085, 982, 961, 911, 873, 811, 737, 668, 653. ^{1}H NMR

(300 MHz, $CDCl_3$, ppm): δ 0.80-0.95 (-C***H***$_3$ of the RAFT chain end and backbone protons), 1.00-2.80 (alkyl protons of RAFT agent and polypentafluorostyrene backbone protons), 2.74-2.79 (>C***H***-CH=CH-C***H***<), 3.23-3.50 (-C***H*****$_2$**SC(S)S-), 3.50-4.00 (-C***H*****$_2$**OC(O)C$(CH_3)_2$), 5.30-5.50 (-C_6F_5C***H***SC(S)S$C_{12}H_{25}$), 6.03-6.16 (-C***H***=C***H***-). ^{13}C NMR (75 MHz, $CDCl_3$, ppm): δ 28.0-30.0, 31.0-32.5, 36.0-40.0, 114, 136, 139,143,146.

Synthesis of α-norbornenyl POSS Isobutyl (NB-POSS).

The chain end modification of POSS Maleimide Isobutyl was done by mixing furan (1.5 g, 22.1 mmol), POSS maleimide isobutyl (10.0 g, 10.4 mmol) in 15mL toluene. The reaction was stirred at 70 ^{o}C for 36 h. After removing the excess furan by vacuum, the product was collected by precipitation in cold methanol three times. Yield: 5.8 g (54 %). M_n = 1023 Da. IR (cm^{-1}): 2954, 2870, 1775, 1704, 1464, 1401, 1366, 1331, 1230, 1101, 1038, 956, 920, 879, 838, 742, 649. ^{1}H NMR (300 MHz, $CDCl_3$, ppm): δ 0.52-0.70 (-SiC***H*****$_2$**CH$(CH_3)_2$ and -SiC***H*****$_2$**CH_2CH_2-), 0.86-1.04 (-$SiCH_2$CH(C***H*****$_3$**$)_2$), 1.56-1.76 (-$SiCH_2$C***H*****$_2$**CH_2-), 1.76-1.96 (-$SiCH_2$C***H***$(CH_3)_2$), 2.80-2.86 (-C(O)C***H***(CH)-C***H***(CH)C(O)-), 3.40-3.52 (>NC***H*****$_2$**CH_2CH_2-), 5.22-5.26 (-C***H***-O-C***H***- of oxo-norbornenyl groups), 6.48-6.56 (-C***H***=C***H***-).

ROMP-based synthesis of PPFS-POSS molecular brush copolymers with varying PPFS/POSS ratio.

Three stock solutions were prepared: 1) NB-PPFS solution (0.7327 g NB-PPFS polymer was dissolved in 5.00 mL CH_2Cl_2, 5.23 × 10^{-2} mmol/mL); 2) NB-POSS solution (0.2677g NB-POSS polymer was dissolved in 5.00 mL CH_2Cl_2,.5.23 × 10^{-2} mmol/mL); 3) Grubbs' catalyst solution (0.0076 g the modified 2nd generation Grubbs catalyst was

dissolved in 1.95 mL CH_2Cl_2, 5.23×10^{-3} mmol/mL). Nine PPFS-POSS molecular brush copolymers were synthesized from the same stock solutions by adjusting the feeding amount of NB-PPFS and NB-POSS. To vial 1, 0.90 mL solution 1 and 0.10 mL solution 2 were mixed; to vial 2, 0.80 mL solution 1 and 0.20 mL solution 2 were mixed… By decreasing the volume of solution 1 by a decrement of 0.10 mL and increasing the volume of solution 1 by an increment of 0.10 mL, nine vials of mixtures of NB-PPFS and NB-POSS can be obtained. To all the vials, 0.10 mL solution 3 was added to trigger the ROMP and all the reactions were quenched by ethyl vinyl ether after 2 h. Nine PPFS-POSS molecular brush copolymers can be obtained by precipitating the polymer solutions in methanol.

ROMP-based synthesis of PPFS-POSS hetero-grafted molecular brush copolymers.

To a solution of Grubbs' catalyst in CH_2Cl_2 (9.7 mg/mL, 1.8 mL, 1 equiv.) under nitrogen in a scintillation vial capped with a septum was added a CH_2Cl_2 solution of **NB-PPF**S (99.6 mg/mL, 5.0 mL, 50 equiv.) *via* an nitrogen-flushed syringe. The reaction was allowed to stir at room temperature for 3 min, and an aliquot of the reaction mixture (100 μL) was withdrawn (for the analysis of the first block) (PDI=1.08). After that, a CH_2Cl_2 solution of **NB-POSS** (237.1 mg/mL, 6.2 mL, 50 equiv) was added to the living polymerization mixture immediately to allow for the second ROMP reaction. Another 3 min later, the polymerization was quenched by addition of a small amount of ethyl vinyl ether. The final diblock molecular brush was obtained after precipitating the reaction mixture in methanol.

Construction of nanostructures from molecular brush copolymers in 9/1 acetone/methanol.

Molecular brush copolymer solutions were prepared in CH_2Cl_2 first at a high concentration (100mg/mL). 100 μL of each solution was added to 9/1 acetone/methanol (10 mL) slowly to trigger the self-assembly of molecular brushes. During the addition, the solution was kept stirring. After that, all the self-assembled solutions were sealed and kept at RT for 3 days before TEM analysis.

REFERENCES

(1) A. Bianco, K. Kostarelos and M. Prato "Applications of carbon nanotubes in drug delivery." *Curr. Opin. Chem. Biol.* **2005**, *9*, 674-679.

(2) N. Nasongkla, E. Bey, J. M. Ren, H. Ai, C. Khemtong, J. S. Guthi, S. F. Chin, A. D. Sherry, D. A. Boothman and J. M. Gao "Multifunctional polymeric micelles as cancer-targeted, MRI-ultrasensitive drug delivery systems." *Nano Lett.* **2006**, *6*, 2427-2430.

(3) I. Roy, T. Y. Ohulchanskyy, D. J. Bharali, H. E. Pudavar, R. A. Mistretta, N. Kaur and P. N. Prasad "Optical tracking of organically modified silica nanoparticles as DNA carriers: A nonviral, nanomedicine approach for gene delivery." *Proc. Natl. Acad. Sci. U. S. A.* **2005**, *102*, 279-284.

(4) L. Zhang, F. X. Gu, J. M. Chan, A. Z. Wang, R. S. Langer and O. C. Farokhzad "Nanoparticles in medicine: Therapeutic applications and developments." *Clin. Pharmacol. Ther.* **2008**, *83*, 761-769.

(5) J. H. Gao, H. W. Gu and B. Xu "Multifunctional Magnetic Nanoparticles: Design, Synthesis, and Biomedical Applications." *Accounts Chem. Res.* **2009**, *42*, 1097-1107.

(6) S. Helveg, C. Lopez-Cartes, J. Sehested, P. L. Hansen, B. S. Clausen, J. R. Rostrup-Nielsen, F. Abild-Pedersen and J. K. Norskov "Atomic-scale imaging of carbon nanofibre growth." *Nature* **2004**, *427*, 426-429.

(7) H. A. Becerril, J. Mao, Z. Liu, R. M. Stoltenberg, Z. Bao and Y. Chen "Evaluation of solution-processed reduced graphene oxide films as transparent conductors." *ACS Nano* **2008**, *2*, 463-470.

(8) M. Lazzari and M. A. Lopez-Quintela "Block copolymers as a tool for nanomaterial fabrication." *Adv. Mater.* **2003**, *15*, 1583-1594.

(9) C. A. Mirkin, R. L. Letsinger, R. C. Mucic and J. J. Storhoff "A DNA-based method for rationally assembling nanoparticles into macroscopic materials." *Nature* **1996**, *382*, 607-609.

(10) P. W. K. Rothemund "Folding DNA to create nanoscale shapes and patterns." *Nature* **2006**, *440*, 297-302.

(11) H. G. Cui, Z. Y. Chen, S. Zhong, K. L. Wooley and D. J. Pochan "Block copolymer assembly via kinetic control." *Science* **2007**, *317*, 647-650.

(12) Z. Y. Chen, H. G. Cui, K. Hales, Z. B. Li, K. Qi, D. J. Pochan and K. L. Wooley "Unique toroidal morphology from composition and sequence control of triblock copolymers." *J. Am. Chem. Soc.* **2005**, *127*, 8592-8593.

(13) S. Zhong, H. G. Cui, Z. Y. Chen, K. L. Wooley and D. J. Pochan "Helix self-assembly through the coiling of cylindrical micelles." *Soft Matter* **2008**, *4*, 90-93.

(14) Z. B. Li, E. Kesselman, Y. Talmon, M. A. Hillmyer and T. P. Lodge "Multicompartment micelles from ABC miktoarm stars in water." *Science* **2004**, *306*, 98-101.

(15) J. D. Lichtenhan "Polyhedral oligomeric silsesquioxanes - building-blocks for silsesquioxane-based polymers and hybrid materials." *Comments Inorganic Chem.* **1995**, *17*, 115-130.

(16) G. Z. Li, L. C. Wang, H. L. Ni and C. U. Pittman "Polyhedral oligomeric silsesquioxane (POSS) polymers and copolymers: A review." *J. Inorg. Organomet. Polym.* **2001**, *11*, 123-154.

(17) H. Y. Xu, S. W. Kuo, J. S. Lee and F. C. Chang "Preparations, thermal properties, and T-g increase mechanism of inorganic/organic hybrid polymers based on polyhedral oligomeric silsesquioxanes." *Macromolecules* **2002**, *35*, 8788-8793.

(18) J. C. Huang, C. B. He, Y. Xiao, K. Y. Mya, J. Dai and Y. P. Siow "Polyimide/POSS nanocomposites: interfacial interaction, thermal properties and mechanical properties." *Polymer* **2003**, *44*, 4491-4499.

(19) J. Wu and P. T. Mather "POSS Polymers: Physical Properties and Biomaterials Applications." *Polym. Rev.* **2009**, *49*, 25-63.

(20) K. T. Powell, C. Cheng and K. L. Wooley "Complex amphiphilic hyperbranched fluoropolymers by atom transfer radical self-condensing vinyl (co)polymerization." *Macromolecules* **2007**, *40*, 4509-4515.

(21) W. J. Du, A. M. Nystrom, L. Zhang, K. T. Powell, Y. L. Li, C. Cheng, S. A. Wickline and K. L. Wooley "Amphiphilic Hyperbranched Fluoropolymers as Nanoscopic

F-19 Magnetic Resonance Imaging Agent Assemblies." *Biomacromolecules* **2008**, *9*, 2826-2833.

(22) J. W. Bartels, C. Cheng, K. T. Powell, J. Q. Xu and K. L. Wooley "Hyperbranched fluoropolymers and their hybridization into complex amphiphilic crosslinked copolymer networks." *Macromol. Chem. Phys.* **2007**, *208*, 1676-1687.

(23) E. T. Kang and Y. Zhang "Surface modification of fluoropolymers via molecular design." *Adv. Mater.* **2000**, *12*, 1481-1494.

(24) S. R. Coulson, I. Woodward, J. P. S. Badyal, S. A. Brewer and C. Willis "Super-repellent composite fluoropolymer surfaces." *J. Phys. Chem. B* **2000**, *104*, 8836-8840.

(25) T. R. Dargaville, G. A. George, D. J. T. Hill and A. K. Whittaker "High energy radiation grafting of fluoropolymers." *Prog. Polym. Sci.* **2003**, *28*, 1355-1376.

(26) G. Moad, E. Rizzardo and S. H. Thang "Living radical polymerization by the RAFT process." *Aust. J. Chem.* **2005**, *58*, 379-410.

(27) G. Moad, E. Rizzardo and S. H. Thang "Radical addition-fragmentation chemistry in polymer synthesis." *Polymer* **2008**, *49*, 1079-1131.

(28) Z. Li, K. Zhang, J. Ma, C. Cheng and K. L. Wooley "Facile Syntheses of Cylindrical Molecular Brushes by a Sequential RAFT and ROMP "Grafting-Through" Methodology." *J. Polym. Sci. Pol. Chem.* **2009**, *47*, 5557-5563.

(29) J. A. Love, J. P. Morgan, T. M. Trnka and R. H. Grubbs "A practical and highly active ruthenium-based catalyst that effects the cross metathesis of acrylonitrile." *Angew. Chem.-Int. Edit.* **2002**, *41*, 4035-4037.

(30) Y. Xia, J. A. Kornfield and R. H. Grubbs "Efficient Synthesis of Narrowly Dispersed Brush Polymers via Living Ring-Opening Metathesis Polymerization of Macromonomers." *Macromolecules* **2009**, *42*, 3761-3766.

(31) Y. Xia, B. D. Olsen, J. A. Kornfield and R. H. Grubbs "Efficient synthesis of narrowly dispersed brush copolymers and study of their assemblies: the importance of side-chain arrangement." *J. Am. Chem. Soc.* **2009**, *131*, 18525-18532.

(32) Z. Li, J. Ma, C. Cheng, K. Zhang and K. L. Wooley "Synthesis of Hetero-Grafted Amphiphilic Diblock Molecular Brushes and Their Self-Assembly in Aqueous Medium." *Macromolecules* **2010**, *43*, 1182-1184.

(33) G. Riess "Micellization of block copolymers." *Prog. Polym. Sci.* **2003**, *28*, 1107-1170.

Chapter 6

Conclusions

This dissertation focuses on the development of a new "bottom-up" approach to prepare robust well-defined nanostructures with precise control over their structure, composite and dimensions, with the ultimate goal to assemble single small molecules to complicated structures by covalent bonds totally. By taking advantage of recent advances in living polymerization techniques and combing them rationally, such as ring opening metathesis polymerization (ROMP), living/controlled radical polymerization (CRP), ring opening polymerization (ROP) and chain end modification, we have developed an efficient and facile "grafting through" strategy to synthesize a variety of molecular brushes from different norbornenyl group functionalized macromonomers, including polystyrene, poly(4-acetoxystyrene), poly(pentafluorostyrene), poly(methyl acrylate), poly(*t*-butyl acrylate), poly(methyl methacrylate), poly(*t*-butyl methacrylate), polylactide, poly(ethylene glycol) and polyhedral oligomeric silsesquioxane (POSS). Details about the design and realization of the "grafting through" strategy can be found in **Chapter 1** and **Chapter 2**. It should be pointed out that the types of macromonomers that are compatible with this strategy can go beyond this scope - by principle, all the functional groups that are compatible with the Grubbs' catalysts can be incorporated into molecular brush frameworks by our "grafting through" method.

The complexity of the resulting molecular brushes can be increased further by introducing block structures to either the backbone or side chains, using the "livingness"

characters of the employed polymerization techniques. Those block molecular brushes can be building blocks to construct more complicated nanostructures and push the self-assembly of polymers from linear block copolymers to complex macromolecular architectures.

In **Chapter 3**, the livingness of ROMP is utilized to achieve the one-pot synthesis of hetero-grafted diblock molecular brush structures by polymerizing different macromonomer sequentially using the modified 2nd generation Grubbs' catalyst as the initiator. The key parameter to this synthesis is the polymerization time to build the first block of the molecular brush. Short polymerization time leads to incomplete conversion of the first block macromonomer, while long polymerization time leads to chain-end deaths. A specific type of diblock brushes [P(NB-*g*-P*t*BA)-*b*-P(NB-*g*-PS)] was prepared from polystyrene and poly(*t*-butyl acrylate) macromonomers and then these diblock molecular brushes were chemically transformed to amphiphilic nanostructures, whose aqueous solution self-assembly study revealed that *ca.* 60-80 unimers were assembled to a more complicated nanostructure.

In **Chapter 4**, molecular brushes with block structures along the side chains are synthesized and characterized. *a*-Norbornyl-polystyrene-*b*-poly(methyl acrylate)-*b*-poly(*t*-tubyl acrylate) macromomonomers were synthesized from sequential RAFT polymerizations of respective monomers and then transformed into molecular brush frameworks by ROMP. After converting both macromonomers and molecular brushes to amphiphilic structures, they were assembled into nanostructures by dialysis from common solvent to water. Their compositional consistency was guaranteed by the "grafting through" strategy and enabled us to study the difference of their self assembly

behaviors which may be caused by molecular brush architecture only. It was found that nanostructures from linear macromonomers showed globular structures, while nanostructures from amphiphilic molecular brushes exhibited cylindrical structures. In this study, we have demonstrated a hierarchical process that assembles linear triblock copolymers into a complicated nanostructure. They form concentric globular sub-units through strong chemical bonds first, followed by the supramolecular assembly *via* weak non-covalent interactions to afford one-dimensionally-assembled, dynamic cylindrical nanostructures.

In **Chapter 5**, the efficiency of the "grafting through" strategy is further utilized to synthesize PPFS-POSS molecular brush copolymers (9 polymers at one time), whose PPFS/POSS ratio from 0.1 to 0.9 with an increment of 0.1. Nanostructures assembled from them exhibit similar sizes and morphologies, but different mechanical properties. Lower PPFS/PPFS ratio leads to flexible and looser nanostructures and the arrangement of PPFS blocks and POSS blocks in molecular brushes may influence mechanical properties as well.

It is hoped that this dissertation has conveyed the notion that a "grafting through" strategy has been built up to construct molecular brushes with well-defined structures, whose compositions, structures and dimensions are all controlled precisely. As an attempt to create nanostructures by "bottom-up" methods, this "grafting-through" strategy has been proven to be efficient, facile and versatile. Besides the examples that have been listed in the chapters of this dissertation, molecular brushes with more complicated structures and more advanced functionality can be prepared from small molecular moieties that are compatible with metathesis reactions. The increasing complexity of the molecular brush structures promises a great potential to apply them for the construction of more complicated hierarchical

nanostructures, which may meet the needs of complicated nanostructures to handle complicated issues in material science, catalysis and biomedicine.